Impermeable recurve seawalls to reduce wave overtopping

by
Talia Schoonees

Thesis presented in fulfilment of the requirements for the degree of MEng(Research) in the Faculty of Engineering at Stellenbosch University

Supervisor: Mr Geoff Toms

April 2014

Declaration

By submitting this thesis electronically, I declare that the entirety of the work contained therein is my own, original work, that I am the sole author thereof (save to the extent explicitly otherwise stated), that reproduction and publication thereof by Stellenbosch University will not infringe on any third party rights and that I have not previously in its entirety or in part submitted it for obtaining any qualification.

Date: .....

Abstract

Sea-level rise due to climate change results in deeper water next to existing coastal structures, which in turn enables higher waves to reach these structures. Wave overtopping occurs when wave action discharges water over the crest of a coastal structure. Therefore, the higher waves reaching existing structures will cause higher wave overtopping rates. One possible solution to address increasing overtopping, is to raise the crest level of existing coastal structures. However, raising the crest level of a seawall at the back of a beach, will possibly obstruct the view to the ocean from inland.

Alternatively, recurves can be incorporated into the design of both existing and new seawalls. The recurve wall reduces overtopping by deflecting uprushing water seawards as waves impact with the wall. The main advantage of seawalls with recurves is that their crest height can be lower, but still allow for the same wave overtopping rate as vertical seawalls without recurves.

This project investigates the use of recurve seawalls at the back of a beach to reduce overtopping and thereby reducing the required wall height. The objectives of the project are twofold, namely: (1) to compare overtopping rates of a vertical seawall without a recurve and seawalls with recurves; and (2) to determine the influence that the length of the recurve overhang has on the overtopping rates.

To achieve these objectives, physical model tests were performed in a glass flume equipped with a piston type wave paddle that is capable of active wave absorption. These tests were performed on three different seawall profiles: the vertical wall and a recurve section with a short and a long seaward overhang, denoted as Recurve 1 and Recurve 2 respectively. Tests were performed with 5 different water-levels, while the wall height, wave height and period, and seabed slope remained constant. Both breaking and non-breaking waves were simulated.

A comparison of test results proves that the two recurve seawalls are more effective in reducing overtopping than the vertical seawall. The reduction of overtopping can be as high as 100%, depending on the freeboard and wave conditions.

Recurve 2 proves to be the most efficient in reducing overtopping. However, in the case of a high freeboard (low water-level at the toe of the structure), the reduction in overtopping for Recurve 1 and Recurve 2 was almost equally effective. This is because all water from the breaking waves is reflected. Even for the simulated lower relative freeboard cases, the recurve walls offer a significant reduction in overtopping compared with the vertical wall.

A graph is presented which shows that the length of the seaward overhang influences the overtopping performance of the seawall. As the seaward overhang length increases, the wave overtopping rate decreases. However, for high freeboard cases the length of the seaward overhang becomes less important. The graph gives designers an indication of how recurves can be designed to reduce seawall height while retaining low overtopping. It is recommended that further model tests be performed for additional overhang lengths.

Incorporation of recurves into seawall design represents an adaptation to problems of sea-level rise due to global warming.

Opsomming

Stygende seevlak as gevolg van klimaatverandering, veroorsaak dat dieper water langs bestaande kusstrukture voorkom. Gevolglik kan hoër golwe hierdie strukture bereik. Golfoorslag vind plaas wanneer water oor die kruin van ‘n kusstruktuur, hoofsaaklik deur golfaksie, spat of vloei. Dus sal hoër golfhoogtes tot verhoogde golfoorslag lei. Een moontlike oplossing vir hierdie verhoogde golfoorslag is om die kruinhoogte van bestaande kusstrukture te verhoog. In die geval van ‘n seemuur aan die agterkant van ‘n strand, kan hoër strukture egter die see-uitsig na die see vanaf die land belemmer. Om hierdie probleem te vermy, kan terugkaatsmure in die ontwerp van bestaande en nuwe seemure ingesluit word.

Terugkaatsmure verminder golfoorslag deurdat opspattende water, afkomstig van invallende golwe terug, na die see gekaats word. Die grootste voordeel van ‘n terugkaatsmuur is dat hierdie tipe muur ‘n laer kruinhoogte as die vertikale seemuur sonder ‘n terugkaatsbalk, vir dieselfde golfoorslagtempo kan hê.

Hierdie projek ondersoek dus die gebruik van terugkaatsmure aan die agterkant van ‘n strand met die doel om golfoorslag te verminder en sodoende die vereiste muurhoogte te verminder. Die doelwit vir die projek is tweeledig: (1) om die golfoorslagtempo van terugkaatsmure te vergelyk met dié van ‘n vertikale muur sonder ‘n terugkaatsbalk; en (2) om die invloed van die terugkaatsmuur se oorhanglengte op die golfoorslagtempo te bepaal.

Om bogenoemde doelwitte te bereik, is fisiese modeltoetse in ‘n golfkanaal, wat met ‘n suiertipe golfopwekker toegerus is en wat aktiewe golfabsorbering toepas, uitgevoer. Hierdie toetse is op drie verskillende seemuurprofiele, naamlik ‘n vertikale muur en ‘n terugkaatsmuur met ‘n kort en lang oorhang, genaamd “Recurve 1” en “Recurve 2” onderskeidelik, uitgevoer. Die muurhoogte, die seebodemhelling asook die golfhoogte en –periode is tydens al die toetse konstant gehou. Vir elke profiel is toetse by 5 verskillende watervlakke vir beide brekende en ongebreekte golwe uitgevoer.

Uit die toetsresultate is dit duidelik dat terugkaatsmure meer effektief as vertikale mure is om golfoorslag te beperk. Die vermindering van golfoorslag kan tot 100% wees, afhangende van die vryboord en golftoestande.

Daar is bevind dat “Recurve 2” golfoorslag die effektiefste verminder. In die geval van hoë vryboord (lae watervlak by die toon van die struktuur) is daar egter gevind dat “Recurve 1” en “Recurve 2” die

golfoorslag feitlik ewe goed beperk. Dit is die geval aangesien alle water van die brekende golwe weerkaats word. In die geval van ‘n lae vryboord, word die voordeel van die terugkaatsmuur teengewerk deurdat daar ‘n kleiner verskil in golfoorslagtempo’s tussen die drie profiele is.

‘n Grafiek is voorgelê wat wys dat die lengte van die terugkaatsmuur se oorhang golfoorslag beperk. ‘n Groter oorhanglengte van die terugslagmuur veroorsaak ‘n groter vermindering in golfoorslag. Vir gevalle met ‘n hoë vryboord, is daar egter gevind dat die oorhanglengte van die terugslagmuur minder belangrik is. Hierdie grafiek gee ontwerpers ‘n aanduiding van hoe terugslagmure ontwerp kan word met ‘n lae hoogte terwyl ‘n lae oorslagtempo behou word.

Die gebruik van terugslagmure bied ‘n aanpassing vir die probleme van seevlakstyging, as gevolg van klimaatverandering.

Acknowledgements

First and foremost I would like to express gratitude to my study supervisor, Mr. Geoff Toms, for his support and guidance throughout my thesis.

In addition, I would like to thank Mr. K. Tulsi from the CSIR, for his advice and suggestions regarding the physical model tests.

Without the help of the staff at the Hydraulic Laboratory at the University of Stellenbosch this project would truly not have been possible. My sincerest thanks to Mr C. Visser, Mr N. Combrinck, Mr J. Nieuwoudt and Mr A. Lindoor. Thanks also to Mr L. Rabie, a masters student, who volunteered to help in the laboratory.

Last, but not least, I would like to thank my family for their love and support throughout my studies.

Table of Contents

Page

Declaration i
Abstract ii
Opsomming iv
Acknowledgements vi
Table of Contents vii
List of figures ix
List of tables xi
List of symbols and acronyms xii
Chapter 1: Introduction 1
1.1 Background 1
1.2 Objective 3
1.3 Definitions 3
1.4 Brief Chapter overview 4
Chapter 2: Literature Review 5
2.1 General 5
2.2 Defining overtopping and its safety limits 5
2.3 Review of design guidance for recurve seawalls 6
2.3.1 Early studies 7
2.3.2 Japanese studies 9
2.3.3 CLASH project 10
2.3.4 Recent studies 15
2.4 Examples of recurve type seawalls 19
2.5 Physical modelling in wave overtopping studies 26
2.5.1 Scale and laboratory effects 26
2.5.2 Wave overtopping laboratory measurement methods 31
2.5.3 Test duration 32
2.5.4 Wave spectra 33
2.6 Conclusions 34
Chapter 3: Physical model tests 36
3.1 Scope of model tests 36

3.2 Test facility 36
3.3 Model set-up 37
3.4 Model scale 45
3.5 Test procedure 45
3.6 Test duration 46
3.7 Data acquisition 46
3.8 Test conditions and schedule 47
3.9 Repeatability and accuracy 48
3.10 Sensitivity runs 48
Chapter 4: Results 49
4.1 General 49
4.2 Results 49
Chapter 5: Analysis and discussion 57
5.1 Introduction 57
5.2 Measured test results 57
5.2.1 Repeatability and accuracy of tests 62
5.2.2 Sensitivity of overtopping rates to wave period 67
5.3 Comparison of measured results with EurOtop calculation tool 68
5.4 Other considered factors 74
5.4.1 Safety evaluation for pedestrians, vehicles and buildings 74
5.4.2 Additional factors to be considered 77
5.5 Applicability of results to a case study 77
Chapter 6: Conclusion and recommendations 81
6.1 General 81
6.2 Findings from literature review 81
6.3 Findings of physical model tests 82
6.4 Conclusions 83
6.5 Recommendations for further research 83
References 85
Appendix A 89

List of figures

Page

Figure 1: Typical behaviour of recurve and vertical seawall 2
Figure 2: Classification of recurves 3
Figure 3: Definition sketch 4
Figure 4: Proposed recurve profile by Berkeley-Thorn and Roberts (1981) 7
Figure 5: Proposed profile of the Flaring Shaped Seawall 9
Figure 6: FSS with vertical wall to reduce water spray 10
Figure 7: High and low free board cases 12
Figure 8: Decision chart for design guidance of recurve walls 13
Figure 9: Parameter definition sketch 13
Figure 10: EurOtop calculation tool: schematisation of vertical wall 14
Figure 11: EurOtop calculation tool: schematisation of recurve wall 14
Figure 12: Recurve wall at shoreline 16
Figure 13: Recurve wall positioned seawards of shoreline 16
Figure 14: Wave return wall on a smooth dike 17
Figure 15: Overtopping results for wave return wall of 5 cm with different parapet angles β 18
Figure 16: Wave overtopping of vertical seawall, parapet wall and recurve wall 19
Figure 17: Recurve wall in Abu Dhabi, United Arab Emirates 19
Figure 18: High recurve seawall at Sandbanks Peninsula southwest of Bournemouth, Dorset, United Kingdom 20
Figure 19: Stepped seawall with recurve at Burnham-on-Sea, Somerset, United Kingdom 20
Figure 20: Seawall at St. Mary's Bay, United Kingdom 21
Figure 21: Recurve seawall with rock armour at Scarborough, United Kingdom 21
Figure 22: Recurve seawall near Dymchurch, United Kingdom 22
Figure 23: Recurve seawall at Kailua-Kona, Hawaii 22
Figure 24: Another recurve type seawall at Kailua-Kona, Hawaii 23
Figure 25: Recurve seawall at Ocean Beach, San Francisco, CA, USA 23
Figure 26: Construction of the Flaring Shaped Seawall (FSS) in Kurahashi-jima, Hiroshima, Japan 24
Figure 27: FSS at Kurahashi-jima, Hiroshima, Japan 24
Figure 28: Recurve wall in Cape Town, South Africa 25
Figure 29: Damaged recurve wall in Strand, South Africa 25

Figure 30: Typical cross-section of battered seawall....29
Figure 31: Full scale test at Ostia, Italy....30
Figure 32: Overtopping tank suspended from load cell....32
Figure 33: JONSWAP spectrum....33
Figure 34: Comparison of the JONSWAP and Pierson-Moskowitz spectra....34
Figure 35: Seawall profiles with 3 different overhang lengths (model dimensions in mm)....37
Figure 36: Recurve structure with bed slopes....38
Figure 37: Irregularities in built-in slope....40
Figure 38: Recurve 2 profile....41
Figure 39: Schematisation of layout behind the structure to collect overtopped water....41
Figure 40: Waterproof plastic to guide water into overtopping container....42
Figure 41: Weighed bin outside the flume....42
Figure 42: Measuring needle and pump in overtopping container....43
Figure 43: Sheets to prevent water from splashing out of the flume....43
Figure 44: Calculating the allowable frequency range in HR DAQ....44
Figure 45: Probe spacing....44
Figure 46: Screenshot of the EurOtop Calculation tool for wave overtopping (vertical wall)....50
Figure 47: Screenshot of EurOtop calculation tool (Recurve)....51
Figure 48: Recurve 1 during model testing....56
Figure 49: Recurve 2 during model testing....56
Figure 50: Graph displaying all test results....58
Figure 51: Graph showing average measured data....59
Figure 52: The influence of the overhang length on mean overtopping rate....61
Figure 53: Influence of wave period on overtopping results....67
Figure 54: Comparison of measured and calculated overtopping rates for vertical wall....69
Figure 55: Comparison of measured and calculated overtopping rates for Recurve 1....70
Figure 56: Comparison of measured and calculated overtopping rates for Recurve 2....71
Figure 57: Vertical wall: predicted versus measured overtopping rates....72
Figure 58: Recurve 1: predicted versus measured overtopping rate....73
Figure 59: Recurve 2: predicted versus measured overtopping rate....74
Figure 60: Current recurve wall in Strand....78
Figure 61: Example of how to apply results of this project in case study....80

List of tables

Page

Table 1: Allowable or tolerable overtopping rates 6
Table 2: Description of symbols used in calculation tool 15
Table 3: Values of geometry parameters 17
Table 4: Scale ratios of the Froude law 27
Table 5: Typical beach slopes along the South African coast 38
Table 6: Applicable scale used 45
Table 7: Test series and conditions (prototype) 48
Table 8: Results of series A – Vertical wall 52
Table 9: Results of series B – Recurve 1 53
Table 10: Results of series C – Recurve 2 54
Table 11: Results of series D – Wave period sensitivity 55
Table 12: Reduction in overtopping due to Recurve 1 and 2 60
Table 13: Repeated tests of series A 63
Table 14: Repeated tests of series B 63
Table 15: Repeated tests of series C 64
Table 16: Repeated tests of series D 64
Table 17: Measured H_{max} and $H_{2\%}$ 66
Table 18: Summary of average prototype overtopping rates 75
Table 19: Summary of used parameters 78
Table 20: Results for case study calculations 80

List of symbols and acronyms

B	Height of FSS (m)
B_r	Width of seaward overhang in front of main vertical wall (m)
CoV	Coefficient of variation (%)
EL	Wave level (m)
FSS	Flaring Shaped Seawall
g	Gravitational acceleration (m/s^2)
H	Local wave height (m)
h	Water depth at the toe of the structure (m)
$H_{2\%}$	Wave height exceeded by 2% of waves (m)
h_c	Critical crest elevation of FSS (m)
H_i	Incident wave height (m)
H_{m0}	Spectral significant wave height (m)
H_{max}	Maximum wave height in the wave train (m)
h_n	Height of nose (m)
h_r	Height of recurve wall section at top of vertical wall (m)
H_r	Reflected wave height (m)
H_s	Significant wave height (m)
h_s	Water depth at the toe of the structure (m)
h_t	Height of wave return wall on dike (m)
h_w	Height of vertical wall on FSS (m)
k	Effective recurve factor
k’	adjusted k-factor
K_r	Bulk reflection coefficient
LLD	Land Levelling Datum

MSL Mean Sea-Level

P_c Height of vertical wall section from still water-level to bottom of recurve (m)

q Overtopping rate (l/s per m)

R_c Freeboard (m)

SLR Sea-Level Rise

SWL Still Water-level

T Wave period (s)

T_p Peak wave period (s)

α Angle of recurve (^{O})

β Parapet nose angle (^{O})

ɣ JONSWAP enhancement factor

μ Average

λ Dimensionless height of the wave return wall's nose

σ Standard deviation

Chapter 1: Introduction

1.1 Background

Wave overtopping occurs when wave action discharges water over the crest of a coastal structure. Coastal structures protect infrastructure (walkways, roads, buildings and land) as well as humans (especially pedestrians) from the impacts of the coastal environment. The crest height of coastal structures is often determined by the allowable wave overtopping during extreme conditions measured in litres per second per metre (l/s per m).

Apart from waves, water-level is an important parameter when considering overtopping. Due to climate change and its concomitant rise in sea level, deeper water occurs next to existing coastal structures. Consequently, coastal engineers are confronted with higher wave heights, which result in an increase in wave overtopping. The levels of land and infrastructure safety behind coastal structures are thus compromised. Raising the crest height of existing coastal structures is one possible solution to this problem.

However, the view of the ocean can be obstructed and access to the beach denied when the crest height of coastal structures, particularly a seawall at the back of the beach, is raised. An obstructed view and lack of access can have a negative impact on a beach's appeal as a tourist attraction. An alternative solution is to incorporate recurves into seawall design. The main advantage of recurve seawalls is that their crest height can be lower than that of vertical walls to allow for the same wave overtopping rates.

A recurve is a form of seaward overhang of a seawall, designed to reduce wave overtopping. Seaward overhangs are also known as a parapet, bullnose, wave return wall or a recurve. Although there are certain distinctions between the different types of overhangs, hereafter the term recurve will collectively be used.

The seaward overhang of a recurve wall deflects uprushing water seawards. When no seaward overhang is present as in the case of a vertical wall, water splashes vertically upwards and over the wall during wave impact. Wind can increase overtopping rates by blowing the uprushing water landwards. Therefore, recurve walls are often incorporated into seawall design in order to reduce wave overtopping. Figure 1 shows the typical behaviour of a recurve and vertical seawall as described above.

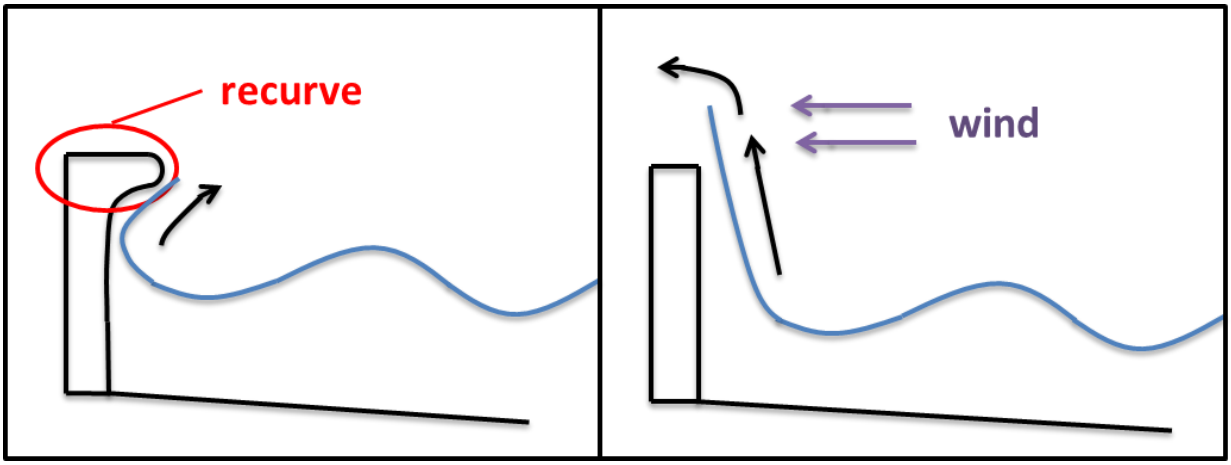

Figure 1: Typical behaviour of recurve and vertical seawall

Recurve walls can primarily be classified into three categories; namely: Type 1: large recurves, Type 2: small recurves; and Type 3: recurves on a vertical wall (Allsop, 2013). A large recurve is defined as a wall where the recurve forms the major part of the wall, as illustrated in Figure 2(a). A small recurve is defined as a wall where the recurve is a minor construction on part of the wall; for example, a curve added to a small wall on top of a rock berm or dike, Figure 2(b). The third type of recurve wall is characterised by a recurve sited at the top of a vertical seawall, as seen in Figure 2(c).

At the back of some beaches along the coast of South Africa, for example, Strand in False Bay, vertical seawalls serve as landward protection from the impacts of overtopping. A sea wall should not obstruct the view of the sea as beaches in South Africa are important for recreation and as tourist attractions. With sea-level rise resulting in an increase in wave overtopping, a possible solution will be to incorporate recurves into seawall design to reduce overtopping. By reducing overtopping, the raising of the crest height of the seawalls can be limited and, in turn, the possible obstruction of the view from the walkway to the beach, can be avoided.

This study focuses on the use of recurves at the top of a vertical seawall (Type 3; Figure 2(c)) to address the predicted increase of wave overtopping rates at the back of beaches due to sea-level rise. There are other possible solutions to limit wave overtopping, such as rubble slopes against seawalls and offshore breakwaters. However, these solutions are not included within the scope of this study. The forces on the recurve wall are also not considered and investigated within this project.

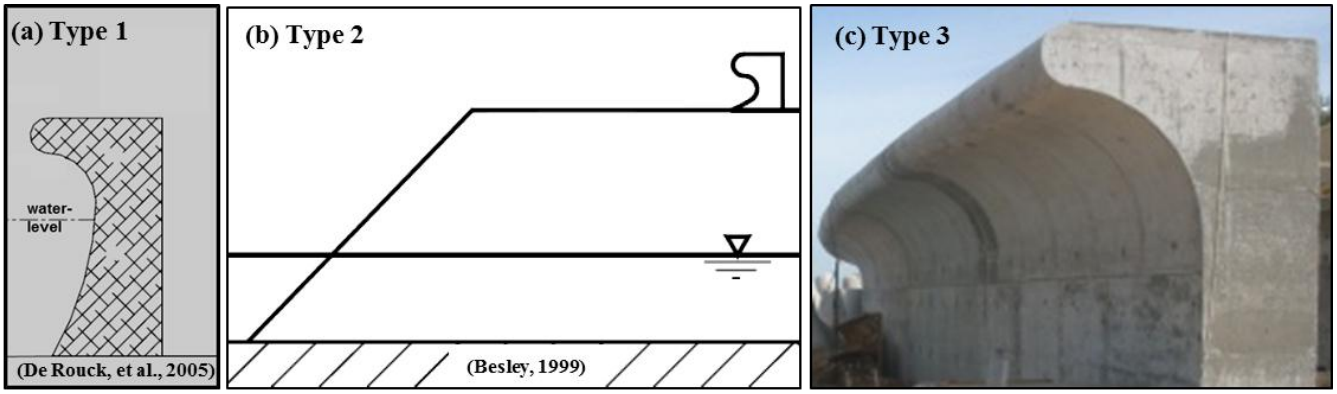

Figure 2: Classification of recurves

Although recurves are often incorporated into seawall design, literature offers little design guidance for recurve walls, as discussed in Chapter 2. The earliest studies on recurve seawall design propose overtopping reduction factors. Using these reduction factors, the overtopping rate for a recurve wall can be adjusted to calculate the required crest level with existing overtopping formulas for vertical walls.

Design guidance on the shape of recurve walls is based on limited research. Existing studies did not specifically investigate the use of recurve walls at the back of a beach nor the optimal recurve profile, to reduce overtopping. According to the literature, no systematic studies have been performed to test the influence of the recurve seawall overhang length in reducing overtopping.

1.2 Objective

This project aims to explore the use of a recurve at the top of a vertical seawall (Type 3) to reduce overtopping. The specific objectives are to:

- Compare overtopping rates for a vertical seawall and a recurve seawall
- Determine the influence of the length of the recurve overhang in reducing overtopping

Although different lengths of recurve overhangs are tested, it is not the objective of this project to provide comprehensive design guidelines.

1.3 Definitions

For the purpose of this study, a recurve wall is defined as a vertical, impermeable seawall with a curved or straight seaward overhang sited at the top of the seawall. The recurve wall is situated at the back of a beach. Figure 3 illustrates the case as defined for this project.

The freeboard of a structure (R_c) is defined as the vertical distance between the water-level (EL) and the crest level of the structure, Figure 3. The wave heights for the two levels (H_1 and H_2) are indicated for each water-level (EL_1 and EL_2). In addition, Figure 3 presents the geometric parameters of a recurve; height (h_r), overhang length (B_r), and angle (α), as defined for this project.

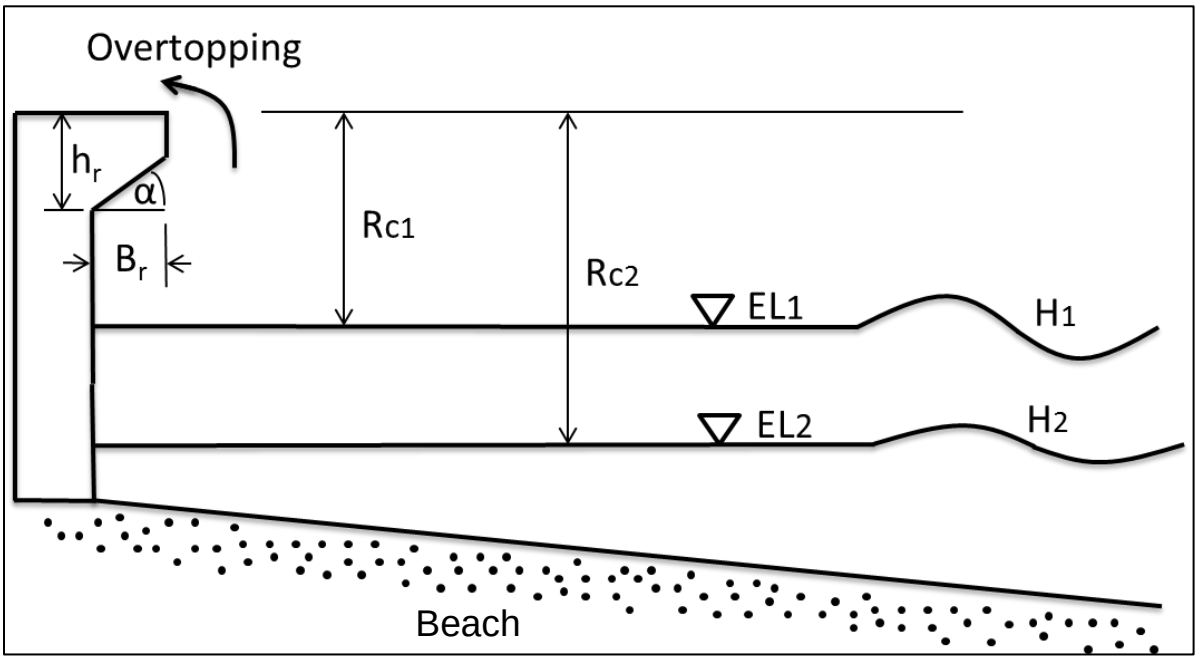

Figure 3: Definition sketch

1.4 Brief Chapter overview

The report consists of six chapters, including the current chapter. Chapter 2, the literature review, aims to review available research on recurve seawall design. Within the chapter, proposed recurve profiles in existing literature are collected and reviewed. The literature review also includes research on physical model testing of wave overtopping.

Chapter 3 describes the scope of the physical model tests and outlines the methodology followed to perform the tests.

Chapter 4 presents the results of all the performed physical model tests, whereas in Chapter 5 these results are analysed and presented as graphs. In addition, these graphs are interpreted and discussed.

The report concludes with Chapter 6, in which the conclusions of the project are given and recommendations regarding future research are made.

Chapter 2: Literature Review

2.1 General

The literature review presents research that forms the basis of this study, and aims to give insight into overtopping studies and the physical modelling of recurve walls. Examples of constructed recurve walls are also included.

2.2 Defining overtopping and its safety limits

Overtopping can occur in three different modes (EurOtop, 2007). The first mode of overtopping is referred to as the "green water overtopping case", which occurs when wave run-up levels are high enough for water to flow over the crest of the coastal structure. Thus, EurOtop (2007) defines green water overtopping as "a continuous sheet of water that passes over the crest".

The second type of overtopping, "splash water overtopping", takes place as waves break on the structure and significant volumes of splash passes over the crest of the structure. The splash water passes over the wall due to either the momentum of the water or the effect of an onshore wind (EurOtop, 2007).

The third and least troublesome type of overtopping occurs when water passes over the crest of a structure as spray. This spray is produced by wind action on wave crests and is usually not significant to the total overtopping volume in spite of strong winds (EurOtop, 2007). Wind effects are not included within the scope of this project. Consequently, only the first two modes of overtopping are considered.

Studies have investigated the allowable overtopping rates for certain safety conditions. As this project focuses on the overtopping of a seawall at the back of a beach, the allowable mean overtopping rates (q) for the conditions applicable to this study only, are presented in Table 1 (CIRIA, et al., 2007); (EurOtop, 2007).

Table 1: Allowable or tolerable overtopping rates

	Mean overtopping rate q (l/s per m)
Pedestrians	
Unsafe for unaware pedestrians, no clear view of the sea, relatively easily upset or frightened, narrow walkway or proximity to edge	q > 0.03
Unsafe for aware pedestrians, clear view of the sea, not easily upset or frightened, able to tolerate getting wet, wider walkway	q > 0.1
Unsafe for trained staff, well shod and protected, expected to get wet, overtopping flows at lower levels only, no falling jet, low danger of fall from walkway	q > 1 - 10
Vehicles	
Unsafe for driving at moderate or high speed, impulsive overtopping giving falling or high velocity jets	q > 0.01 - 0.05
Unsafe for driving at low speed, overtopping by pulsating flows at low levels only, no falling jets	q > 10 - 50
Buildings and infrastructure	
No damage	q > 0.001
Minor damage to fitting etc.	0.001 < q < 0.03
Structural damage	q > 0.03
Damage to grassed or lightly protected promenade behind seawall	q > 50
Damage to paved or armoured promenade behind seawall	q > 200

(CIRIA, et al., 2007); (EurOtop, 2007)

2.3 Review of design guidance for recurve seawalls

Recurves have often been included in seawall design to reduce overtopping in the past. Even though designers often include recurves, little design guidance on the shape of seaward overhangs exists. This section of the literature review focuses on the review of recurve design aspects and the examination of recurve wall profiles.

2.3.1 Early studies

Physical model tests of the Kent Northern seawall in the United Kingdom (UK), were conducted in an early study by Berkeley-Thorn and Roberts (1981). Berkeley-Thorn and Roberts (1981) propose a recurve profile, Figure 4, to be sited at the crest of a sloped seawall (Type 2). The physical model of the Kent Northern seawall was tested under severe conditions where the wave wall crest height was less than the tested wave crest elevation. The model recurve seawall proved to be ineffective in these severe conditions. However the study concluded that recurve walls are more effective under less severe conditions and far superior to vertical seawalls (Berkeley-Thorn & Roberts, 1981).

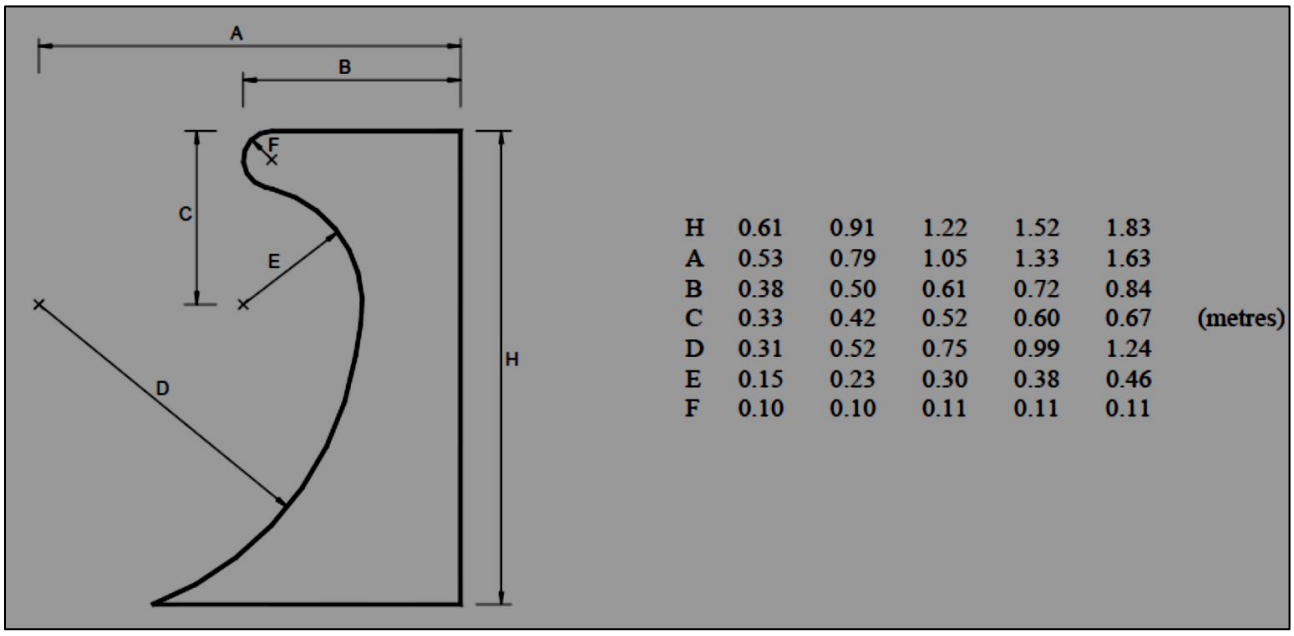

H	0.61	0.91	1.22	1.52	1.83	
A	0.53	0.79	1.05	1.33	1.63	
B	0.38	0.50	0.61	0.72	0.84	
C	0.33	0.42	0.52	0.60	0.67	(metres)
D	0.31	0.52	0.75	0.99	1.24	
E	0.15	0.23	0.30	0.38	0.46	
F	0.10	0.10	0.11	0.11	0.11	

Figure 4: Proposed recurve profile by Berkeley-Thorn and Roberts (1981)

(Besley, 1999)

Owen and Steele (1991) undertook physical model tests and proposed a design method whereby wave overtopping discharges of recurve wave return walls can be estimated. The model tests were performed with the same profile (Type 2) as proposed by Berkeley-Thorn and Roberts (1981). Owen and Steele (1991) suggest that this proposed profile is probably one of the most effective recurve profiles, because the water is deflected seawards at a very shallow angle above the horizontal. Overtopping reduction factors for recurve seawalls were also proposed. It was found that the height of the recurve wall, as well as the discharge incident on the recurve wall were the primary factors influencing the wall's overtopping performance.

The United States of America (US) Army Corps of Engineers (1991) found in a study that a recurve wall significantly reduces overtopping. This study was undertaken to determine the effectiveness of a parapet at the top of a riprap protected embankment (Type 2) to reduce overtopping. Vertical parapets with different heights, as well as a recurve wall were tested. The US Army Corps of Engineers (1991) conclude that the recurve wall proves to be surprisingly effective as their results indicate that the overtopping rates over the recurve wall are only about 9 percent of the rates for a vertical parapet. The study suggests that the recurve wall may be successful because the riprap significantly reduces the intensity of the wave uprush once the water reaches the recurve wall above the water line on the berm.

Herbert et al. (1994) conducted a study to quantify the overtopping performance of recurve and vertical seawalls on a sloped seawall (Type 2) by using physical model tests. The study only used the proposed recurve profile of Berkeley Thorn & Roberts (1981) for the tests even though a wide range of profiles have been built along the UK coastline. The model tests show that the effectiveness of the recurve wall performance is dependent on the height of the recurve wall relative to the still water-level (freeboard). The results indicate that a recurve wall can significantly reduce overtopping compared to a case with no recurve wall.

A study by Franco et al. (1994) researched wave overtopping of vertical and composite breakwaters, including recurve and vertical parapets at the top of caisson breakwaters (Type 3). The physical model test results show that the crest of the recurve seawall can be lowered by 30 % to get the same overtopping rate for a vertical seawall without a recurve. However Franco et al. (1994) states that this is only applicable to relatively small overtopping rates.

The UK Environmental Agency Overtopping Manual (Besley, 1999) is a compilation and summary of previous research on overtopping performance of seawalls. This manual was intended to offer guidelines to flood and coastal engineers for the assessment of existing coastal structures and the design of new seawalls. Besley (1999) presents the reduction factors as proposed by Owen and Steele (1991). In addition, Besley (1999) claims that the recurve profile as proposed by Berkeley-Thorn and Roberts (1981), Figure 4, is very efficient and that alternative profiles may be significantly less effective.

2.3.2 Japanese studies

Different profiles for a non-wave overtopping seawall were researched in Japan. Kamikubo et al. (2000) recommend a non-wave overtopping seawall which has a deep circular cross-section, named the Flaring Shaped Seawall (FSS), Figure 5. The FSS (Type 1) was recommended as this profile has the lowest vertical uplift force and the lowest wave pressure. The FSS was compared with a conventional vertical seawall using physical model tests. These tests indicated that the crest elevation of the FSS can be lower than the conventional vertical seawall as it limits wave overtopping more effectively. However, the measured wave pressures were found to be very high on the portion above the still water surface.

Kamikubo et al. (2003) later extended the research of the proposed non-wave overtopping seawall, looking particularly at the Flaring Shaped Seawall (FSS). The non-overtopping FSS has a significantly lower crest height compared with a conventional wave absorbing vertical seawall. This study proposes to include a vertical wall at the tip of the FSS to effectively reduce water spray, Figure 6. The FSS weakness is that the shape is difficult to form in reinforced concrete as there is not sufficient cover for reinforcement in the slender parts at the crest and at the base (Kortenhaus, et al., 2003). However, this recurve profile has been built in Japan, Figures 26 and 27.

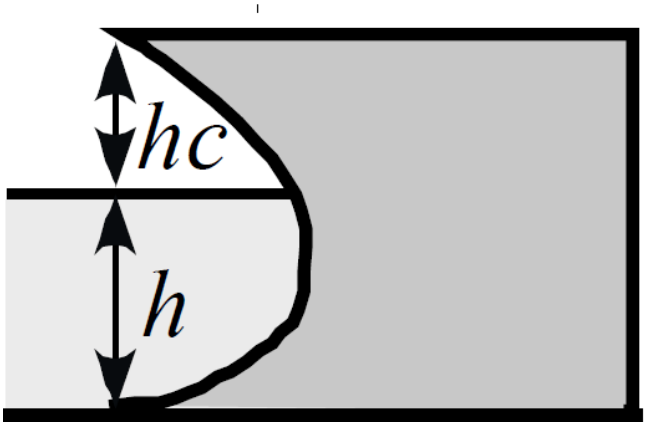

Symbol	Description
B	Seawall height (m)
h	Water depth in front of seawall (m)
h_c	Critical crest elevation (m)
h_w	Height of vertical wall (m)
H_0	Incident wave height (m)

Figure 5: Proposed profile of the Flaring Shaped Seawall

(Kamikubo, et al., 2003)

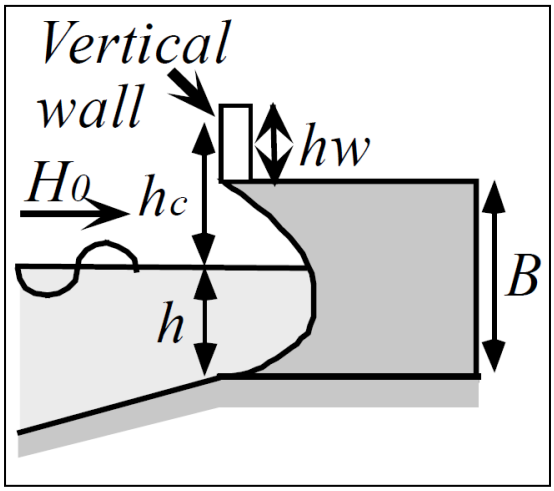

Figure 6: FSS with vertical wall to reduce water spray

(Kamikubo, et al., 2003)

2.3.3 CLASH project

The European Union (EU) funded CLASH project (Crest Level Assessment of coastal Structures by full scale monitoring, neural network prediction and Hazard analysis on permissible wave overtopping) was a collaborative study between several European countries: Belgium, Germany, Denmark, Spain, Italy, the Netherlands and the United Kingdom. The need for the study originated from two observations (De Rouck, et al., 2005):

> "(1) The proven fact that small scale model testing under predicts wave run-up on rough slopes;
>
> (2) The lacking of generally applicable prediction methods for crest height design or assessment with respect to wave overtopping."

Two overall CLASH objectives were developed from these two observations. The first objective was to validate the present design methods by using full scale monitoring of wave overtopping, small scale laboratory modelling, and numerical modelling, in order to solve the issue of scale effects and possible underpredictions. The second objective was to use numerous available data sets on overtopping to develop a generally applicable design method (De Rouck, et al., 2005).

From the CLASH study, De Rouck et al. (2005) found that the number of waves generated per test has an influence on the average wave overtopping measurements. A comparison of overtopping results

from tests using 200 waves with tests using 1000 waves, showed a 20% difference in mean overtopping results.

Further studies by Kortenhaus et al. (2003) and Pearson et al. (2004) were partly facilitated by the CLASH collaboration.

According to a study by Kortenhaus et al. (2003), parapet and recurve seawalls have often been incorporated into seawall design, even though no general design guidance has been available. This study proposes a reduction factor for wave overtopping of parapet and Type 3 recurve seawalls which is dependent on the geometrical profile. Earlier studies of recurve walls have mostly been investigated by case studies and only a few generic investigations have been conducted.

Wave energy can be deflected completely with a relatively high crest freeboard. However, it was found that with a lower freeboard, or in many high wave conditions, overtopping is not effectively reduced and that the wall shape had no significant effect compared with a conventional seawall (Kortenhaus, et al., 2003). Figure 7 illustrates a high freeboard (R_{c1}) and a low freeboard case (R_{c2}).

According to Kortenhaus et al. (2003) a recurve wall is most effective when the shape of the recurve, together with the freeboard, prevents green water from overtopping the seawall. With larger relative freeboards, the wave energy is completely deflected seawards away from the wall. Lower freeboards and/or higher waves prevent wave energy from being fully deflected and therefore the recurve wall is no longer effective, resulting in large overtopping. When a recurve wall is small, the influence of a recurve is relatively small on green water overtopping.

As Pearson et al. (2004) states, it is surprising that with such a long history of the design of recurve walls, very few systematic studies on, and even less generic guidance for the incorporation of recurve walls into seawall design exists. To address this shortcoming Pearson et al. (2004) formulates generic guidance for the crest level design of recurve walls (Type 3).

In Kortenhaus et al. (2003) a generic method for the prediction of the reduction in overtopping of recurve walls was proposed. The reduction was quantified with a reduction factor, the so-called k-factor. The k-factor is defined as follows:

$$k = \frac{q_{recurve}}{q_{no\ recurve}}$$

Where $q_{recurve}$ = overtopping rate of a test where recurve is present

$q_{no\ recurve}$ = overtopping rate of the same test with a vertical wall (same crest height as recurve wall)

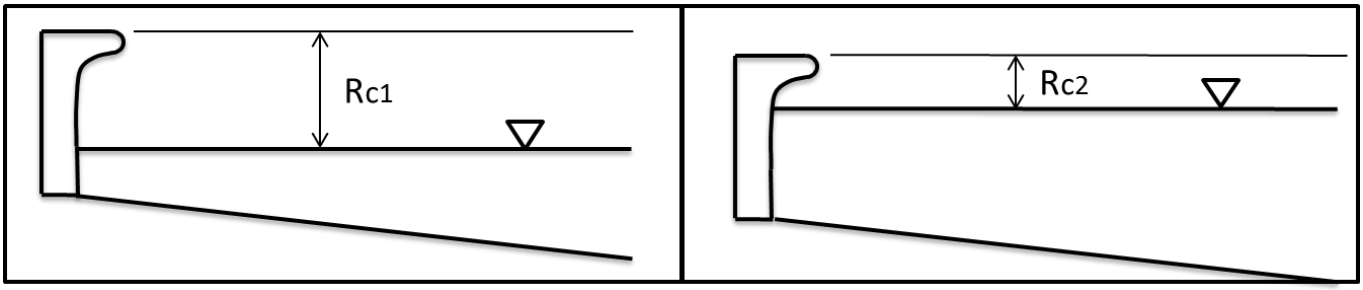

Figure 7: High and low free board cases

However, the calculated k-factors from the test results presented a scatter for large reductions in overtopping. Pearson et al. (2004) proposed a method to reduce the scatter in test results. This method introduces the adjusted k-factor (k'). The outcome of this study was a decision chart to give design guidance for recurve walls, Figures 8 and 9. The decision chart enables the designer to determine a reduction factor for a recurve wall, based on the dimensions of the recurve wall profile and freeboard. The designer can use vertical wall equations to estimate the mean overtopping rate ($q_{no\ recurve}$). Once the reduction factor (k) and $q_{no\ recurve}$ are known, the estimated overtopping rate for a recurve wall ($q_{recurve}$) can be calculated.

The EurOtop Overtopping Manual provides current practice and therefore extends and revises guidance on wave overtopping predictions provided in previous manuals such as the CIRIA/CUR Rock Manual, the Revetment Manual by McConnel (1998), British Standard BS6349, the US Coastal Engineering Manual and ISO TC98. The EurOtop includes the research obtained from the CLASH project (EurOtop, 2007).

As described in EurOtop (2007), the CLASH project introduced a Neural Network tool for the prediction of overtopping rates for particular structures under given wave conditions and water-levels. The Neural Network predicts overtopping rates by using the CLASH database.

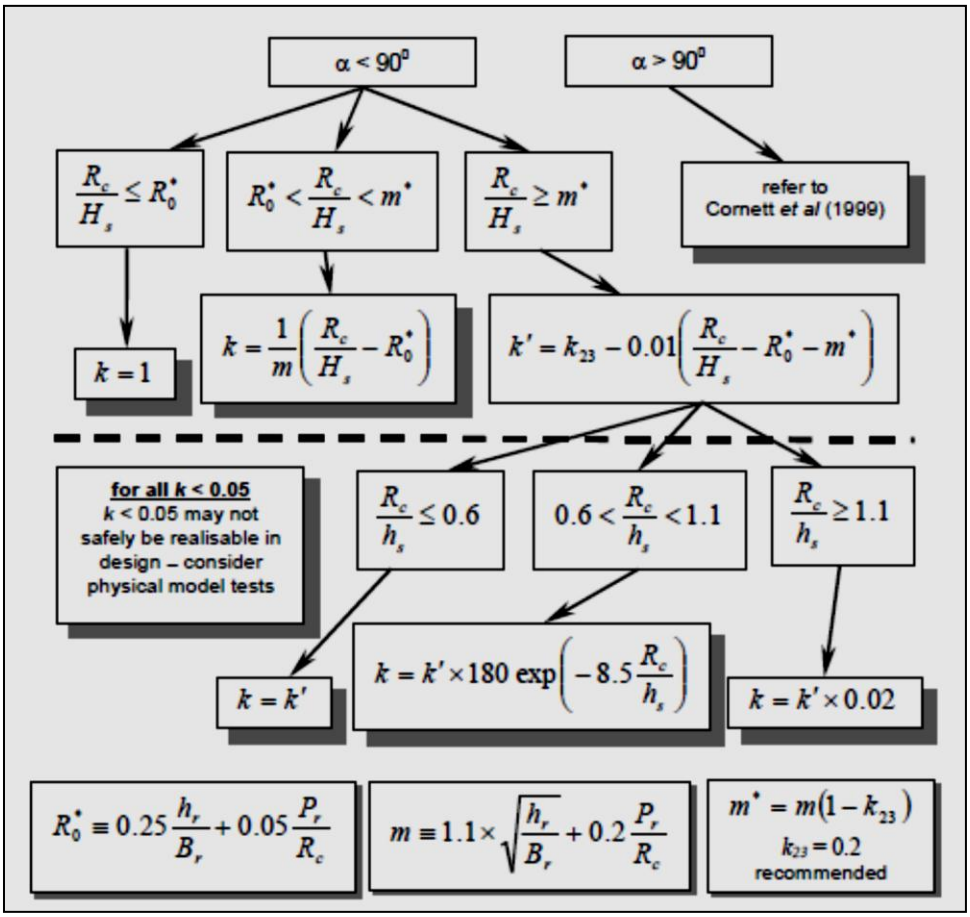

Figure 8: Decision chart for design guidance of recurve walls

(Pearson, et al., 2004)

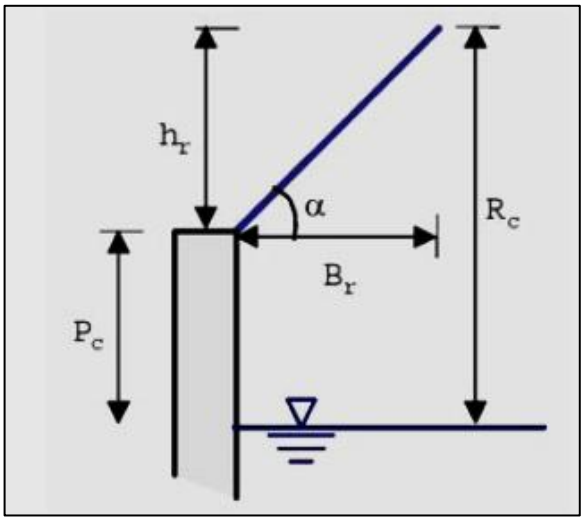

Symbol	Description
α	Angle of recurve (^{O})
R_c	Freeboard (m)
H_s	Significant wave height (m)
k	Effective recurve factor (-)
k'	Adjusted k-factor (-)
B_r	Width of parapet overhang (m)
h_r	Height of parapet (m)
$P_c = P_r$	Relative elevation (m)

Figure 9: Parameter definition sketch

(Pearson, et al., 2004)

EurOtop also developed a calculation tool from the empirical formulae presented in the EurOtop Overtopping Manual. The calculation tool can be used as a preliminary prediction for overtopping discharges (HR Wallingford, n.d.). Figures 10 and 11 show the schematisation of the input parameters of the calculation tool for the vertical and recurve wall, respectively. Table 2 gives the description of the symbols.

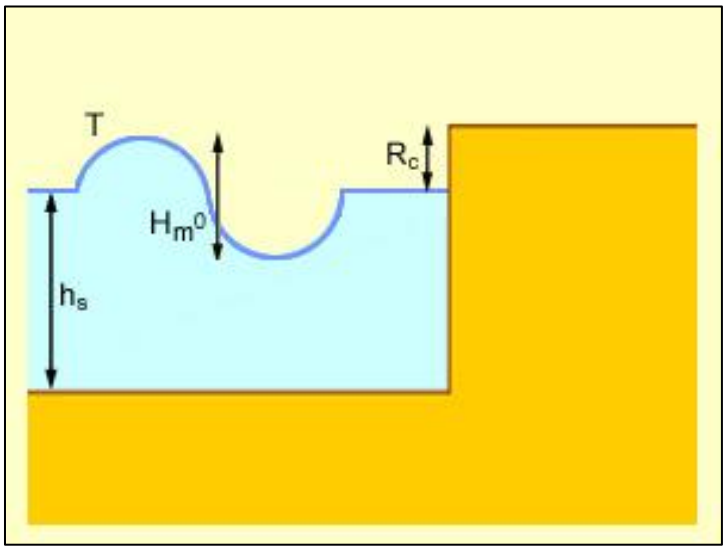

Figure 10: EurOtop calculation tool: schematisation of vertical wall (HR Wallingford, n.d.)

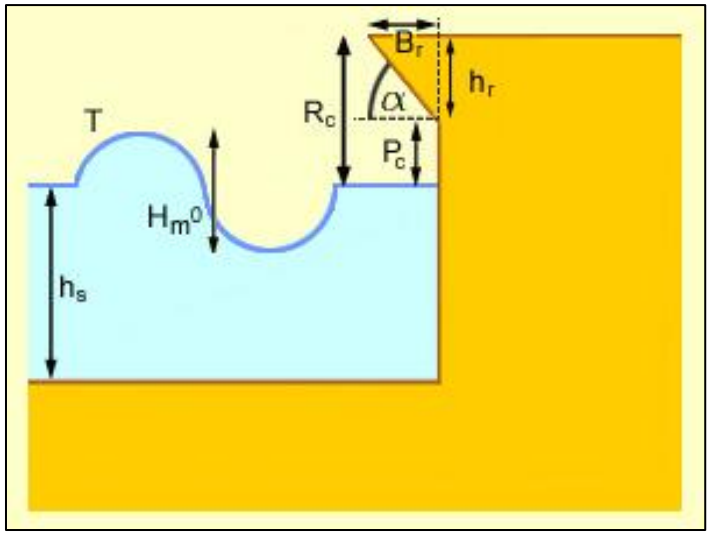

Figure 11: EurOtop calculation tool: schematisation of recurve wall (HR Wallingford, n.d.)

Table 2: Description of symbols used in calculation tool

Symbol	Description	Unit
T	Wave period	s
h_s	Water depth at toe of the structure	m
H_{m0}	Estimate of significant wave height of spectral analysis	m
R_c	Crest freeboard of structure	m
h_r	Height of recurve wall section at top of vertical wall	m
B_r	Width of seaward overhang in front of main vertical wall	m
P_c	Height of vertical wall section from still water-level to bottom of recurve	m
α	Angle of recurve	o

To address model uncertainty, two approaches can be followed with the calculation tool, namely the probabilistic and deterministic approaches. The probabilistic approach implies that if the collected data is normally distributed, about 50% of the collected data points exceed the prediction of the approach, while 50% are under the prediction (EurOtop, 2007).

The deterministic approach is based on a mean overtopping value plus one standard deviation and thus results in higher overtopping rates. The standard deviation is determined by the comparison of model data and model predictions and provides safety in prediction. The deterministic approach is generally a safer approach as it takes the model uncertainty of wave overtopping into account.

The next section presents research on recurve type walls which follows after the CLASH project.

2.3.4 Recent studies

Allsop et al. (2007) presents different solutions to protect buildings and people against wave overtopping for a number of cases in Europe. Within the study, the wave overtopping of two different recurve configurations (both Type 1) with the same crest level were tested under the same conditions. The recurve wall at the shoreline, Figure 12, proved to reduce overtopping by 2 to 9 times, compared with a vertical wall at the same location and with the same crest level. With this recurve, the incoming wave reaches the seawall, fills the recurve and is guided back seawards by the curved shape of the recurve.

However, the recurve wall positioned seawards from the shoreline, Figure 13, only reduces wave overtopping up to 3 times compared with a vertical wall in the same test conditions. The reason for this limited reduction in wave overtopping can be explained by the influence of the vertical toe of the recurve wall. When the incoming wave reaches the vertical toe, the water is projected vertically upwards instead of filling and following the shape of the recurve. Consequently, the beneficial effect of the recurve is lost since it has almost the same performance as a vertical wall (Allsop, et al., 2007).

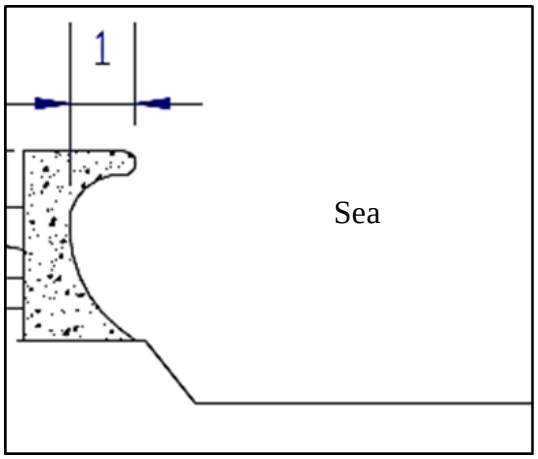

Figure 12: Recurve wall at shoreline

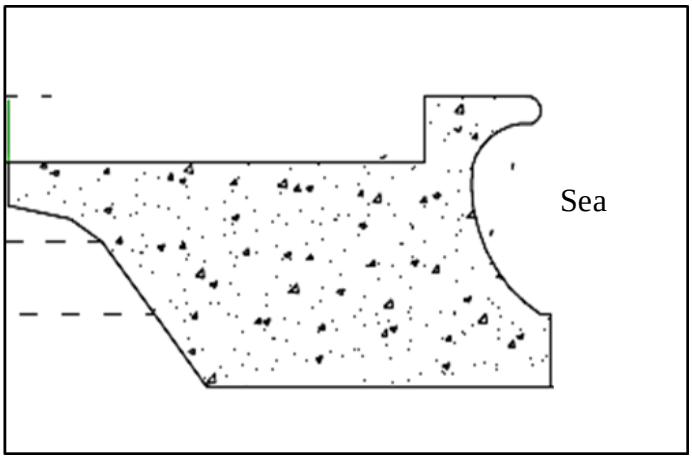

Figure 13: Recurve wall positioned seawards of shoreline

(Allsop, et al., 2007)

Van Doorslaer & De Rouck (2010) investigated the reduction of wave overtopping of a smooth dike by incorporating a wave return wall or parapet (Type 2; Figure 14(a)). The study included only non-breaking waves on smooth dikes. One of the objectives of the study was to determine the optimal geometry of the wave return wall. This objective was achieved by investigating the combined influence of the angle of the wave return wall's nose (β) and the dimensionless height of the wave return wall's nose ($\lambda = h_n/h_t$), Figure 14(b).

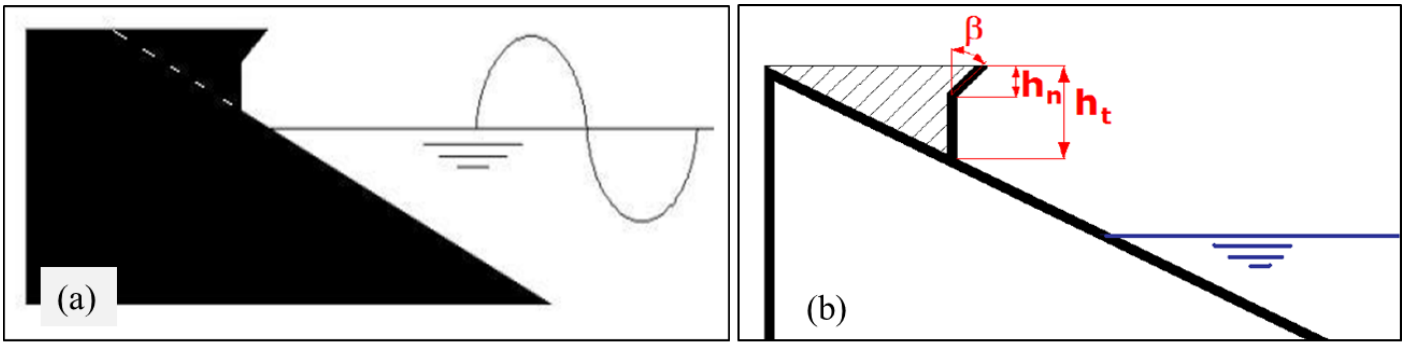

Figure 14: Wave return wall on a smooth dike

(Van Doorslaer & De Rouck, 2010)

A total of 92 wave flume tests with different h_t, β and λ combinations were performed. Table 3 gives the different values for the tested geometry parameters.

Table 3: Values of geometry parameters

h_t (cm)	2, 5, 8
β (°)	15, 30, 45, 60
λ	1/8, 1

The results for h_t = 5cm for the different wave return angles are presented in Figure 15. The smooth dike has a slope of 1:2 and a wall height of 5cm as indicated on the graph by ½ and VW5 respectively (Van Doorslaer & De Rouck, 2010).

Figure 15 shows that the angle of the wave return wall has an influence on overtopping results. It is evident from the results, that the overtopping rate is most reduced with a β of 60°. However, Van Doorslaer & De Rouck (2010) advise that the design of wave return walls include a nose angle (β) of 45° for the ease of construction and to limit wave impact on the nose.

Veale et al. (2012) conducted a study to determine the optimal geometry of wave return walls to be constructed on an existing sea dike at Wenduine, Belgium (Type 2). The crest height of the seawall must be as low as possible to avoid obstruction of the view to the ocean. For this reason, the use of parapet and recurve walls, among others, was considered. The study was supported by physical model flume tests at the Flanders Hydraulics Research laboratory in Antwerp, Belgium.

The wave return wall design for this study was based on the findings and recommendations of Van Doorslaer & De Rouck (2010). A nose angle (β) of 50^{O} was used for the design. Figure 16 shows the response to wave overtopping of three different walls on a sea dike (Veale, et al., 2012). All three wall sections have the same crest levels and the tests were conducted under the same conditions and wave train. The mean overtopping rate (q) from the results of the overtopping tests for each wall section is indicated below each image. The vertical wall with parapet and the recurve wall are both equally effective in reducing overtopping, compared with the vertical wall. The effectiveness can be explained as evident from the images that show the incoming wave reflected back seawards, rather than upwards as for the vertical wall.

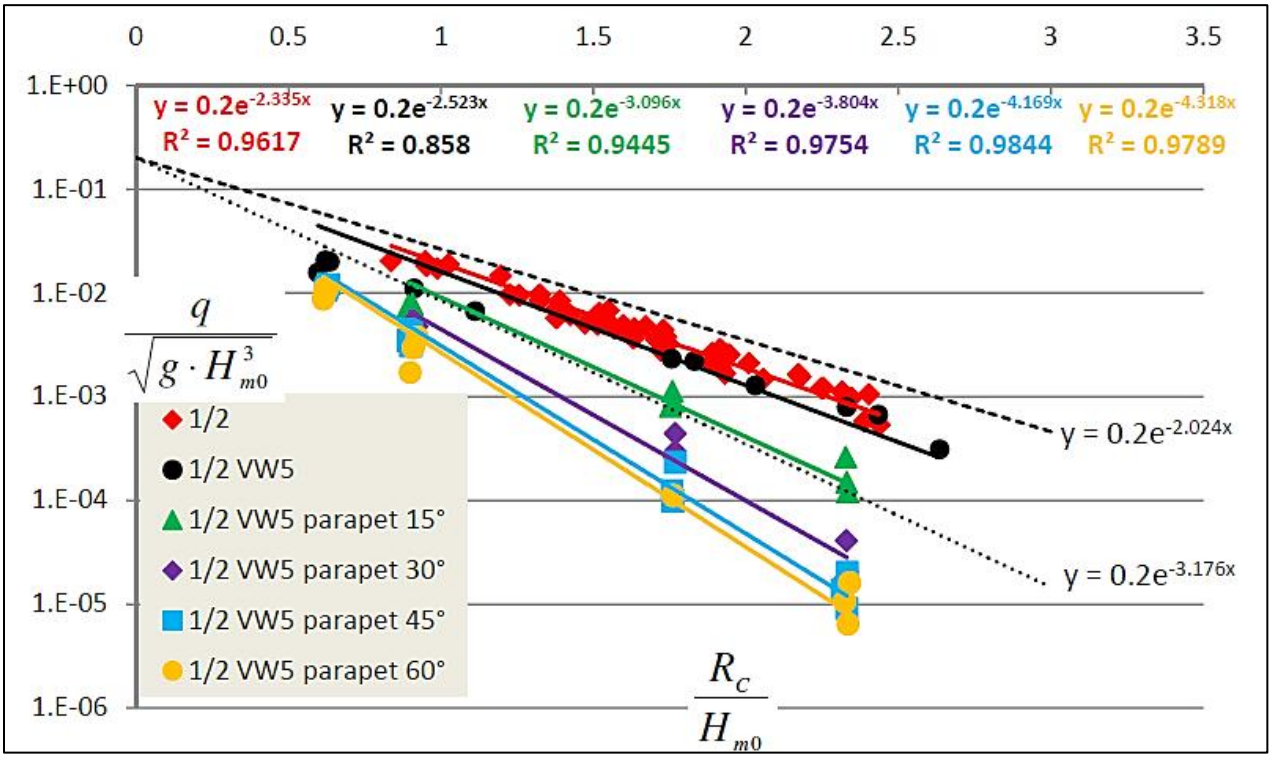

Figure 15: Overtopping results for wave return wall of 5 cm with different parapet angles β (Van Doorslaer & De Rouck, 2010)

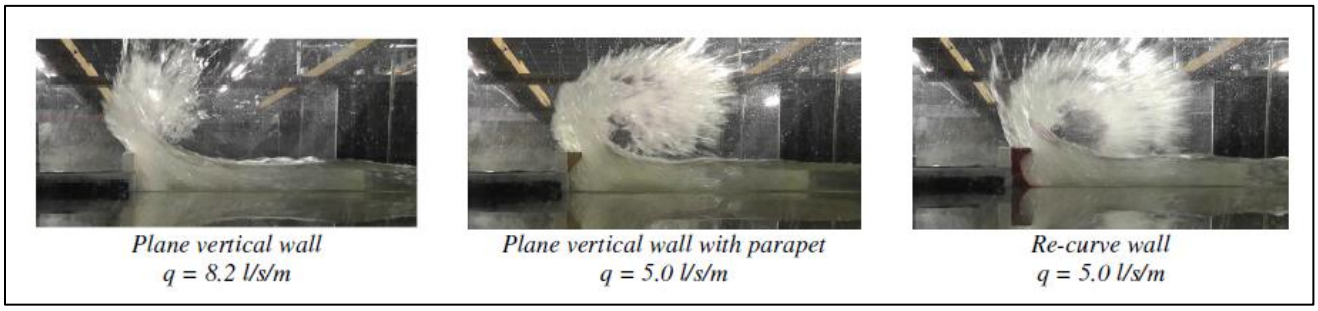

Figure 16: Wave overtopping of vertical seawall, parapet wall and recurve wall

(Veale, et al., 2012)

2.4 Examples of recurve type seawalls

Recurve type seawalls are incorporated into seawall design around the world. The use of recurves in seawall design is common, especially along the coast of England. This section gives a few examples of different types of recurve walls constructed around the world, Figures 17 to 29. Recurves are still regularly used in designs.

Figure 17: Recurve wall in Abu Dhabi, United Arab Emirates

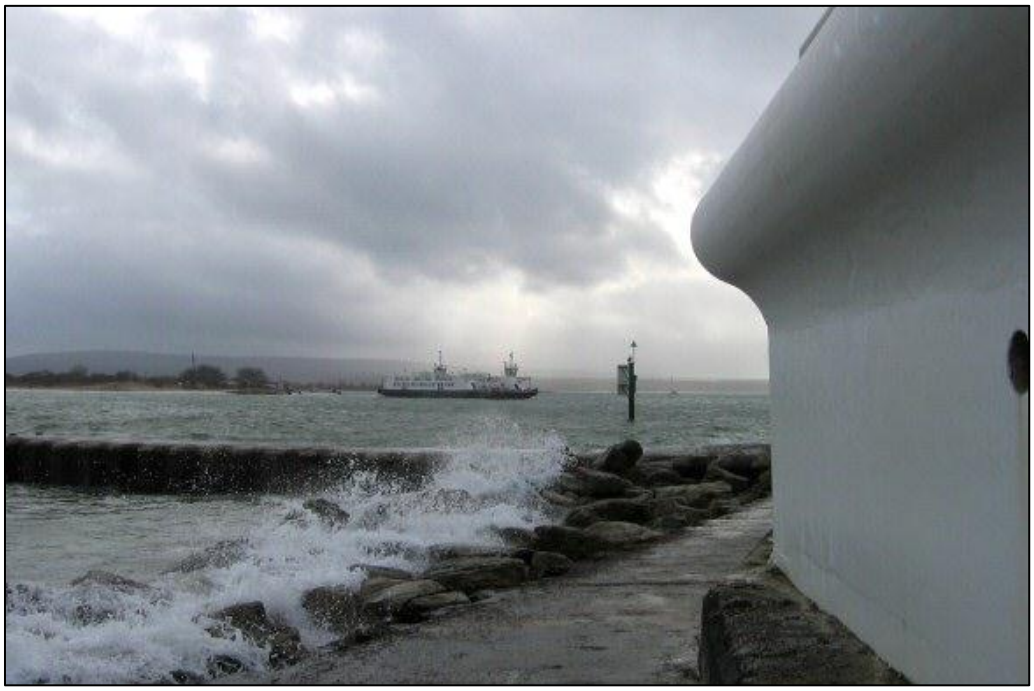

Figure 18: High recurve seawall at Sandbanks Peninsula southwest of Bournemouth, Dorset, United Kingdom

(West, 2013)

Figure 19: Stepped seawall with recurve at Burnham-on-Sea, Somerset, United Kingdom

(Grainger, 2009)

Figure 20: Seawall at St. Mary's Bay, United Kingdom

(Willson, 2008)

Figure 21: Recurve seawall with rock armour at Scarborough, United Kingdom

(Bennett, 2009)

Figure 22: Recurve seawall near Dymchurch, United Kingdom

(PIANC, n.d.)

Figure 23: Recurve seawall at Kailua-Kona, Hawaii

(Hawaii Real Estate, n.d.)

Figure 24: Another recurve type seawall at Kailua-Kona, Hawaii

(West Hawaii Today, 2013)

Figure 25: Recurve seawall at Ocean Beach, San Francisco, CA, USA

(Noble Consultants, Inc., 2011)

Figure 26: Construction of the Flaring Shaped Seawall (FSS) in Kurahashi-jima, Hiroshima, Japan (Kamikubo, n.d.)

Figure 27: FSS at Kurahashi-jima, Hiroshima, Japan (Kamikubo, n.d.)

Figure 28: Recurve wall in Cape Town, South Africa

Figure 29: Damaged recurve wall in Strand, South Africa

Physical model tests are a cost-effective way to evaluate wave overtopping before building a structure. The next section focuses on the scale and laboratory effects that occur with physical model tests and describes how wave overtopping is measured on a small scale.

2.5 Physical modelling in wave overtopping studies

2.5.1 Scale and laboratory effects

When performing physical model tests, processes take place naturally without the simplifying assumptions that are necessary for analytical or numerical models. As physical model tests are performed on a smaller scale, data collection is much less expensive than field data collection (Hughes, 1995).

However, physical model testing has certain implications: scale and laboratory effects. Scale effects occur due to the inability to scale all relevant forces acting within the model correctly. Laboratory effects are the result of the inability to simulate all prototype conditions in the model, for example, wind (Hughes, 1995).

Schüttrumpf & Oumeraci (2005) researched the scale and laboratory effects in crest level design. The results of physical model tests are influenced by scale and laboratory effects. In order to produce accurate results, a physical model must therefore be carefully set up to ensure the minimisation of scale and laboratory effects. This study found that scale effects for wave overtopping affect mostly low overtopping rates as a result of surface tension and viscosity (Schüttrumpf & Oumeraci, 2005).

For wave overtopping, gravitational forces play the largest role, leading to the use of the Froude similitude law. A Froude model neglects friction, viscosity and surface tension. According to Hughes (1995) a scale ratio is defined as: "the ratio of a parameter of the prototype to the value of the same parameter of the model." Symbolically, the scale ratio (N_X) is presented as follows:

$$N_X = \frac{X_p}{X_m} = \frac{Value\ of\ X\ in\ prototype}{Value\ of\ X\ in\ model} \qquad \text{(Hughes, 1995)}$$

Table 4 presents the scale ratios used for the scaling of parameters in physical models when applying the Froude law.

Table 4: Scale ratios of the Froude law

Characteristic	Dimension	Froude
Geometric		
Length	$[L]$	N_L
Area	$[L^2]$	$N_L{}^2$
Volume	$[L^3]$	$N_L{}^3$
Kinematic		
Time	$[T]$	$N_L^{1/2} N_\rho^{1/2} N_\gamma^{-1/2}$
Velocity	$[LT^{-1}]$	$N_L^{1/2} N_\rho^{-1/2} N_\gamma^{1/2}$
Acceleration	$[LT^{-2}]$	$N_\gamma N_\rho^{-1}$
Discharge	$[L^3T^{-1}]$	$N_L^{5/2} N_\rho^{-1/2} N_\gamma^{1/2}$
Kinematic Viscosity	$[L^2T^{-1}]$	$N_L^{3/2} N_\rho^{-1/2} N_\gamma^{1/2}$
Dynamic		
Mass	$[M]$	$N_L^3 N_\rho$
Force	$[MLT^{-2}]$	$N_L^3 N_\gamma$
Mass Density	$[ML^{-3}]$	N_ρ
Specific Weight	$[ML^{-2}T^{-2}]$	N_γ
Dynamic Viscosity	$[ML^{-1}T^{-1}]$	$N_L^{3/2} N_\rho^{1/2} N_\gamma^{1/2}$
Surface Tension	$[MT^{-2}]$	$N_L^2 N_\gamma$
Volume Elasticity	$[ML^{-1}T^{-2}]$	$N_L N_\gamma$
Pressure and Stress	$[ML^{-1}T^{-2}]$	$N_L N_\gamma$
Momentum, Impulse	$[MLT^{-1}]$	$N_L^{7/2} N_\rho^{1/2} N_\gamma^{1/2}$
Energy, Work	$[ML^2T^{-2}]$	$N_L^4 N_\gamma$
Power	$[ML^2T^{-3}]$	$N_L^{7/2} N_\rho^{-1/2} N_\gamma^{3/2}$

(Hughes, 1995)

For normal test conditions, where the Weber number is between 30 and 3000, the influence of surface tension is negligible. The Weber number (We) is defined as $We = \frac{(v_A h_A \rho_W)}{\sigma 0}$, where υ_A = the wave run-up velocity at still water-level, σ_0 = surface tension, ρ_W = density of the fluid and h_A = layer thickness at still water-level (Schüttrumpf & Oumeraci, 2005).

Viscosity affects model results when the overtopping Reynolds number is below 10^3 (Schüttrumpf & Oumeraci, 2005). The higher viscosity will cause lower overtopping rates and higher friction. The overtopping Reynolds number under 10^3, as defined below, occurs for freeboard heights close to the wave run-up height, which is the case for small overtopping rates (Schüttrumpf & Oumeraci, 2005).

$$Re_q = \frac{2(R - R_C)^2}{vT}$$

Where R = wave run-up height, R_C = characteristic wave run-up height, υ= characteristic velocity and T = characteristic wave period.

The effect of viscosity and surface tension is reduced to acceptably low levels when using a large scale with the Froude law under normal test conditions.

According to Hughes (1995) laboratory effects in short-wave physical models are mainly due to:

- The physical constraints of boundaries on the water flow
- The occurrence of unintentional nonlinear effects because of the mechanical generation of waves
- The simplification of prototype forcing conditions; for instance, representing prototype wave conditions as unidirectional

When using a two-dimensional wave flume, as in this project, cross-waves frequently develop when energetic wave conditions are being generated by a mechanical wave paddle. As mentioned above, the mechanical wave generation can also create unwanted nonlinear effects. Nonlinear effects can be higher harmonics in finite-amplitude regular waves or spurious long waves (Hughes, 1995).

A boundary effect for wave flumes can occur from re-reflecting waves from the wave paddle. This happens as waves reflect from a structure, travel back to the wave paddle and are again reflected towards the model structure. In nature, reflected waves from a structure will continue to travel into the

ocean and will not be a constraint. This laboratory effect can be eliminated if active wave absorption is implemented at the wave paddle by absorbing unwanted reflected wave energy (Hughes, 1995).

Pearson et al. (2002) investigated wave overtopping of battered seawalls, Figure 30, by measuring overtopping discharges for large and small scale physical model tests.

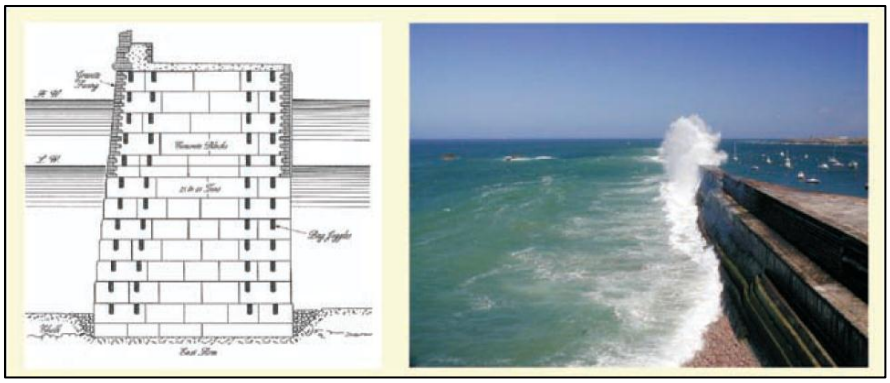

Figure 30: Typical cross-section of battered seawall

(EurOtop, 2007)

According to Pearson et al. (2002), the most common laboratory effects are the absence of wind and the use of fresh water instead of seawater. Wind has very little influence during heavy overtopping, although wind effects will be more important for small discharges. Even though fresh water is used instead of sea water, there is no evidence that this model effect influences wave overtopping (Pearson, et al., 2002).

Comparing the measurements of large and small scale physical model tests, the results from the study suggest that scale effects are not significant for mean or peak overtopping volumes under impulsive wave conditions for battered seawalls. The results suggest that scale effects are likely to be minimal for pulsating waves (Pearson, et al., 2002).

Pearson et al. (2002) also found that the prediction methods of Besley (1999) may be used for mean overtopping discharges under conditions of significant or dominant impulsive waves at battered walls. The mean overtopping is well-predicted without any significant scale effects.

The European Commission OPTICREST project found that wave run-up on rough slopes has been underestimated in small scale physical model tests due to scale or laboratory effects. Therefore the same effects are expected to influence wave overtopping model results because part of the run-up

overtops the seawall. One of the main objectives of the CLASH project is to solve the problem of suspected scale and laboratory effects for wave overtopping (De Rouck, et al., 2005).

The objective of the CLASH study was achieved by comparing wave overtopping measurements at three different coastal sites with the measurements of scale models of the sites. The three sites are as follows:

- Rubble-mound breakwater armoured with flattened Antifer cubes (Zeebrugge, Belgium)
- Rock armoured rubble-mound breakwater in shallow water (Ostia, Italy; Figure 31)
- Vertical seawall with rubble-mound toe protection (Samphire Hoe, United Kingdom)

Figure 31: Full scale test at Ostia, Italy

(De Rouck, et al., 2005)

The three prototype sites were modelled in at least two different laboratories. The wave overtopping results of the models were compared with the prototype results in order to develop new guidance on possible scale and laboratory effects (De Rouck, et al., 2005).

The CLASH project concluded that prototype and laboratory wave overtopping measurements, as well as empirically predicted wave overtopping rates for vertical walls are in close proximity. Differences in measurements and predictions can be ascribed to laboratory effects due to the absence of wind in the

wave flume. De Rouck et al. developed a generic method for adjusting measured overtopping results for wind effects. This generic method was developed by comparing measured overtopping data with and without wind (De Rouck, et al., 2005).

A study by Pullen et al. (2008) investigated field and laboratory measurements of mean overtopping discharges. The study provided a detailed description of the field study methodologies and of the two corresponding physical model tests performed within the CLASH project for the vertical seawall at Samphire Hoe (Southampton, UK).

The results confirm that no scale effects have to be considered for wave overtopping discharges of vertical or near-vertical seawalls. It was found that the absence of wind causes laboratory effects for wave overtopping measurements. Wind increases the discharge in instances of low overtopping discharge, but its effect is negligible with much higher discharges (Pullen, et al., 2008).

2.5.2 Wave overtopping laboratory measurement methods

In an early study, Owen and Steele (1991) measured overtopping in a set of five overtopping intervals, where overtopping discharges were collected in a calibrated tank. A float monitors the difference in water-level in the tank. Overtopping volumes and rates can be calculated from the water-level difference.

In a study by Franco et al. (1994), wave overtopping was measured by a tray suspended through a load cell to a supporting beam, Figure 32. The load cell takes a signal reading after every overtopping wave. This enables the measurement of the individual volume for every overtopping event and the number of overtopping waves. The mean discharge for each test can be easily calculated from these measurements. In this study long test durations with no less than 1000 waves were performed in order to increase the statistical validity of the average overtopping measurements.

The accuracy of the overtopping measurement system was tested before the model tests were undertaken (Franco, et al., 1994). This was done by directing known volumes of water into the measurement container. Data from the load cell were then fed into an algorithm to determine and quantify individual overtopping events (Franco, et al., 1994).

In Pearson et al. (2002) overtopping was measured by directing the overtopping discharges with a chute from the seawall to a measuring container suspended from a load cell. Separate overtopping events

were detected by two parallel strips of metal tape which run along the crest of the structure. These strips function as a switch closed by the water. With the measurement of wave-by-wave overtopping volumes, the additional mass of water in the overtopping tank was measured after every overtopping event (Pearson, et al., 2002).

Pearson et al. (2002) attempts to reduce possible uncertainties in determining incident and inshore wave conditions. These measurements were taken by a wave gauge put in the same location where the structure for the model test would be erected. The flumes were equipped with active wave absorption systems to remove reflected waves from the seawall during overtopping tests.

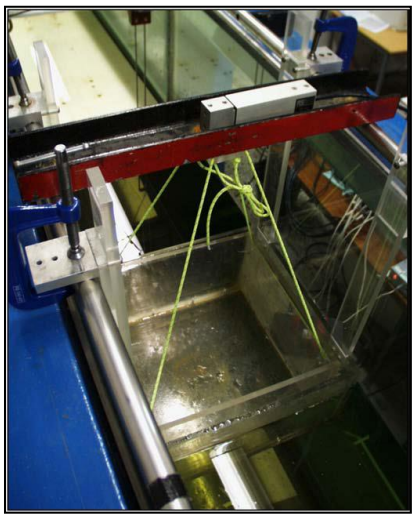

Figure 32: Overtopping tank suspended from load cell

(Pullen, et al., 2008)

2.5.3 Test duration

A study by Reis et al. (2008) investigated the influence of test duration in the modelling of wave overtopping. The number of waves in physical model tests is important for studies of wave overtopping. The correct balance between the total duration of the model tests and the required accuracy of the measurements has to be achieved. A total of 87 physical model tests were performed with different test durations.

The results of the study indicate that the convergence of the mean wave overtopping discharge to a constant value is not clear. However, the variability in the measured values of the mean overtopping discharge decrease in general with an increasing number of waves ranging between 1100 to about 1400 waves. Further reduction of the variability was small for more waves.

Measurements obtained from a single test give little indication of the expected wave overtopping discharge, because the mean overtopping discharge varies from test to test even if the test is performed under the same conditions. For this reason, Reis et al. (2008) recommends that several tests of the same short duration should be undertaken rather than one test with a very long duration. It is particularly important to undertake several short tests when active wave absorption is absent or inefficient, in order to avoid re-reflections by the wave paddle.

According to Reis et al. (2008), a small difference in wave height of the largest waves within a wave train, could have a large impact on the mean overtopping discharge. Small overtopping rates and short test durations are especially affected by such differences in wave heights. For this reason it is important to evaluate the maximum wave heights and not only the significant wave height.

2.5.4 Wave spectra

JONSWAP (Joint North Sea Wave Project) spectrum waves were mainly generated in the studies discussed and are typical for the North Sea and the South African coast (Rossouw, 1989). The JONSWAP spectrum is an extension of the single-parameter Pierson-Moskowitz (PM) spectrum for a fully developed sea. The JONSWAP spectrum represents a fetch-limited sea-state or in other words, a growing sea, and has a sharper peak than the PM spectrum. The JONSWAP spectrum is expressed as shown in Figure 33.

Figure 34 gives the symbol definition and the comparison of the JONSWAP spectrum and the PM spectrum (U.S. Army Corps of Engineers, 2001).

$$E(f) = \frac{\alpha g^2}{(2\pi)^4 f^5} \exp\left[-1.25\left(\frac{f}{f_p}\right)^{-4}\right]\gamma^{\exp\left[-\frac{\left(\frac{f}{f_p}-1\right)^2}{2\sigma^2}\right]}$$

$$f_p = 3.5\left[\frac{g^2F}{U_{10}^3}\right]^{-0.33} \quad ; \quad \alpha = 0.076\left[\frac{gF}{U_{10}^2}\right]^{-0.22} \quad ; \quad 1 \le \gamma \le 7$$

$$\sigma = 0.07 \quad for\ f \le f_p \quad and \quad \sigma = 0.09 \quad for \quad f > f_p$$

Figure 33: JONSWAP spectrum

(U.S. Army Corps of Engineers, 2001)

Where α = equilibrium coefficient

σ = dimensionless spectral width parameter,

with value 0.07 for $f \leq fp$ and value 0.09 for $f > fp$

γ = peak enhancement factor

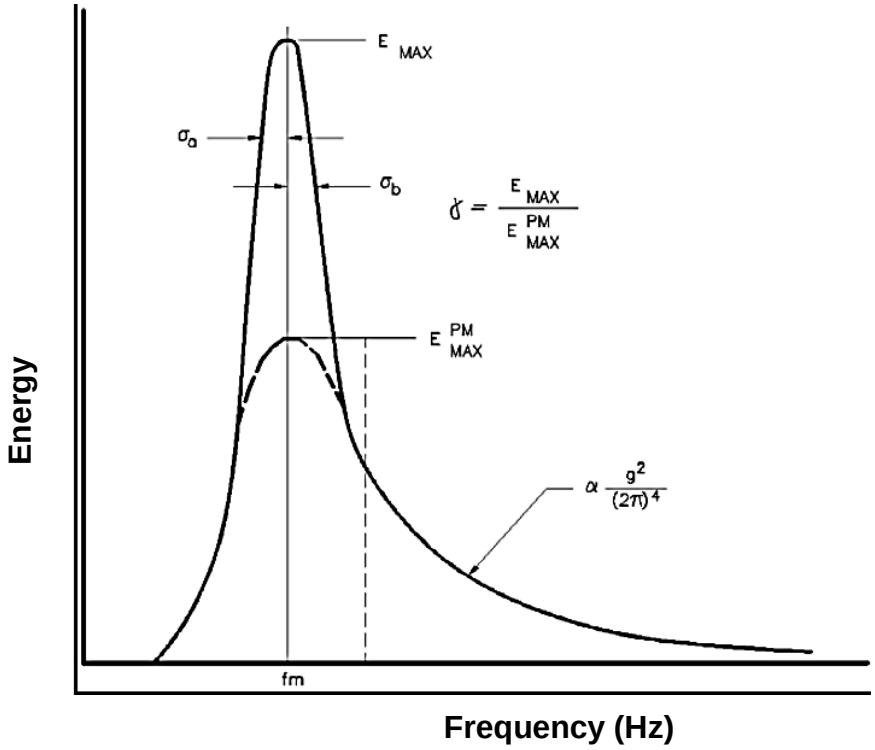

Figure 34: Comparison of the JONSWAP and Pierson-Moskowitz spectra

(U.S. Army Corps of Engineers, 2001)

2.6 Conclusions

Berkeley-Thorn and Roberts (1981) proposed a recurve profile which was used in several studies. Besley (1999) claims that this recurve profile proves to be very effective and that other profiles may be found to be significantly less effective.

Kamikubo (2000 & 2003) investigated the use of a deep, circular cross-section, namely the Flaring Shaped Seawall (FSS). The non-overtopping FSS has a significantly lower crest height compared with

a conventional wave absorbing vertical seawall. Although Kortenhaus et al. (2003) suggest that the profile of the FSS will be difficult to form with reinforced concrete; a FSS has been built in Japan.

Within the framework of the CLASH project, two studies were undertaken to formulate generic guidance for recurve walls. A generic method for the prediction of the reduction in overtopping of recurve walls was proposed in Kortenhaus et al. (2003). However, the test results presented a scatter for large reductions in overtopping. Pearson et al. (2004) proposed a method to reduce the scatter in test results. The outcome is a decision chart to give design guidance for recurve walls.

From all the wave-overtopping studies investigated, it can be concluded that scale effects have little influence on wave overtopping of vertical seawalls, provided the scale is large enough to reduce the effect of viscosity and surface tension to acceptably low levels. Laboratory effects also play a small role, although the failure to include wind in modelling plays a role in certain cases. Reis et al. (2008) suggest that tests should be repeated, as the mean overtopping rates vary from test to test, even if performed under the same conditions. The number of waves per test and the largest wave heights in the wave train are also very important.

Design guidance on the shape of recurve walls is based on limited research and no systematic studies were performed to test the influence of the recurve seawall overhang length in reducing overtopping. Consequently, this project investigates the influence of the length of the overhang of the recurve wall on wave overtopping discharges.

Chapter 3: Physical model tests

3.1 Scope of model tests

The main objective of the physical model tests is to determine the influence of the overhang length of a recurve wall on wave overtopping. To achieve this objective, physical model tests were performed with three different seawall profiles under the same marine conditions, i.e. water-level, input wave height and period. The overtopping is measured for each seawall profile to compare the influence of the length of a seaward overhang on overtopping rates.

The seawall profile shapes were as follows (model dimensions of overhang B_r given):

- Vertical wall (B_r = 0 mm)
- Recurve 1 with small overhang (B_r = 30 mm)
- Recurve 2 with large overhang (B_r = 60 mm)

Figure 35 displays the three different seawall profiles with model dimensions. As a result of the varying overhang length B_r and the fixed overhang height at the wall h_r (50 mm), the angle of the overhang also changes. However, all other dimensions remain constant.

The bed slopes and wall height within the flume were kept unchanged in all the physical model tests. Other test conditions are discussed in Section 3.8.

The effect of wind was not included in the scope of this project; consequently, only “green water overtopping” and “splash water overtopping” were measured in this model tests.

3.2 Test facility

All physical model tests were performed in a 2D glass flume at the Hydraulic Laboratory of the Civil Engineering Department of the University of Stellenbosch. The flume is 30 m long, 1 m wide and has a maximum operational depth of 0.8 m. Waves are generated with a piston type wave paddle from Hydraulic Research Wallingford (HR Wallingford), which is capable of generating regular and irregular waves. The wave paddle is equipped with dynamic wave absorption, which absorbs the reflected waves returning from the seawall.

Waves were measured with four resistance probes. The voltage signals, recorded by the wave probes, were captured by a connected computer. HR DAQ, a data acquisition and analysis software package

developed by HR Wallingford, analysed the volt signals to convert them to water-level readings in metres. Resistance wave probes are very sensitive to changes in properties, such as water temperature and water quality. For this reason, the wave probes were calibrated before every test.

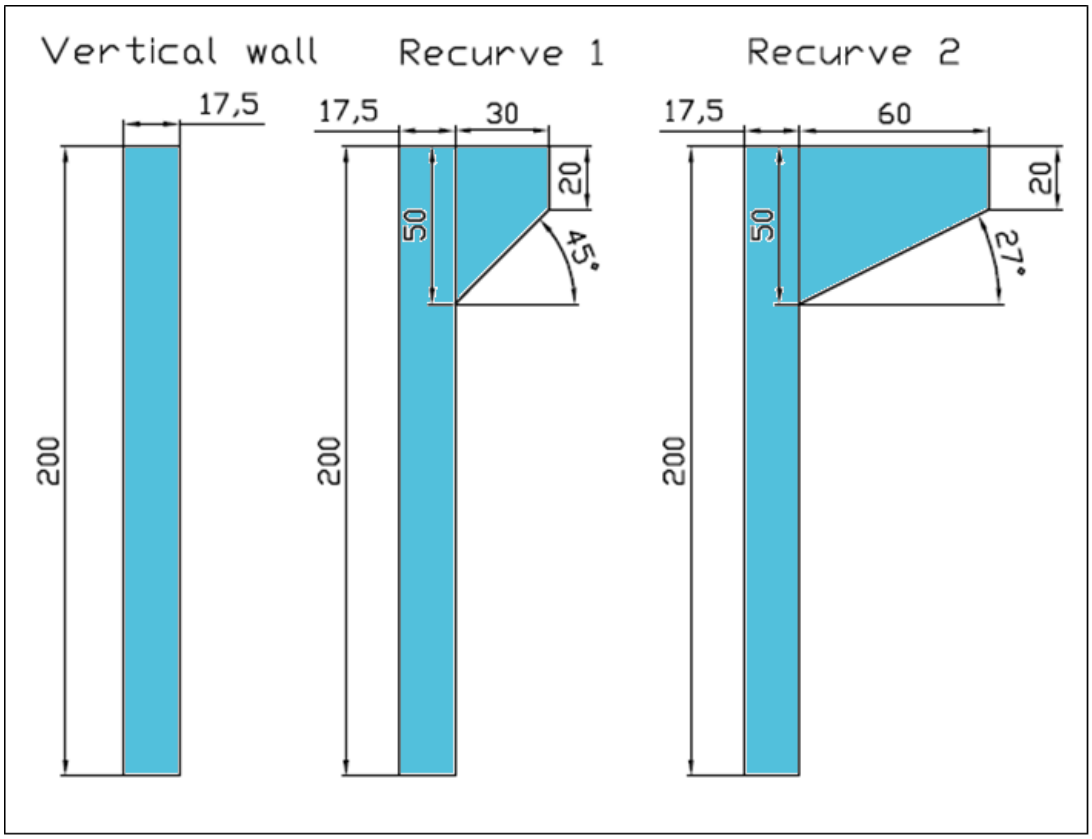

Figure 35: Seawall profiles with 3 different overhang lengths (model dimensions in mm)

3.3 Model set-up

As already mentioned, the built-in bed within the flume was kept unchanged throughout all the physical model tests. The flume had an average nearshore slope of 1:50. An additional upper beach slope of approximately 1:20 was built-in for this project immediately before the seawall to resemble a typical South African beach. The 1:20 beach was selected as an average slope after considering a few locations along the South African coast, Table 5. The mean slopes presented in the table are calculated between -1 m MSL (Mean Sea-Level) and +1m MSL.

Measurements show that the built-in slope in fact has an average of 1:18.6. Figure 36 shows a schematisation of the built-in slopes before the seawall. It was also noted that the built-in slope was not

precisely level from side to side but also had a sideways slope as is evident in Figure 37. The blue line in the figure indicates the water-level across the flume. However, these inaccuracies in the bed slope were found to have an insignificant effect on the measured overtopping rates in the project.

The detailed long section of the flume bed (including the additional 1:18.6 beach slope) is presented in Appendix A.

Table 5: Typical beach slopes along the South African coast

Location	**Slope (-1 m to +1 m MSL)**	**Source**
False Bay	1: 16.5	(WNNR, 1983)
Richards bay	1: 42.0	(Schoonees, et al., 2008)
Groot brak/Glentana	1: 32.0	(WSP Africa Coastal Engineers, 2012)
Saldanha	1: 11.5	(Schoonees & Theron, 2003)
Table bay	1: 41.5	(Soltau, 2009)
Average	**1: 22**	

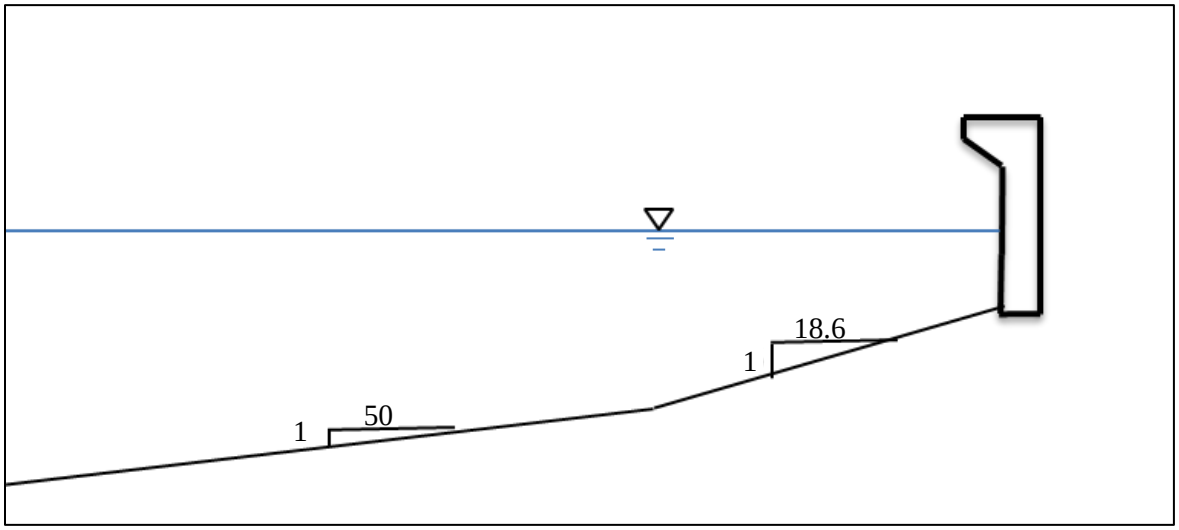

Figure 36: Recurve structure with bed slopes

The seawall was built-in at a distance of 28 m from the wave paddle and stretched across the entire width of the flume.

The three different seawall profiles were made of marine plywood and painted to protect the wood from swelling. The vertical wall formed the base structure for each seawall profile. For the recurve profiles, the overhang was bolted onto the vertical wall. This ensured that all the structures were in exactly the same location. It also ensured time efficiency when changing the seawalls. The seawall profiles were sealed off with a silicon base material in order to keep the water within the flume from seeping around the ends of the structure. Figure 38 shows the sealed off Recurve 2 profile, viewed through the flume glass side-wall. The blue section of the seawall profile is bolted onto the vertical wall.

The overtopping was measured by collecting the overtopped water in a metal container, which was located behind the structure in the flume, Figure 39. A sheet of waterproof plastic was spanned with a slope to guide all overtopped water into the metal container, Figure 40. When the container was full, the water was pumped into bin(s) on the outside of the flume to be weighed with a scale capable of an accuracy of ±20 grams, Figure 41. Since model tests were performed with fresh water, the density of the water was assumed to be 1000 kg/m^3.

The water could be pumped out of the metal container only to a certain water-level, leaving the metal container with a remaining water-level. For this reason the metal container had a starting water-level before the test, indicated with a measuring needle. After each test the water was pumped out of the overtopping container to the same water-level indicated by the needle. Figure 42 shows the measuring needle and pump in the overtopping container.

Water was pumped into the flume behind the wave paddle to minimise the effect on wave generation while maintaining a consistent water-level within the flume. With breaking waves, water splashes high, causing some water to spill over the sides of the flume. Plates were therefore attached to the sides of the flume to prevent the water from splashing over the side of the flume, Figure 43.

Readings from the wave probes were taken and processed by the HR DAQ software on a connected computer. The required spacing of the probes was determined using the HR DAQ software calculation tool, which applies a least square method (Mansard & Funke, 1980). This is done by entering the distance between each probe and calculating the allowable frequency range of the wave. Figure 44 shows an example of how the allowable frequency range of the waves (0.202 to 1.195 Hz) was calculated with the HR DAQ software for this project.

Figure 45 presents the probe spacing used in all physical model tests, with probe 1 closest to the wave generator. The distance of the probe closest to the structure was determined by one wavelength from the structure, in order to prevent wave breaking from compromising the probe readings. The software requires four probes to perform a reflection analysis. With the reflection analysis the incident wave height was determined from the measured recordings.

As only four probes were available for use during this project, it was deemed best to measure the waves as close as possible to the structure, rather than to measure the deep water waves.

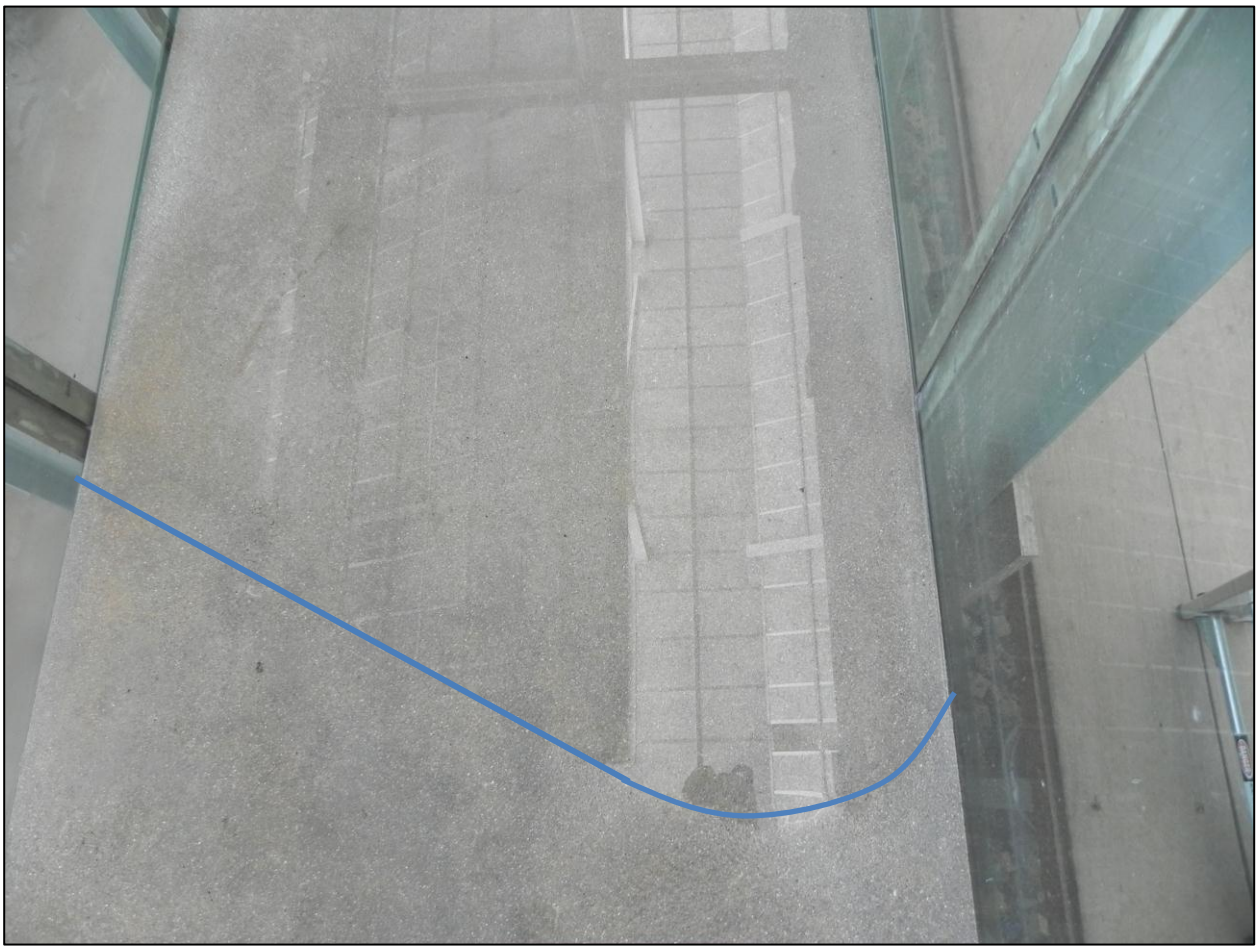

Figure 37: Irregularities in built-in slope

Figure 38: Recurve 2 profile

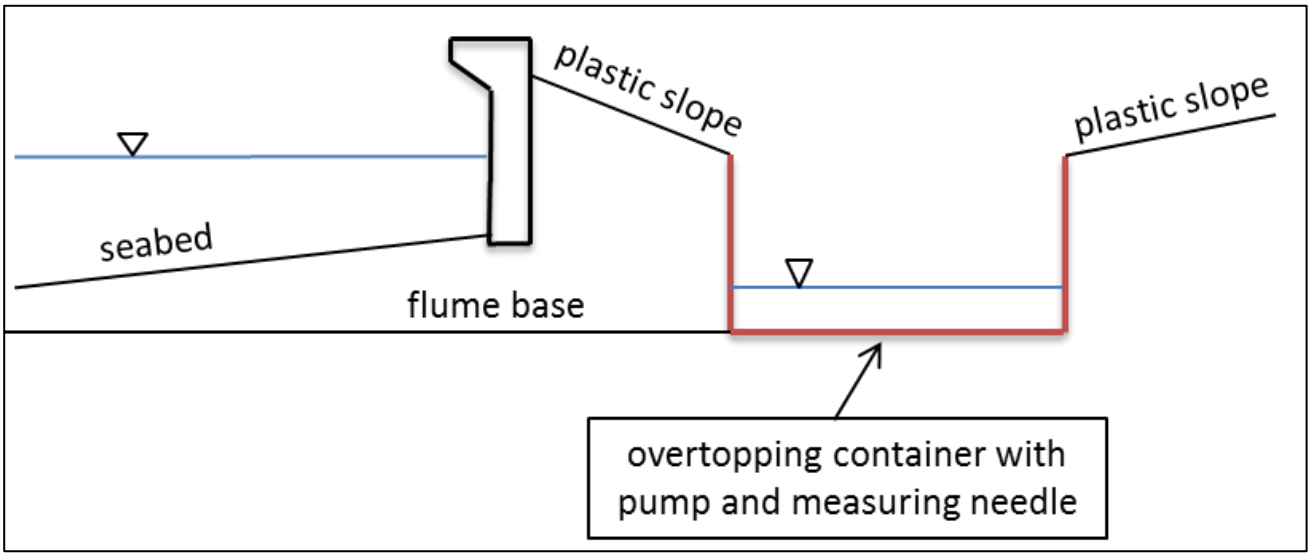

Figure 39: Schematisation of layout behind the structure to collect overtopped water

Figure 40: Waterproof plastic to guide water into overtopping container

Figure 41: Weighed bin outside the flume

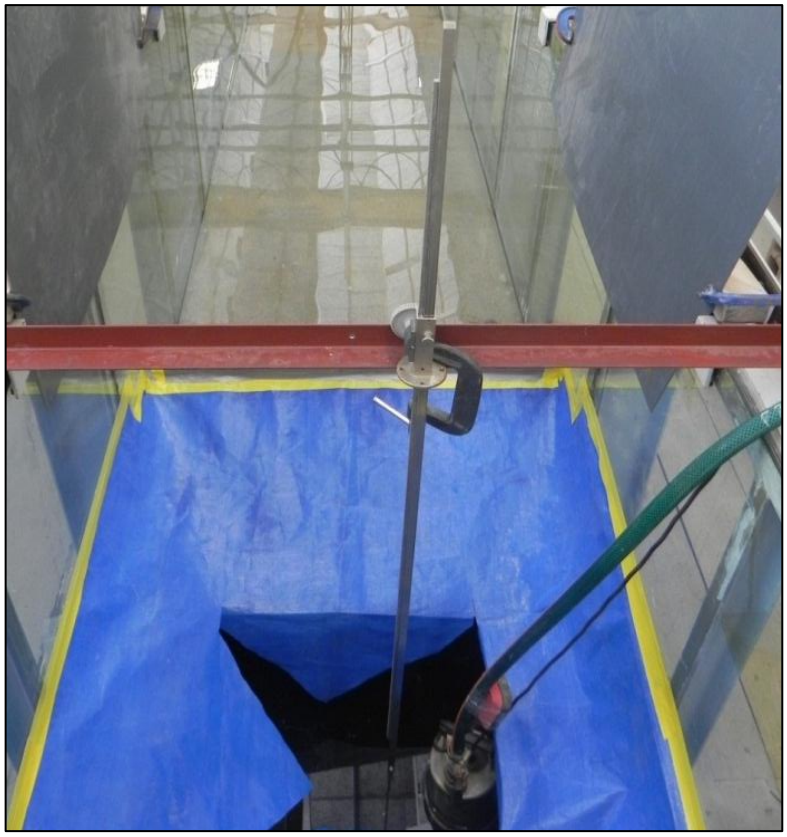

Figure 42: Measuring needle and pump in overtopping container

Figure 43: Sheets to prevent water from splashing out of the flume

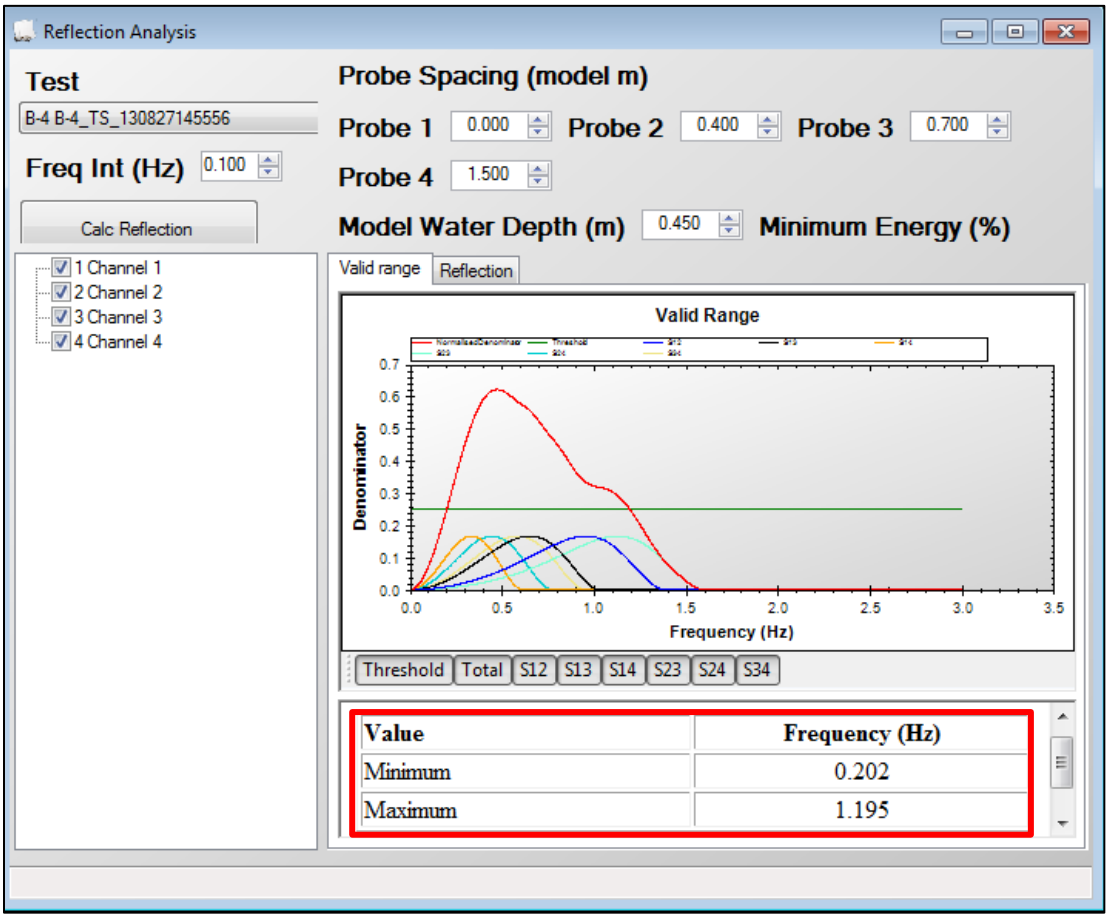

Figure 44: Calculating the allowable frequency range in HR DAQ

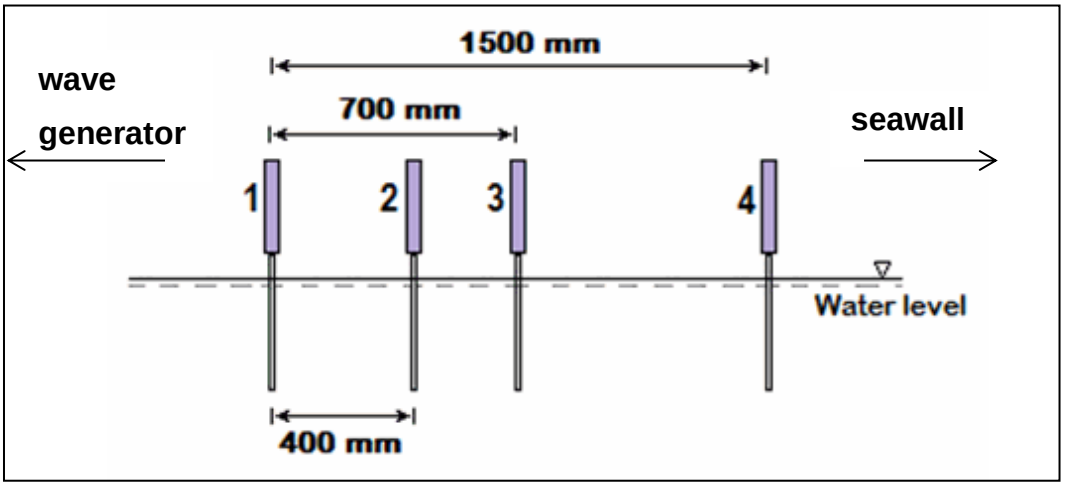

Figure 45: Probe spacing

3.4 Model scale

Physical model tests were performed at a large scale of 1:20 to minimise scale effects. The scale was selected based on the height of the structure, the capacity (performance) of the wave paddle and the difference between water-levels to simulate a realistic tidal range between the lowest and the highest water-level. The Froude similitude scale law was used as described in Section 2.5.1. Table 6 shows a summary of the scales used for this project.

Table 6: Applicable scale used

Scale type	Parameter	Froude scale
Linear scale	Water depth, wavelength, wave height, wall heights	1:20
Time scale	Wave period, test duration	$1:\sqrt{20} = 1: 4.472\ldots$
Mass scale	Mass of overtopped water	$1:20^3 = 1: 8000$

3.5 Test procedure

When the water in the flume remains stagnant for some time, the water can get stratified as the temperature in the upper layer is different from the lower layer. These temperature changes can have an influence on the wave probe readings. Consequently, before a test was performed, the water was stirred by generating a few waves (duration of approximately 100 seconds) to mix the stratified water.

After the water has been mixed, the water-level has to settle and become calm again before the probes can be calibrated. The probes are very sensitive to temperature changes and were therefore calibrated before every test by collecting readings at three different levels.

The measuring needle was set to indicate the starting water-level within the overtopping container before every test. The overtopping water was measured by weighing all water entering the overtopping container during the test duration. The overtopped water was pumped into a bin on the outside of the flume until the water-level in the overtopping container reached the starting water-level. As the overtopping container filled up, the same quantity of water was pumped into the flume at the back of the wave paddle to ensure a constant water-level during the entire test.

3.6 Test duration

The duration of each test was based on a time series that contained at least a 1000 waves, defined by $1000T_p$, where T_p is the peak wave period. Since the test duration was based on the peak wave period, the time series in fact contained more than a 1000 waves. This test duration was selected to improve the statistical validity and to acquire reliable average wave overtopping discharges (Franco, et al., 1994).

3.7 Data acquisition

Three main sets of measurements were recorded for every model test: the overtopping rate, the incident wave height and the wave period. The overtopping rate was measured by weighing the overtopped water.

Wave probe readings were recorded and analysed with the HR DAQ software. The post processing included a spectral analysis and the identification of wave statistics by the zero upward-crossing method. Since the recorded probe readings included both the incident (H_i) and reflected wave height (H_r) recordings, a reflection analysis was required to separate the two wave types. Only the incident waves are important for the analysis of results in this project.

The incident wave height, H_i, is dependent on the bulk reflection coefficient (K_r) and the significant wave height from spectral analysis, H_{m0}. A reflection analysis was performed with the HR DAQ reflection calculator to determine the bulk reflection coefficient. As an H_{m0} was recorded for each probe, an average of all four wave probes was taken as H_{m0} for the calculation of the incident wave height. The following calculations show how the equation for calculating the incident wave heights was derived:

$$H_{m0}{}^2 = H_i{}^2 + H_r{}^2 \quad \text{(Mansard \& Funke, 1980)}$$

$$H_{m0} = \sqrt{(H_i{}^2 + H_r{}^2)}$$

$$H_{m0} = \sqrt{(H_i{}^2 + K_r{}^2 H_i{}^2}$$

$$H_{m0} = H_i\sqrt{(1 + K_r{}^2)}$$

$$\therefore H_i = H_{m0} / \sqrt{(1 + K_r{}^2)}$$

3.8 Test conditions and schedule

The test conditions were selected based on typical values for the case of a seawall at the back of a beach in South Africa. Irregular waves with a JONSWAP spectrum were generated for this project. In the North Sea the JONSWAP wave spectrum has an average enhancement factor of ɣ= 3.3. This average enhancement factor is used in most overtopping studies. In South Africa the peak enhancement factor varies between 1 and 6 with an average peak enhancement factor of ɣ= 2.2 and a standard deviation of 1 (Rossouw, 1989). For this project a peak enhancement factor of ɣ= 3.3 was selected, as it lies within the range of peak enhancement factors for the South African coast and results for this study can be compared to the results of other overtopping studies (which mostly use ɣ= 3.3).

Table 7 shows all the test conditions within the scope of the performed physical model tests. For every seawall profile, tests were performed at five different water-levels. To include both breaking and non-breaking waves in this project, the water-levels were selected to represent two cases of breaking waves (1.0 m and 0.6 m) and three non-breaking cases (2.4 m, 2.0 m and 1.6 m). A prototype significant wave height of 1m (the wave height specified to the wave maker) and wave peak period (Tp) of 10 seconds were selected for the tests. The wave height and wave period were selected to resemble typical conditions for a South African beach.

A wave generation signal file was created for each water-level to ensure that tests with different seawall profiles but with the same water-level, can be compared. The wave generation signal file contains a wave train signal that specifies the conditions of the waves to be generated to the wave generator.

The tests were performed within 4 different series (A-D). Series A to C are the three different wall profiles: vertical wall, Recurve 1 and Recurve 2, respectively. Each of these series tests were performed for 5 specific water-levels and the same wave height and period. Series D tested the sensitivity of the wave period on the overtopping rates. The description for each test series is given in Table 7.

Table 7: Test series and conditions (prototype)

Test series	Seawall profile	Water-levels at toe (m)	H_s (m)	T_p (s)
A	Vertical wall	2.4, 2.0, 1.6, 1.0, 0.6	1	10
B	Recurve 1	2.4, 2.0, 1.6, 1.0, 0.6	1	10
C	Recurve 2	2.4, 2.0, 1.6, 1.0, 0.6	1	10
D	Recurve 2	2.0	1	8, 12

3.9 Repeatability and accuracy

A number of tests were repeated to determine the repeatability and the model uncertainty. In the case where tests are repeated, the average of the respective overtopping discharges is taken to achieve a more reliable overtopping discharge. Chapter 5 expands on these repeated tests.

Small overtopping discharges less than 2 litres could not be measured very accurately due to the size of the overtopping container. Therefore the small overtopping results, less than 0.08 l/s per m, should be interpreted cautiously.

3.10 Sensitivity runs

The influence of the wave period on overtopping discharges was tested by performing test runs with periods of 8 and 12 seconds in Series D, Table 7

.

Chapter 4: Results

4.1 General

A total of 41 physical model tests were completed between 21 August and 8 October 2013. Included in these 41 tests are a number of tests that were repeated with the same test conditions: water-level, wave height, peak wave period and the same wave signal input file. The tests were repeated in an attempt to eliminate uncertainty (random error) in the model tests, as well as to determine the model tests' repeatability.

4.2 Results

The complete results for test series A to D are presented in Tables 8 to 11. The seawall profile shape used in the series is shown next to each table with the model dimensions of the overhang for the two recurve shapes given in millimetres. The result tables show the results in both prototype and model values. The specified significant wave height, H_{m0} (generator), as well as the incident wave height calculated from the probe readings, H_i (probes), are presented in the result tables. The incident wave height was calculated as described in Section 3.7.

In addition to the measured values, calculated overtopping values are also presented. These values are calculated with the EurOtop empirical calculation tool (HR Wallingford, n.d.), by following both deterministic and probabilistic approaches.

The calculated results serve merely as an estimated comparison to the measured results from the physical model tests. Figures 46 and 47 display examples of the EurOtop calculation tool for a vertical and recurve wall, respectively. However, both scenarios deviate from the physical model, as there is no beach slope incorporated into the calculation tool. The schematised recurve wall in the calculation tool also does not correspond exactly to the seawall profiles in this project.

During the model tests it was observed that the water is effectively reflected back seawards, Figures 48 and 49.

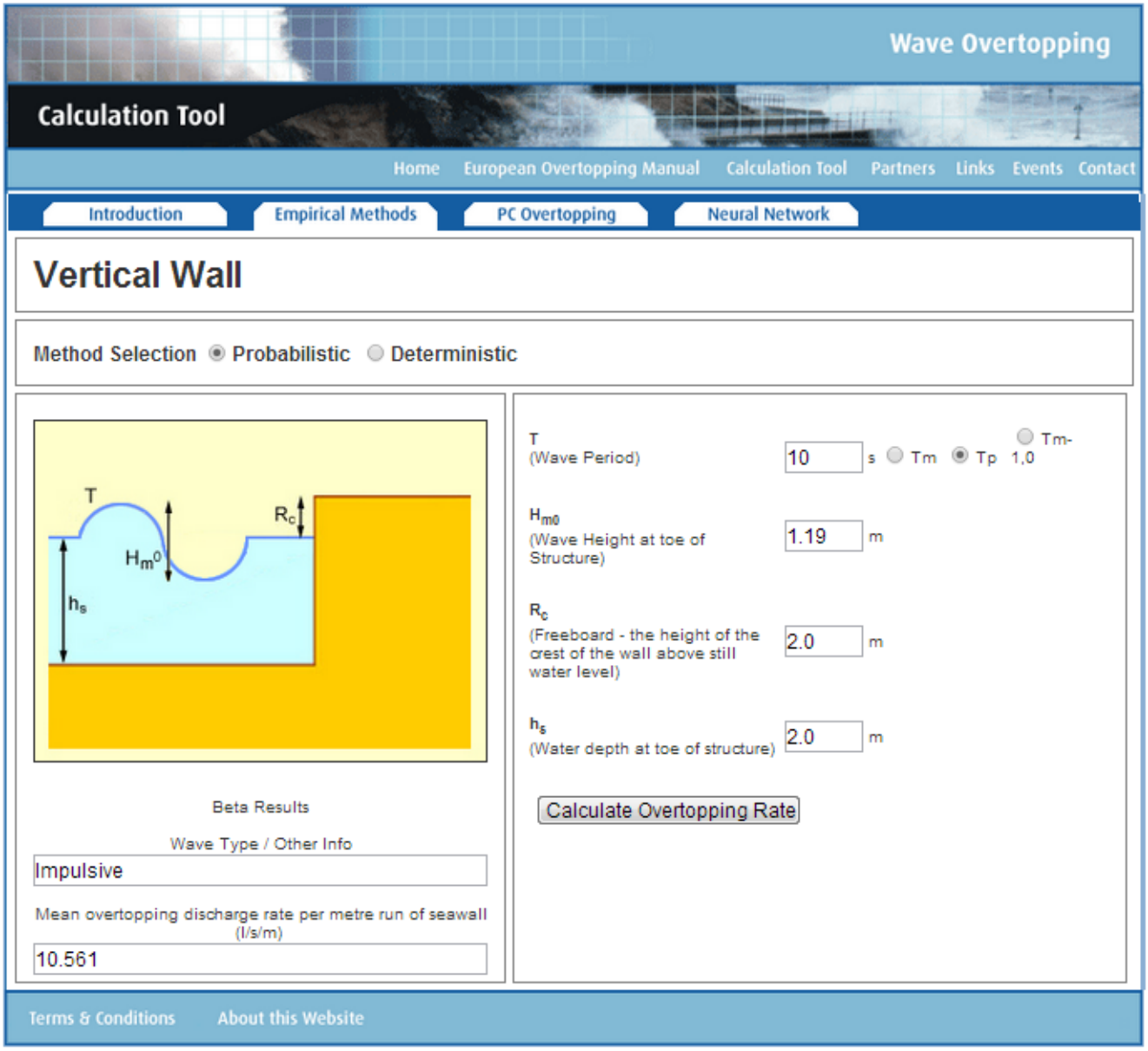

Figure 46: Screenshot of the EurOtop Calculation tool for wave overtopping (vertical wall)

(HR Wallingford, n.d.)

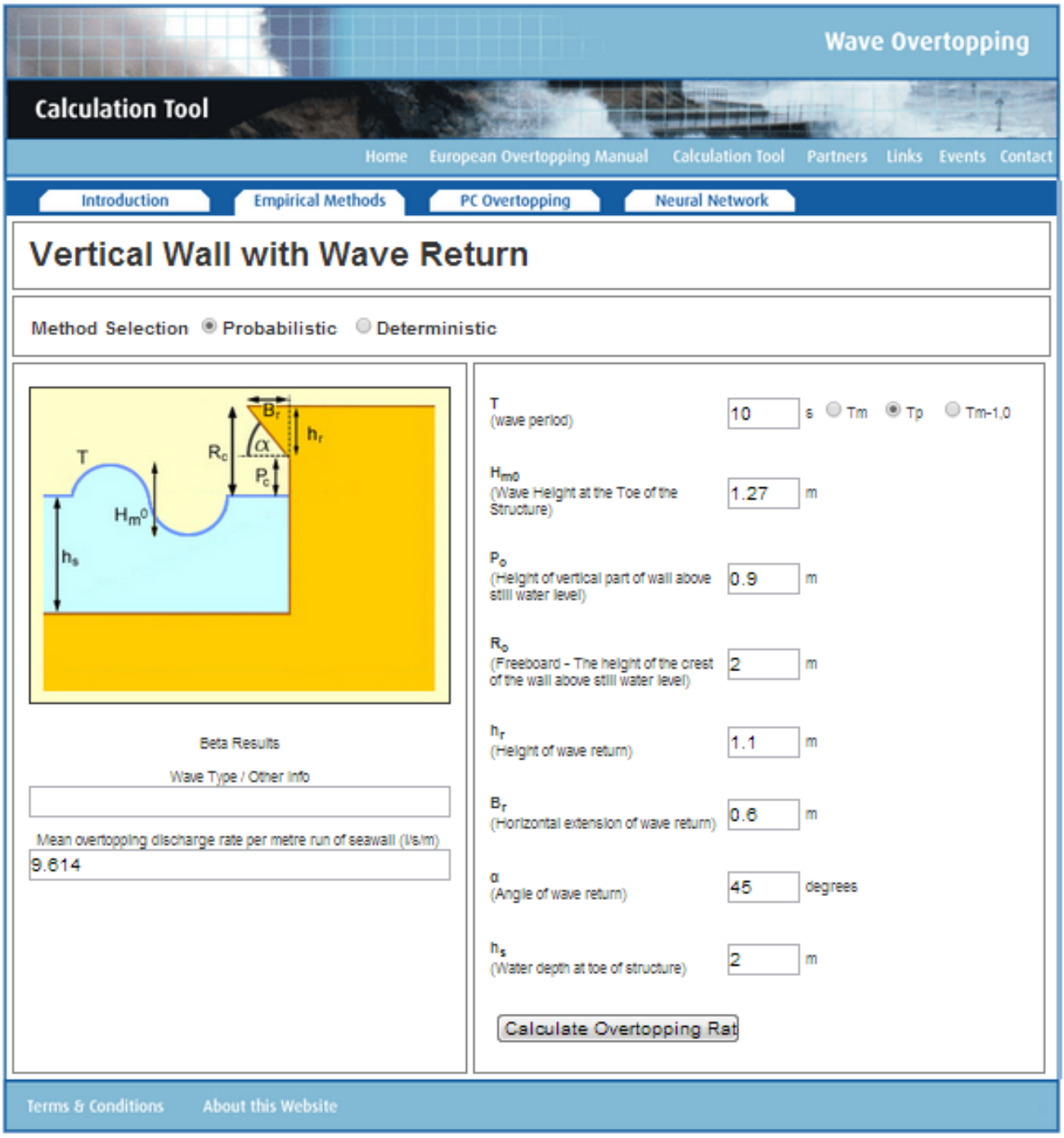

Figure 47: Screenshot of EurOtop calculation tool (Recurve)

(HR Wallingford, n.d.)

Table 8: Results of series A – Vertical wall

		Test number	A-1	A-2	A-3	A-4	A-5	A-6	A-7	A-8	A-9	A-10
		Date	21/08/2013	22/08/2013	23/08/2013	23/08/2013	23/08/2013	23/08/2013	23/08/2013	07/10/2013	07/10/2013	07/10/2013
PROTOTYPE	MEASURED	Water depth at wave paddle (m)	10.4	10.0	10.0	9.4	9.4	9.0	9.0	10.8	10.8	10.8
		Water depth at toe (m)	2.0	1.6	1.6	1.0	1.0	0.6	0.6	2.4	2.4	2.4
		Freeboard R_c (m)	2.0	2.4	2.4	3.0	3.0	3.4	3.4	1.6	1.6	1.6
		Wave period (s)	10.0	10.0	10.0	10.0	10.0	10.0	10.0	10.0	10.0	10.0
		Duration of wave attack (s)	10000	10000	10000	10000	10000	10000	10000	10000	10000	10000
		H_{m0} (probes) (m)	1.19	1.28	1.25	1.25	1.26	1.20	1.21	1.18	1.16	1.19
		Overtopping (l/s per m)	18.19	12.44	12.57	5.15	5.08	1.15	1.18	18.99	17.67	17.93
	CLASH	Probabilistic (l/s per m)	10.56	9.53	8.27	6.00	2.33	1.34	1.37	17.92	16.68	18.57
		Deterministic (l/s per m)	19.71	17.79	16.10	11.20	3.27	1.88	1.93	33.45	31.13	34.66
MODEL	MEASURED	Water depth at wave paddle (m)	0.52	0.50	0.50	0.47	0.47	0.45	0.45	0.54	0.54	0.54
		Water depth at toe (m)	0.10	0.08	0.08	0.05	0.05	0.03	0.03	0.12	0.12	0.12
		Freeboard R_c (m)	0.10	0.12	0.12	0.15	0.15	0.17	0.17	0.08	0.08	0.08
		Wave period (s)	2.236	2.236	2.236	2.236	2.236	2.236	2.236	2.236	2.236	2.236
		Duration of wave attack (s)	2236	2236	2236	2236	2236	2236	2236	2236	2236	2236
		H_{m0} (generator) (m)	0.05	0.05	0.05	0.05	0.05	0.05	0.05	0.05	0.05	0.05
		H_i (probes) (m)	0.0596	0.0639	0.0623	0.0625	0.0629	0.0600	0.0603	0.0588	0.0579	0.0595
		Overtopping (l)	454.78	311.08	314.20	128.66	126.98	28.70	29.46	474.70	441.64	448.22

Table 9: Results of series B – Recurve 1

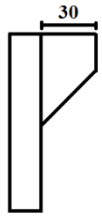

		Test number	B-1	B-2	B-3	B-4	B-5	B-5_2	B-5_3	B-5_4	B-6	B-7	B-8	B-9	B-10
		Date	27/08/2013	27/08/2013	27/08/2013	27/08/2013	28/08/2013	28/08/2013	28/08/2013	28/08/2013	29/08/2013	29/08/2013	04/10/2013	04/10/2013	04/10/2013
PROTOTYPE	MEASURED	Water depth at wave paddle (m)	10.4	10.0	9.4	9.0	10.4	10.4	10.4	10.4	10.0	10.0	10.8	10.8	10.8
		Water depth at toe (m)	2.0	1.6	1.0	0.6	2.0	2.0	2.0	2.0	1.6	1.6	2.4	2.4	2.4
		Freeboard R_c (m)	2.0	2.4	3.0	3.4	2.0	2.0	2.0	2.0	2.4	2.4	1.6	1.6	1.6
		Wave period (s)	10.0	10.0	10.0	10.0	10.0	10.0	10.0	10.0	10.0	10.0	10.0	10.0	10.0
		Duration of wave attack (s)	10000	10000	10000	10000	10000	10000	10000	10000	10000	10000	10000	10000	10000
		H_{m0} (probes) (m)	1.27	1.27	1.29	1.19	1.22	1.21	1.23	1.21	1.24	1.22	1.17	1.16	1.14
		Overtopping (l/s per m)	4.46	0.41	0.02	0.00	3.76	3.65	3.18	4.06	0.42	0.31	10.77	12.12	11.53
	CLASH	Probabilistic (l/s per m)	0.69	0.46	0.13	0.07	0.59	0.57	0.61	0.57	0.42	0.39	11.70	11.42	10.88
		Deterministic (l/s per m)	1.30	0.86	0.18	0.09	1.09	1.06	1.13	1.06	0.78	0.73	21.84	21.32	20.30
MODEL	MEASURED	Water depth at wave paddle (m)	0.52	0.50	0.47	0.45	0.52	0.52	0.52	0.52	0.50	0.50	0.54	0.54	0.54
		Water depth at toe (m)	0.10	0.08	0.05	0.03	0.10	0.10	0.10	0.10	0.08	0.08	0.12	0.12	0.12
		Freeboard R_c (m)	0.10	0.12	0.15	0.17	0.10	0.10	0.10	0.10	0.12	0.12	0.08	0.08	0.08
		Wave period (s)	2.236	2.236	2.236	2.236	2.236	2.236	2.236	2.236	2.236	2.236	2.236	2.236	2.236
		Duration of wave attack (s)	2236	2236	2236	2236	2236	2236	2236	2236	2236	2236	2236	2236	2236
		H_{m0} (generator) (m)	0.05	0.05	0.05	0.05	0.05	0.05	0.05	0.05	0.05	0.05	0.05	0.05	0.05
		H_i (probes) (m)	0.0634	0.0637	0.0644	0.0597	0.0611	0.0607	0.0614	0.0605	0.0621	0.0612	0.0583	0.0581	0.0572
		Overtopping (l)	111.58	10.34	0.5	0.001	94.08	91.26	79.44	101.48	10.56	7.8	269.22	303	288.14

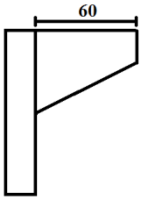

Table 10: Results of series C – Recurve 2

		Test number	C-1	C-2	C-3	C-4	C-5	C-6	C-7	C-8	C-9	C-10	C-11	C-12
		Date	30/08/2013	30/08/2013	03/09/2013	03/09/2013	03/09/2013	03/09/2013	03/09/2013	04/09/2013	04/09/2013	03/10/2013	03/10/2013	03/10/2013
PROTOTYPE	MEASURED	Water depth at wave paddle (m)	10.0	10.0	10.0	9.4	9.0	10.4	10.4	10.4	10.4	10.8	10.8	10.8
		Water depth at toe (m)	1.6	1.6	1.6	1.0	0.6	2.0	2.0	2.0	2.0	2.4	2.4	2.4
		Freeboard R_c (m)	2.4	2.4	2.4	3.0	3.4	2.0	2.0	2.0	2.0	1.6	1.6	1.6
		Wave period (s)	10.0	10.0	10.0	10.0	10.0	10.0	10.0	10.0	10.0	10.0	10.0	10.0
		Duration of wave attack (s)	10000	10000	10000	10000	10000	10000	10000	10000	10000	10000	10000	10000
		H_{m0} (probes) (m)	1.22	1.21	1.29	1.32	1.26	1.25	1.26	1.27	1.28	1.18	1.18	1.19
		Overtopping (l/s per m)	0.06	0.10	0.11	0.05	0.00	1.20	0.83	1.38	0.78	6.17	5.64	6.58
	CLASH	Probabilistic (l/s per m)	0.39	0.38	0.49	0.13	0.08	0.65	0.67	0.69	0.72	2.20	2.20	2.28
		Deterministic (l/s per m)	0.73	0.70	0.92	0.18	0.11	1.21	1.25	1.30	1.34	4.10	4.10	4.25
MODEL	MEASURED	Water depth at wave paddle (m)	0.50	0.50	0.50	0.47	0.45	0.52	0.52	0.52	0.52	0.54	0.54	0.54
		Water depth at toe (m)	0.08	0.08	0.08	0.05	0.03	0.10	0.10	0.10	0.10	0.12	0.12	0.12
		Freeboard R_c (m)	0.12	0.12	0.12	0.15	0.17	0.10	0.10	0.10	0.10	0.08	0.08	0.08
		Wave period (s)	2.236	2.236	2.236	2.236	2.236	2.236	2.236	2.236	2.236	2.236	2.236	2.236
		Duration of wave attack (s)	2236	2236	2236	2236	2236	2236	2236	2236	2236	2236	2236	2236
		H_{m0} (generator) (m)	0.05	0.05	0.05	0.05	0.05	0.05	0.05	0.05	0.05	0.05	0.05	0.05
		H_i (probes) (m)	0.0608	0.0604	0.0647	0.0662	0.0628	0.0627	0.0629	0.0636	0.0640	0.0592	0.0589	0.0597
		Overtopping (l)	1.58	2.38	2.74	1.22	0.00	29.98	20.66	34.38	19.60	154.36	141.00	164.54

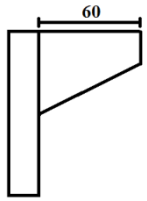

Table 11: Results of series D – Wave period sensitivity

		Test number	D-1	D-2	D-3	D-4	D-5	D-6
		Date	04/09/2013	04/09/2013	30/09/2013	02/10/2013	02/10/2013	03/10/2013
PROTOTYPE	MEASURED	Water depth at wave paddle (m)	10.4	10.4	10.4	10.4	10.4	10.4
		Water depth at toe (m)	2.0	2.0	2.0	2.0	2.0	2.0
		Freeboard R_c (m)	2.0	2.0	2.0	2.0	2.0	2.0
		Wave period (s)	8.0	8.0	8.0	12.0	12.0	12.0
		Duration of wave attack (s)	8000	8000	8000	12000	12000	12000
		H_{m0} (probes) (m)	1.18	1.22	1.12	1.23	1.21	1.22
		Overtopping (l/s per m)	0.28	0.25	0.12	2.42	2.55	2.42
	CLASH	Probabilistic (l/s per m)	0.31	0.36	0.25	0.91	0.85	0.88
		Deterministic (l/s per m)	0.58	0.67	0.47	1.69	1.58	1.63
MODEL	MEASURED	Water depth at wave paddle (m)	0.52	0.52	0.52	0.52	0.52	0.52
		Water depth at toe (m)	0.10	0.10	0.10	0.10	0.10	0.10
		Freeboard R_c (m)	0.10	0.10	0.10	0.10	0.10	0.10
		Wave period (s)	1.789	1.789	1.789	2.683	2.683	2.683
		Duration of wave attack (s)	1789	1789	1789	2683	2683	2683
		H_{m0} (generator) (m)	0.05	0.05	0.05	0.05	0.05	0.05
		H_i (probes) (m)	0.0590	0.0608	0.0559	0.0616	0.0607	0.0610
		Overtopping (l)	5.60	4.90	2.46	72.74	76.48	72.62

Figure 48: Recurve 1 during model testing

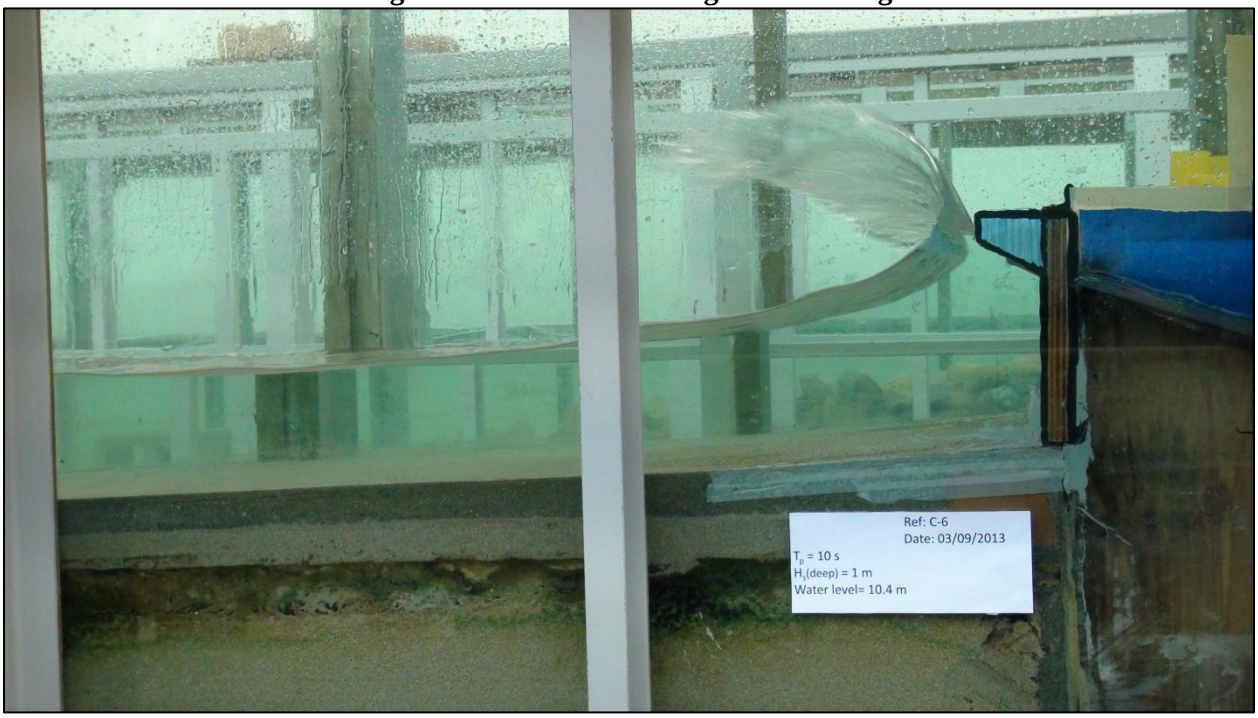

Figure 49: Recurve 2 during model testing

Chapter 5: Analysis and discussion

5.1 Introduction

The results presented in the previous chapter are analysed, interpreted and discussed in order to achieve the objectives of the project. The overtopping performance of a vertical wall is compared with both recurve walls, Recurve 1 and 2, and the influence of the length of the recurve overhang on overtopping rates is evaluated. As an indication of their reliability, the overtopping results were compared with results calculated using the EurOtop calculation tool. This indirectly enables the measurements in this project to be compared with measurements of overtopping from previous studies.

5.2 Measured test results

In terms of overtopping rates, the performance of the vertical wall and the two recurve shapes are compared in Figures 50 and 51. These graphs have a logarithmic vertical axis (dimensionless relative overtopping rate) and a linear horizontal axis (dimensionless relative freeboard) (following EurOtop, 2007).

As mentioned before, certain tests were repeated with the same test conditions. In Figure 50 all the test results are shown as data points on the graph. However, Figure 51 presents the average test results, by taking the average of the results for the repeated tests. In other words, the results of the tests performed under the same conditions, i.e. water-level, wave height and wave period, are averaged to display only one data point for the same input conditions.

Both Figures 50 and 51 indicate that the use of recurve walls offer a definite reduction in wave overtopping rates compared with vertical walls. As the relative freeboard decreases, the effectiveness of the recurves also decreases. Therefore recurves effectiveness in reducing overtopping will be less in instances of a high water-level or large waves ($R_c/H_{m0} \leq 1.4$). In these conditions, most waves pass over the crest of the structure and are not reflected seawards. This observation supports the findings of Kortenhaus et al. (2003) which states that lower freeboards or higher waves result in wave energy not being fully deflected and thus the effectiveness of the recurve is compromised. However, even for the lower relative freeboard cases, recurve walls offer a significant reduction in overtopping compared with the vertical wall.

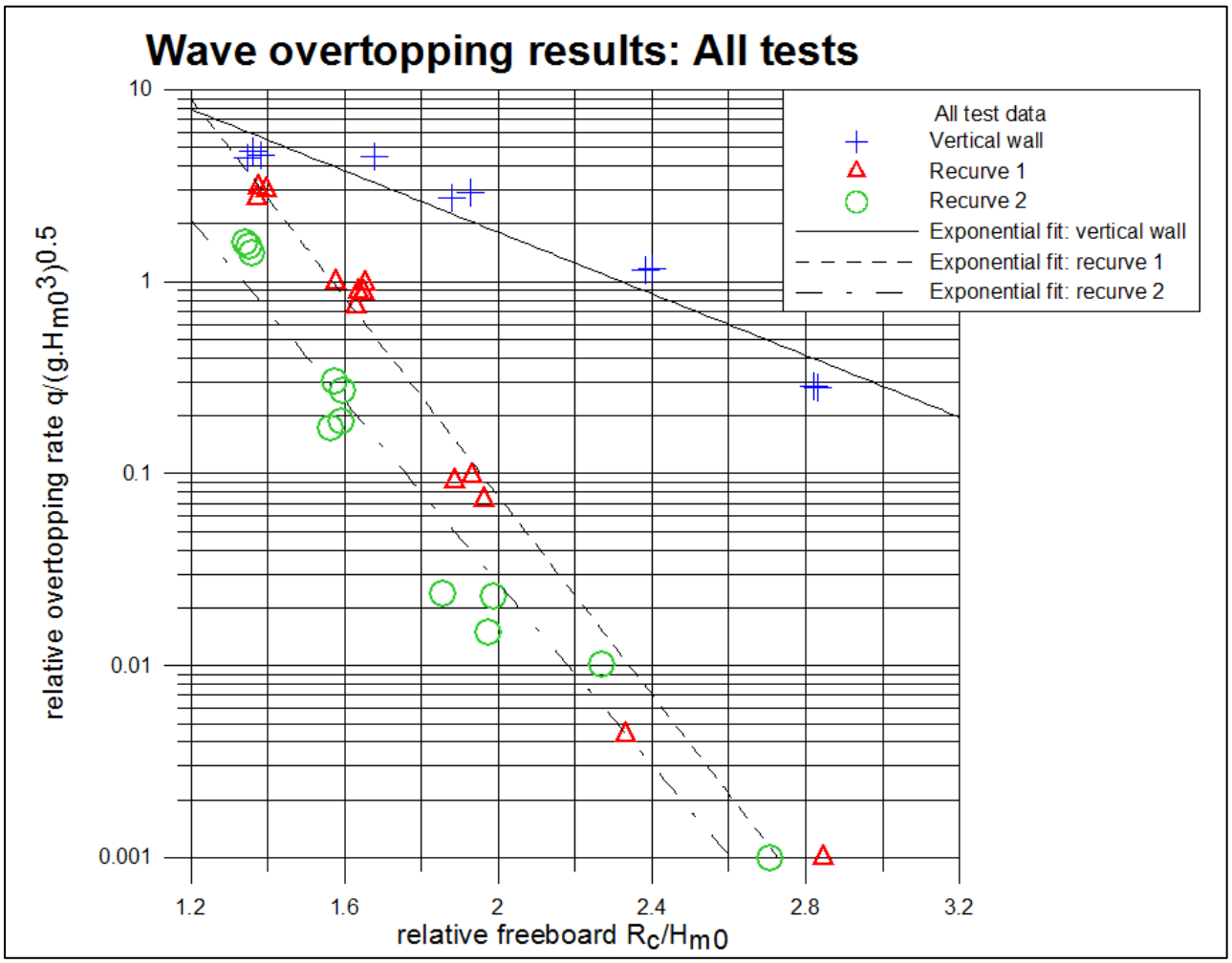

Figure 50: Graph displaying all test results

On the contrary, the figures suggest that the effectiveness of recurves to reduce overtopping is very significant for $R_c/H_{m0} > 1.4$. When wave breaking occurs with lower water level and higher R_c ($R_c/H_{m0} > 2.2$ for the conditions of this project), water easily splashes over the vertical wall with the momentum of the incident waves. Recurve walls effectively prevent these splashes from being carried over the wall, as the recurve reflects the water seawards.

The figures also indicate that Recurve 2, with a large seaward overhang, proves to be more effective in reducing overtopping than Recurve 1, which has a small overhang. In prototype measurements Recurve 1 has a seaward overhang of 0.6 m, whereas Recurve 2 has a seaward overhang of 1.2 m.

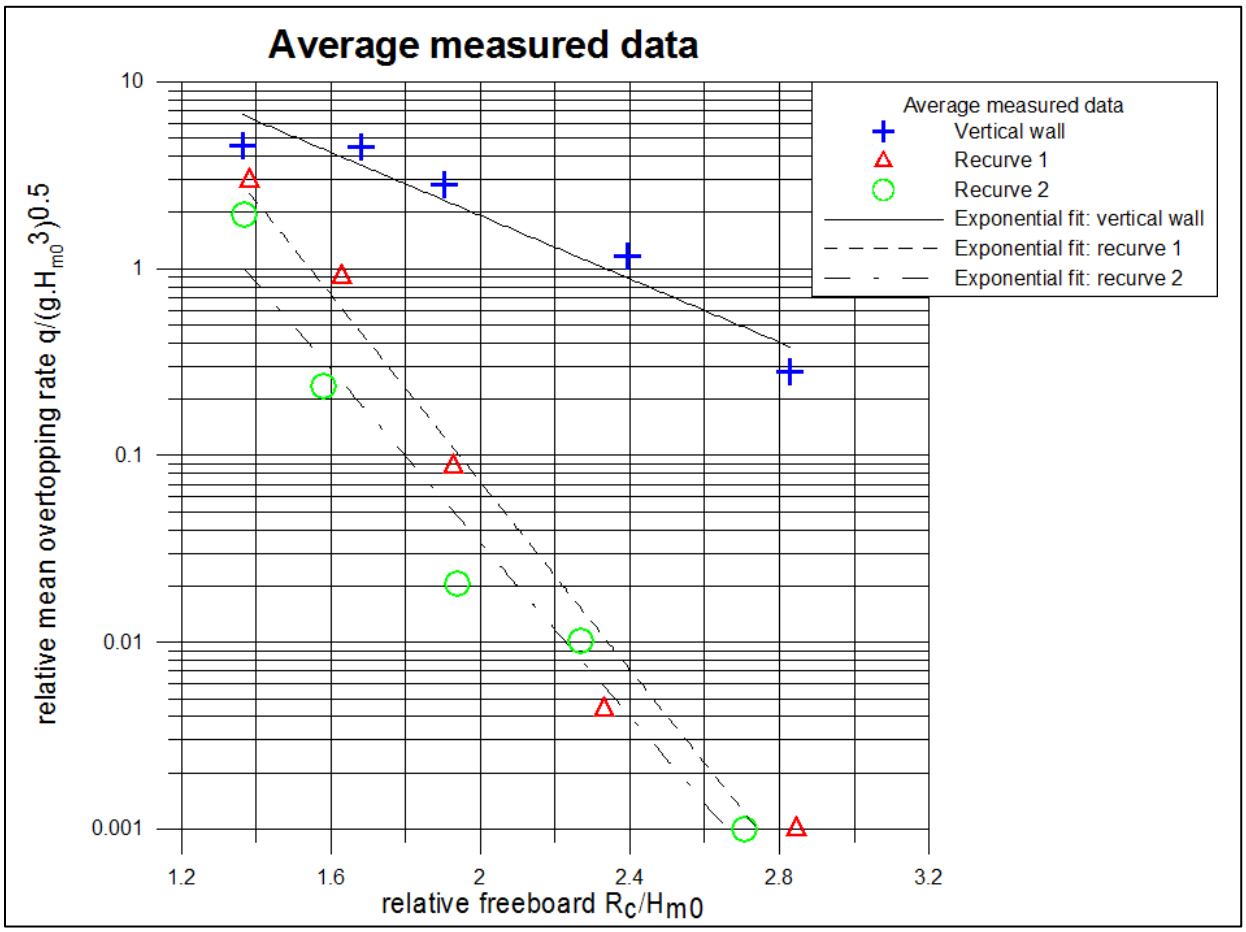

Figure 51: Graph showing average measured data

For cases with high freeboard or large wave heights when R_c/H_{m0} >2.2, both recurves effectively reflect the splash from the incident breaking waves. Consequently, the length of the seaward overhang of the recurves becomes less important in reducing overtopping.

The vertical wall serves as a reference case to which the reduction of overtopping is compared. Table 12 gives the overtopping for each freeboard case for the vertical wall, as well as the percentage in reduction of overtopping for the two recurve sections. For the lowest two freeboard cases, the reduction in overtopping for Recurve 1 is 37% and 79%, and for Recurve 2, 66% and 94% respectively. Therefore, the length of the recurve overhang is still important. For the remaining cases the reduction of overtopping is very similar.

Recurve 2 is overall more efficient in reducing overtopping. Considering the property of reducing overtopping only, the use of the Recurve 2 section would be recommended. However, other properties also need to be considered in the decision making process, such as constructability, cost and case specific factors.

Table 12: Reduction in overtopping due to Recurve 1 and 2 for H_{m0} and T_p=10s

Prototype freeboard (m)	1.6	2.0	2.4	3.0	3.4
Prototype vertical wall overtopping rate (l/s per m)	18.194	18.191	12.506	5.113	1.163
Recurve 1 - reduction in overtopping (%)*	37	79	97	100	100
Recurve 2 - reduction in overtopping (%)*	66	94	99	99	100

*compared to vertical wall

Figure 52 gives a further indication of the influence of the overhang length on the mean overtopping rate. The figure presents the dimensionless relative mean overtopping rate (y-axis) versus the dimensionless relative overhang length (x-axis) as a function of freeboard. Since the generated significant wave height was specified as 1 m in prototype for all tests, the change in relative overhang length and relative overtopping rates are mainly due to the change in overhang length and measured overtopping rates, respectively.

All freeboard cases follow the same trend, showing that as the overhang length increases, the mean overtopping rate decreases. However, the data point with a freeboard of 1.6 m and a relative mean overtopping rate of 18, deviates as it would be expected to have a higher overtopping rate. This deviation is discussed further in Section 5.3. To be certain of the presented trend, it is recommended that further model tests are performed with relative overhang lengths between 0.0 and 0.4 as well as between 0.4 and 1.0.

The largest reduction in mean overtopping occurs between a relative overhang length of 0 (vertical wall) and around 1.5 (Recurve 1). Between Recurve 1 and Recurve 2 (relative overtopping length of around 1) there is a smaller, but still significant, reduction in mean overtopping rates. However, as the freeboard increases, the reduction in overtopping between Recurve 1 and Recurve 2 becomes less significant.

Looking at Figure 52 it is expected that as the relative overhang length increases, the reduction in relative overtopping will, at a certain overhang length, remain constant. However, to make this

conclusion, it is recommended that further tests are performed with relative overhang lengths larger than 1.0.

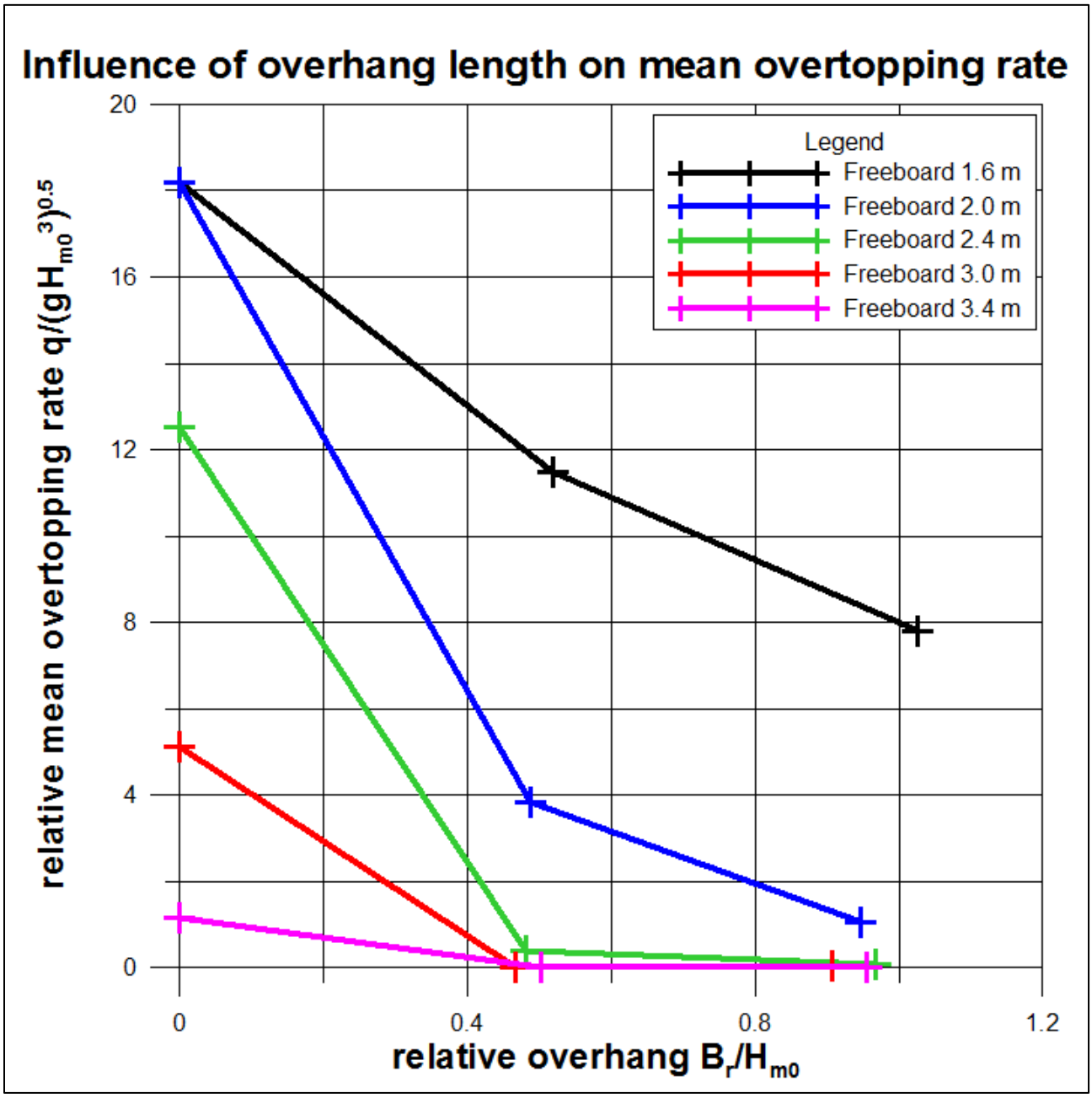

Figure 52: The influence of the overhang length on mean overtopping rate

5.2.1 Repeatability and accuracy of tests

Reis et al. (2008) stated that tests should be repeated, because of the variability in mean overtopping rates between tests, even though tests are performed under the same test conditions. The results from the repeated tests in each test series are presented in Tables 13 to 16.

Despite investigation, no exact reasons could be found for the large variations in overtopping results for some of the repeated tests. Although the wave absorption was kept constant between tests with the same water-levels, it is possible that the performance of the wave absorption could vary between tests, resulting in different overtopping results.

All tests were performed as accurately as possible. Steps were taken to ensure that the water-level in the flume during the test remained constant, for example making sure that water was not spilled, and that the overtopped water was pumped out of the overtopping container to the exact starting water-level after each test. Calibration of the wave probes was executed before every test, to limit the chance that a change in temperature could have a large effect on wave probe readings.

To quantify the variation of the overtopping measurements for the repeated tests under the same test conditions, the coefficient of variation (CoV) was calculated. Since there are too few repeated tests to get an accurate statistical indication of the CoV, it is recommended that additional repeated tests are performed. The CoV is calculated with the following equation:

$$CoV\ (\%) = \frac{\sigma}{\mu} \times 100$$

Where σ = standard deviation of the prototype overtopping rates/ wave heights for test with the same test conditions

μ = average of the prototype overtopping rates/ wave heights for test with the same test conditions

The CoV of overtopping rates ranges between 2.97 % to a maximum value of 38.16%, Tables 13 to 16. A CoV of 38.16% indicates a large variation on overtopping measurements. It should be noted that with low overtopping rates, such as with Test D-1 to D-3, a range difference in model overtopping water of about 3 litres result in a large CoV of 38.16 %. Whereas with high overtopping rates, for example, Test B-1 to Test B-5_4, a range difference of about 30 litres, only results in a CoV of 12.52

%. Consequently the difference in overtopping measurements becomes far more critical for low overtopping rates.

In the CLASH project it was found that overtopping rates differ up to 12 % when tests are repeated (De Rouck, et al., 2005). The EurOtop (2007) states that in the CLASH project the CoV of overtopping rates were found to be about 10 % and 13 % for two different flumes. Compared to these figures, the coefficient of variation for this project is rather large, reaching up to 38.16 %. However, the CLASH database consists of more than 10 000 overtopping tests. Thus it is expected that the CoV for this project will higher than the CoV of the CLASH project.

The average of the repeated tests was taken in order to eliminate the uncertainty in the model tests. Figure 51 shows the averaged measurements, whereas Figure 50 shows all physical model tests. More repetitions were not possible due to time constraints.

Table 13: Repeated tests of series A

	Test number	A-2	A-3	A-4	A-5	A-6	A-7	A-8	A-9	A-10
PROTOTYPE	Water depth at toe (m)	1.6		1.0		0.6		2.4		
	Freeboard R_c (m)	2.4		3.0		3.4		1.6		
	Wave period (s)	10.0		10.0		10.0		10.0		
	Duration of wave attack (s)	10000		10000		10000		10000		
	H_{m0} (probes) (m)	1.28	1.25	1.25	1.26	1.20	1.21	1.18	1.16	1.19
	Overtopping (l/s per m)	12.44	12.57	5.15	5.08	1.15	1.18	18.99	17.67	17.93
MODEL	H_{m0} (generator) (m)	0.05		0.05		0.05		0.05		
	H_i (probes) (m)	0.0639	0.0623	0.0625	0.0629	0.0600	0.0603	0.0588	0.0579	0.0595
	Overtopping (l)	311.08	314.20	128.66	126.98	28.70	29.46	474.70	441.64	448.22
	CoV of overtopping (%)							3.85		

Test conditions
Measured
Coefficient of variation

Table 14: Repeated tests of series B

	Test number	B-1	B-5	B-5_2	B-5_3	B-5_4	B-2	B-6	B-7	B-8	B-9	B-10
PROTOTYPE	Water depth at toe (m)	2.0					1.6			2.4		
	Freeboard R_c (m)	2.0					2.4			1.6		
	Wave period (s)	10.0					10.0			10.0		
	Duration of wave attack (s)	10000					10000			10000		
	H_{m0} (probes) (m)	1.27	1.22	1.21	1.23	1.21	1.27	1.24	1.22	1.17	1.16	1.14
	Overtopping (l/s per m)	4.46	3.76	3.65	3.18	4.06	0.41	0.42	0.31	10.77	12.12	11.53
MODEL	H_{m0} (generator) (m)	0.05					0.05			0.05		
	H_i (probes) (m)	0.0634	0.0611	0.0607	0.0614	0.0605	0.0637	0.0621	0.0612	0.0583	0.0581	0.0572
	Overtopping (l)	111.58	94.08	91.26	79.44	101.48	10.34	10.56	7.80	269.22	303.00	288.14
	CoV of overtopping (%)	12.52					16.03			5.90		

Table 15: Repeated tests of series C

	Test number	C-1	C-2	C-3	C-6	C-7	C-8	C-9	C-10	C-11	C-12
PROTOTYPE	Water depth at toe (m)	1.6			2.0				2.4		
	Freeboard R_c (m)	2.4			2.0				1.6		
	Wave period (s)	10.0			10.0				10.0		
	Duration of wave attack (s)	10000			10000				10000		
	H_{m0} (probes) (m)	1.22	1.21	1.29	1.25	1.26	1.27	1.28	1.18	1.18	1.19
	Overtopping (l/s per m)	0.06	0.10	0.11	1.20	0.83	1.38	0.78	6.17	5.64	6.58
MODEL	H_{m0} (generator) (m)	0.05			0.05				0.05		
	H_i (probes) (m)	0.0608	0.0604	0.0647	0.0627	0.0629	0.0636	0.0640	0.0592	0.0589	0.0597
	Overtopping (l)	1.58	2.38	2.74	29.98	20.66	34.38	19.60	154.36	141.00	164.54
	CoV of overtopping (%)	26.59			27.52				7.70		

Table 16: Repeated tests of series D

	Test number	D-1	D-2	D-3	D-4	D-5	D-6
PROTOTYPE	Water depth at toe (m)	2.0			2.0		
	Freeboard R_c (m)	2.0			2.0		
	Wave period (s)	8.0			12.0		
	Duration of wave attack (s)	8000			12000		
	H_{m0} (probes) (m)	1.18	1.22	1.12	1.23	1.21	1.22
	Overtopping (l/s per m)	0.28	0.25	0.12	2.42	2.55	2.42
MODEL	H_{m0} (generator) (m)	0.05			0.05		
	H_i (probes) (m)	0.0590	0.0608	0.0559	0.0616	0.0607	0.0610
	Overtopping (l)	5.60	4.90	2.46	72.74	76.48	72.62
	CoV of overtopping (%)	38.16			2.97		

Moreover, there is also variation in the H_{m0} wave height readings, which can also impact the overtopping measurements. It should be noted that a small difference in wave height for the largest waves within a wave train, could strongly affect the mean overtopping rates (Reis, et al., 2008). The maximum wave heights should therefore also be considered as a possible reason for the large variation in mean overtopping rates of the repeated tests. Table 17 presents the average $H_{2\%}$, the wave height exceeded by 2% of the waves, and the maximum recorded wave in each wave train, H_{max}, for all tests.

Not all variation in wave overtopping for the repeated tests can be explained by the difference in wave height of the maximum and $H_{2\%}$ waves, since other experimental factors also play a role. However, for example, Test B-1 has notably the highest H_{max} and $H_{2\%}$ (3.38 m and 2.16 m, respectively) compared to the other tests performed under the same conditions. Thus the higher overtopping rate could be the result of the higher H_{max} and $H_{2\%}$.

Also, when comparing Tests C-10 to C-12 with one another, it is evident that Test C-12 (H_{max} =2.87 and $H_{2\%}$ =2.10) with the higher waves result in the highest overtopping rate (H_{max} =2.84; 2.83 and $H_{2\%}$ =2.05; 2.02). Test D-3 has a lower overtopping rate than D-1 and D-2, which were performed under the same conditions. By looking at the measured wave heights, it is clear that the lower overtopping rate is a result of lower wave heights.

It should be noted that the results are presented as dimensionless in Figure 50, because the relative freeboard and mean overtopping rate are expressed relative to the spectral significant wave height (H_{m0}). The wave heights are thus taken into account in the presented results, but this does not necessarily account for the higher waves. In addition, the number of overtopping waves is not considered and was not measured for this project. The number of overtopping waves could also possibly give an indication of why there is such a large variation in some repeated tests.

Table 17: Measured H_{max} and $H_{2\%}$

	Test number	A-8	A-9	A-10	A-2	A-3	A-4	A-5	A-6	A-7
PROTOTYPE	Freeboard R_c (m)	1.6	1.6	1.6	2.4	2.4	3.0	3.0	3.4	3.4
	$H_{s\ probes}$(m)	1.18	1.16	1.19	1.28	1.25	1.25	1.26	1.20	1.21
	H_{max} (m)	2.87	2.79	2.90	2.94	2.91	2.68	2.63	2.36	2.38
	$H_{2\%}$ (m)	2.03	2.02	2.05	2.11	2.05	2.00	1.99	1.97	1.97
	Overtopping (l/s per m)	18.99	17.67	17.93	12.44	12.57	5.15	5.08	1.15	1.18

	Test number	B-8	B-9	B-10	B-1	B-5	B-5_2	B-5_3	B-5_4	B-2	B-6	B-7
PROTOTYPE	Freeboard R_c (m)	1.6	1.6	1.6	2.0	2.0	2.0	2.0	2.0	2.4	2.4	2.4
	$H_{s\ probes}$(m)	1.17	1.16	1.14	1.27	1.22	1.21	1.23	1.21	1.27	1.24	1.22
	H_{max} (m)	2.92	2.80	2.84	3.38	3.09	3.01	3.04	3.20	3.02	2.93	2.89
	$H_{2\%}$ (m)	2.09	2.04	2.02	2.16	2.10	2.06	2.10	2.07	2.05	1.98	1.96
	Overtopping (l/s per m)	10.77	12.12	11.53	4.46	3.76	3.65	3.18	4.06	0.41	0.42	0.31

	Test number	C-10	C-11	C-12	C-6	C-7	C-8	C-9	C-1	C-2	C-3
PROTOTYPE	Freeboard R_c (m)	1.6	1.6	1.6	2.0	2.0	2.0	2.0	2.4	2.4	2.4
	$H_{s\ probes}$(m)	1.18	1.18	1.19	1.25	1.26	1.27	1.28	1.22	1.21	1.29
	H_{max} (m)	2.84	2.83	2.87	3.15	3.11	3.18	3.08	2.81	2.78	2.93
	$H_{2\%}$ (m)	2.05	2.02	2.10	2.12	2.09	2.13	2.10	1.96	1.95	2.06
	Overtopping (l/s per m)	6.17	5.64	6.58	1.20	0.83	1.38	0.78	0.06	0.10	0.11

	Test number	D-1	D-2	D-3	D-4	D-5	D-6
PROTOTYPE	Freeboard R_c (m)	2.0	2.0	2.0	2.0	2.0	2.0
	Wave period (s)	8.0	8.0	8.0	12.0	12.0	12.0
	$H_{s\ probes}$(m)	1.18	1.22	1.12	1.23	1.21	1.22
	H_{max} (m)	2.82	2.84	2.60	3.21	3.13	3.20
	$H_{2\%}$ (m)	1.96	2.05	1.90	2.16	2.13	2.16
	Overtopping (l/s per m)	0.28	0.25	0.12	2.42	2.55	2.42

5.2.2 Sensitivity of overtopping rates to wave period

In Series D, tests were performed with a peak wave period (T_p) of 8 and 12 seconds. Tests in all the other series were performed with a peak wave period of 10 seconds. Series D tests the influence of the wave period on overtopping results. Figure 53 shows the results of comparing mean overtopping rates of tests performed under the same test conditions with varying wave periods.

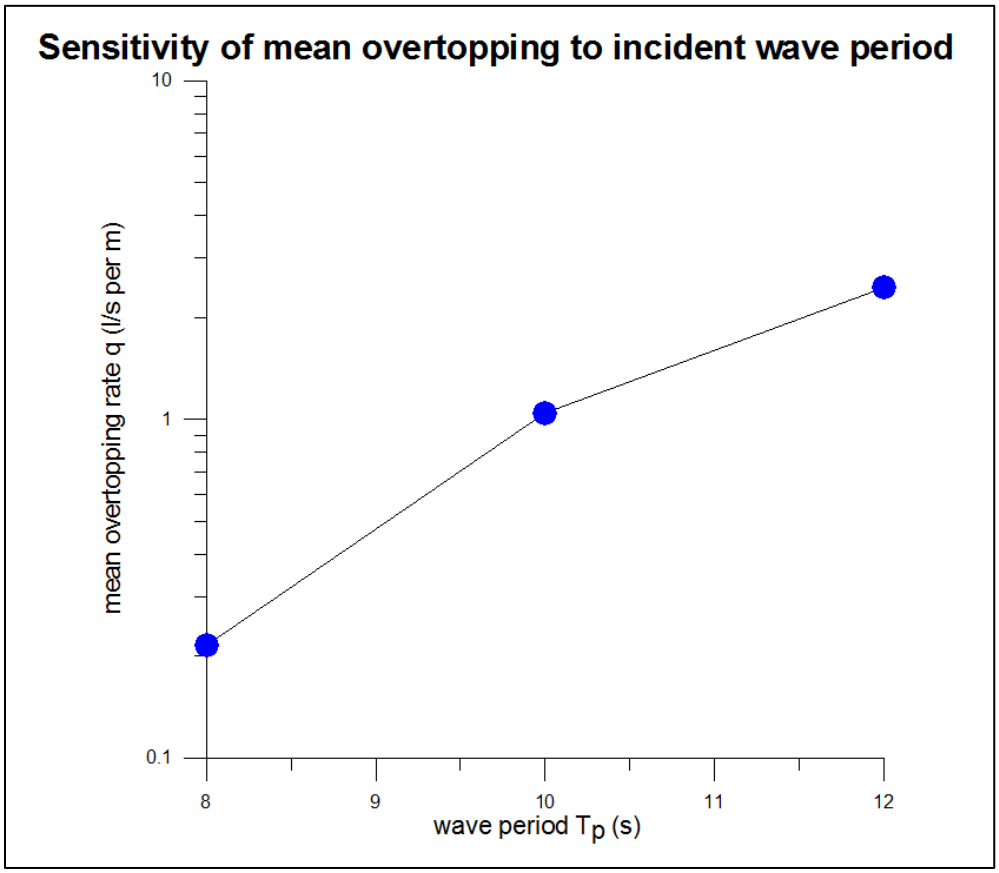

Figure 53: Influence of wave period on overtopping results

Figure 53 indicates that the mean overtopping rate is fairly sensitive to wave period, T_p. This corresponds to Roux's (2013) findings that overtopping rates increase as the wave period increases up to 12 seconds. However, Roux (2013) found that as the wave period increases beyond 12 seconds, the overtopping rate decreases. According to Roux (2013) this decrease in overtopping rates is a result of increase in wave heights from shoaling. Waves with longer periods have longer wavelengths and therefore start shoaling in deeper water. Therefore, waves with periods 14 and 16 seconds broke before

reaching the recurve wall due to the depth-induced breaking limit. Consequently, the waves lost energy and were smaller when reaching the structure, resulting in lower overtopping rates (Roux, 2013).

It is recommended that further tests are performed with a range of wave periods as overtopping results are sensitive to the wave period.

5.3 Comparison of measured results with EurOtop calculation tool

In this section, the results of the different seawall profiles are compared with the predicted overtopping rates calculated by the EurOtop calculation tool. This comparison is made to get an indication of how the results of this project compare with other physical model studies. Both the probabilistic approach and deterministic approach (increased by one standard deviation) are used to calculate the overtopping rate.

Figure 54 compares the measured overtopping rates for the vertical wall from the performed physical model tests for this project, with the calculated overtopping. The measured overtopping rates of the vertical wall generally follow the trend of the calculated overtopping rates. However, deviation from the trend occurs with a relative freeboard smaller than about 1.7.

The data point with relative freeboard at 1.36, presents the average of three tests performed with the same water-level, wave period and wave signal input file. This data point does not follow the trend of the graph, but no exact reasons could be found for this deviation. The three tests representing the data point were performed following the same procedure as all the other tests and no problems were encountered or observed.

In Figure 55 the overtopping measurements (Recurve 1) for the lower freeboard cases ($R_c/H_{m0} < 1.9$) follows a straight line. With $R_c/H_{m0} > 1.9$, the measured wave overtopping is less than the calculated overtopping rates. The measurement of the low overtopping rates requires another technique, since small errors have a significant impact on the measured overtopping rates. For example the use of blotting paper to absorb small quantities of water would be more accurate. This technique was not used, because it is time consuming and a change of model set-up would be required.

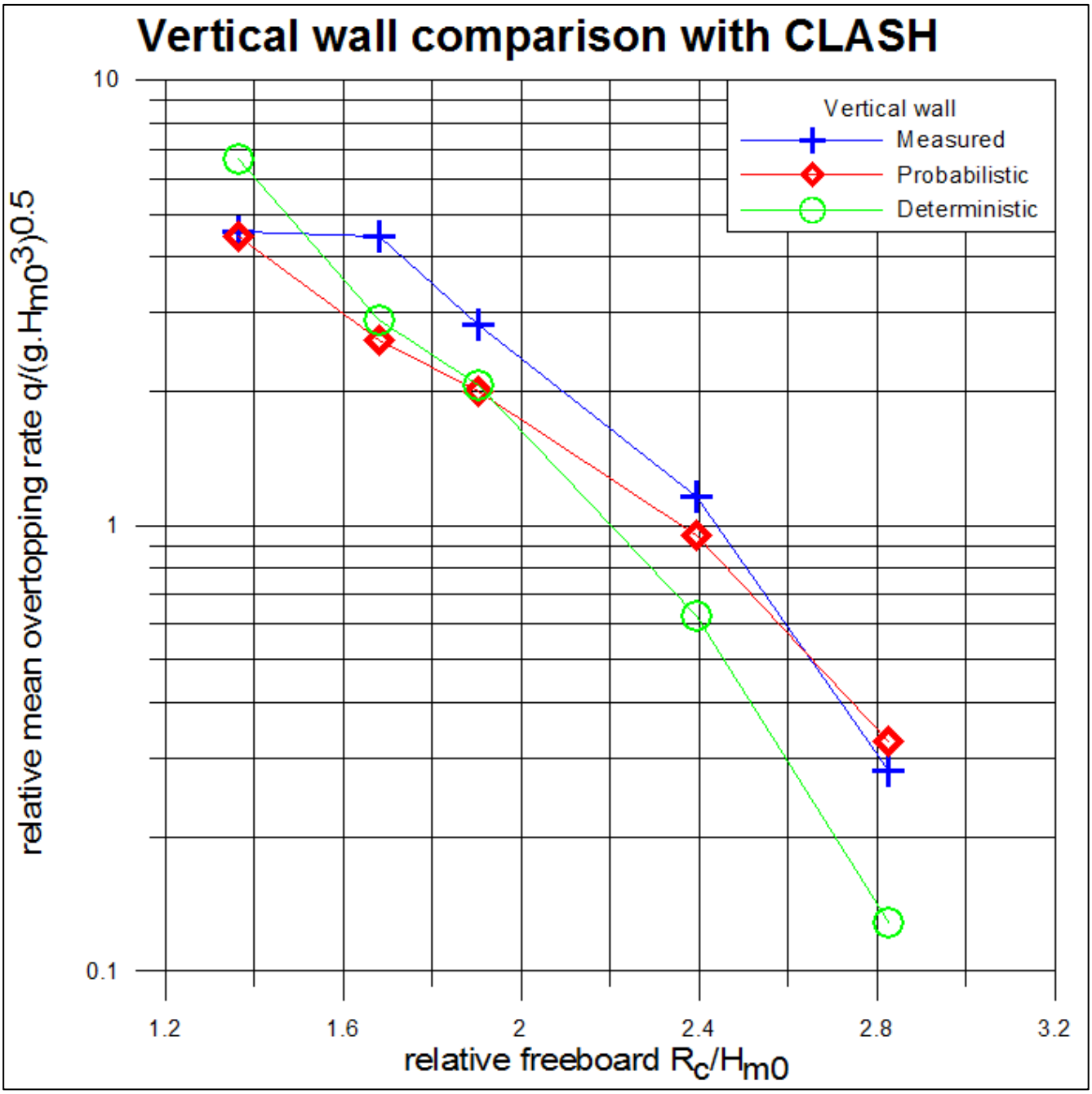

Figure 54: Comparison of measured and calculated overtopping rates for vertical wall

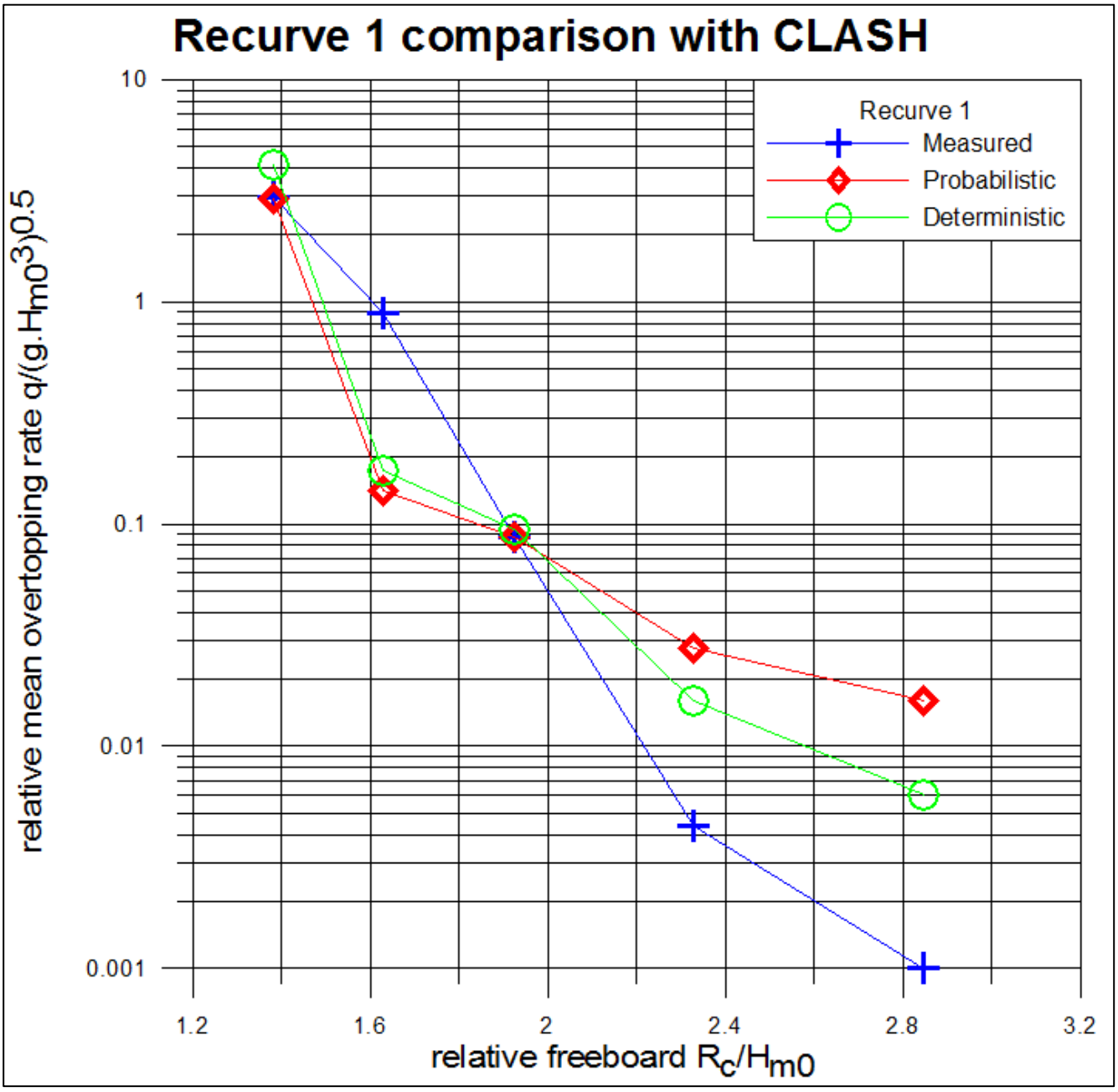

Figure 55: Comparison of measured and calculated overtopping rates for Recurve 1

Recurve 2 is very efficient in reducing overtopping and therefore has small overtopping rates, Figure 56. As discussed above, a better technique should be used to measure small overtopping rates more accurately. In the case of small overtopping rates, it was found that the measured overtopping rates are lower than the EurOtop predicted overtopping rates. This difference in overtopping rates could possibly be reduced by using a more accurate technique to measure small overtopping rates.

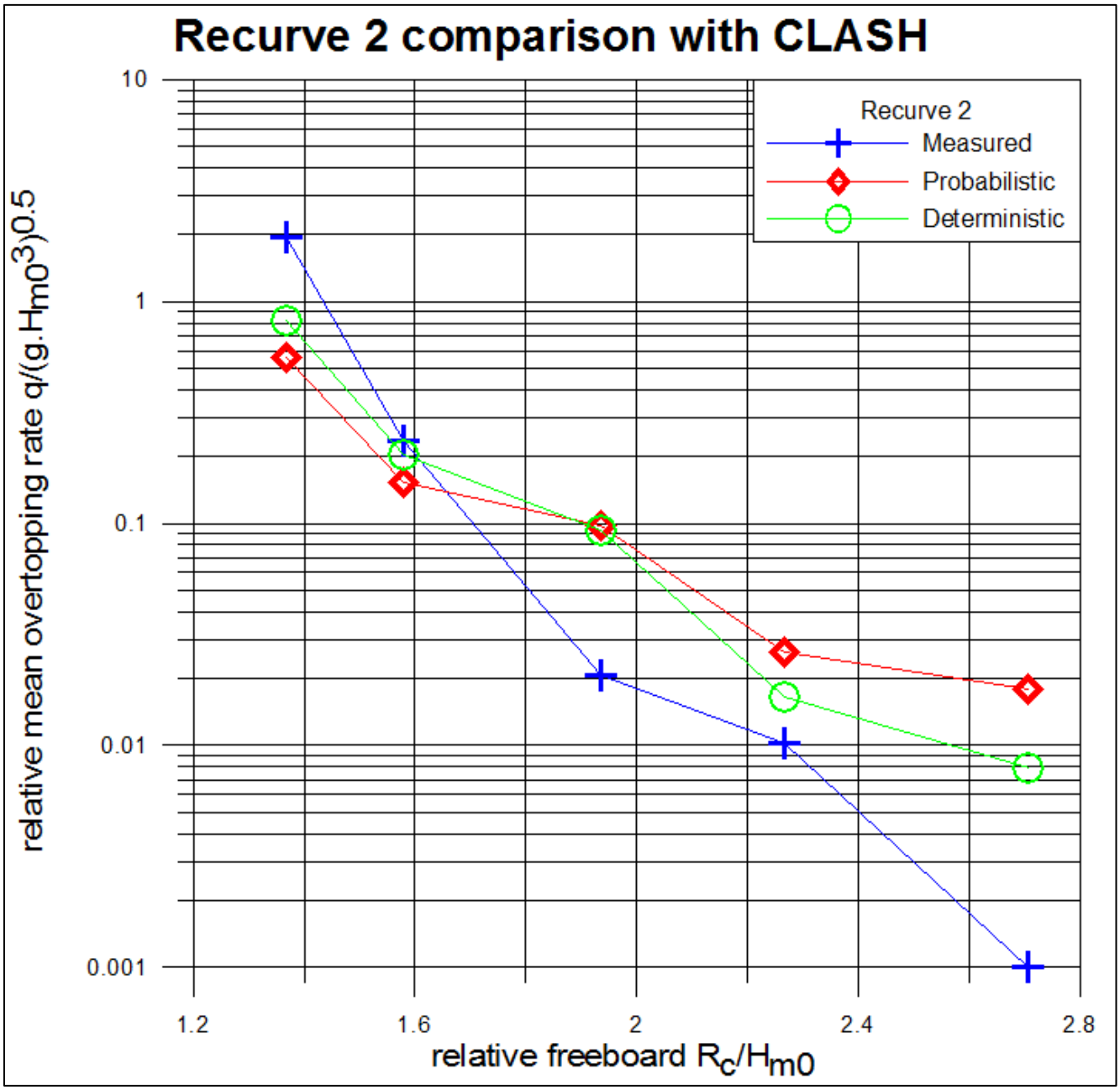

Figure 56: Comparison of measured and calculated overtopping rates for Recurve 2

Figures 57 to 59 present the measured relative overtopping rates versus the relative overtopping rates as predicted by the deterministic approach of the EurOtop calculation tool. These graphs clearly show whether overtopping rates are over- or underpredicted.

For the vertical wall, Figure 57 shows the measured results are close to the predicted results. All tests, except one, are underpredicted. The overpredicted test is the same test that deviates from the trend in

Figure 54. As the deterministic approach was used for the predicted overtopping rates, one standard deviation is included in the calculated results. Therefore, even when comparing the results with the safer approach as set out in EurOtop (2007), the measured overtopping proves to be larger.

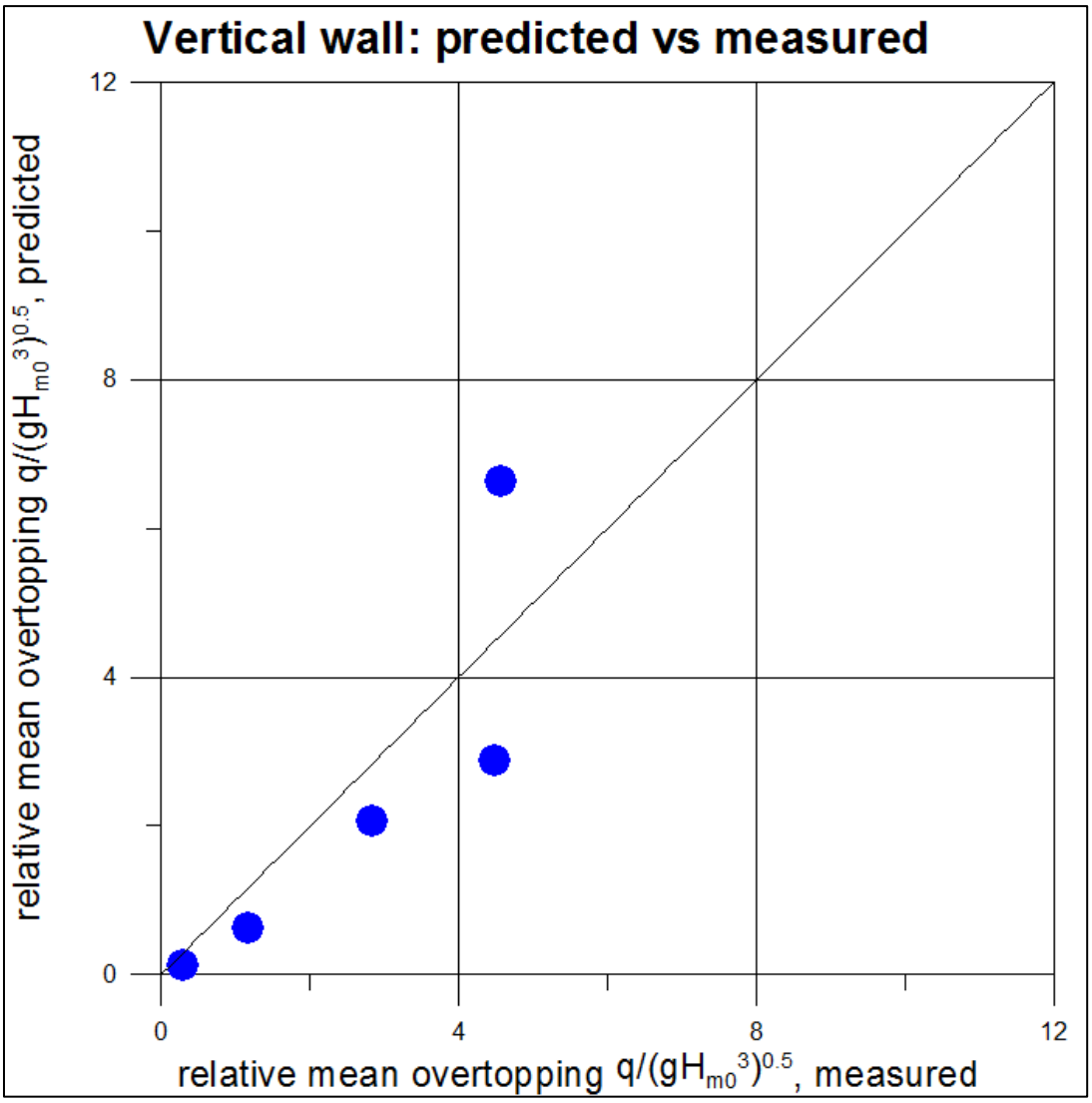

Figure 57: Vertical wall: predicted versus measured overtopping rates

Figure 58 shows that the measured overtopping rates of the recurve profiles for the low relative overtopping rates ($q/(gH_{m0}^3)^{0.5} < 0.4$) are very close to the predicted overtopping rates. In the other two cases with larger relative overtopping rates, one case is underpredicted and the other overpredicted.

In Figure 59 the measured relative overtopping rates compare well with the predicted relative overtopping rates, except one case that is largely underpredicted.

The measured overtopping results do not compare well to the CLASH predictions in all cases. As mentioned before, the modelled case for this project does not exactly correspond to the case in the EurOtop calculation tool. This could possibly explain the deviations of the measured overtopping rates, from the predicted overtopping rates. To fully evaluate the model tests by comparing with the CLASH predictions, further comprehensive tests should be performed.

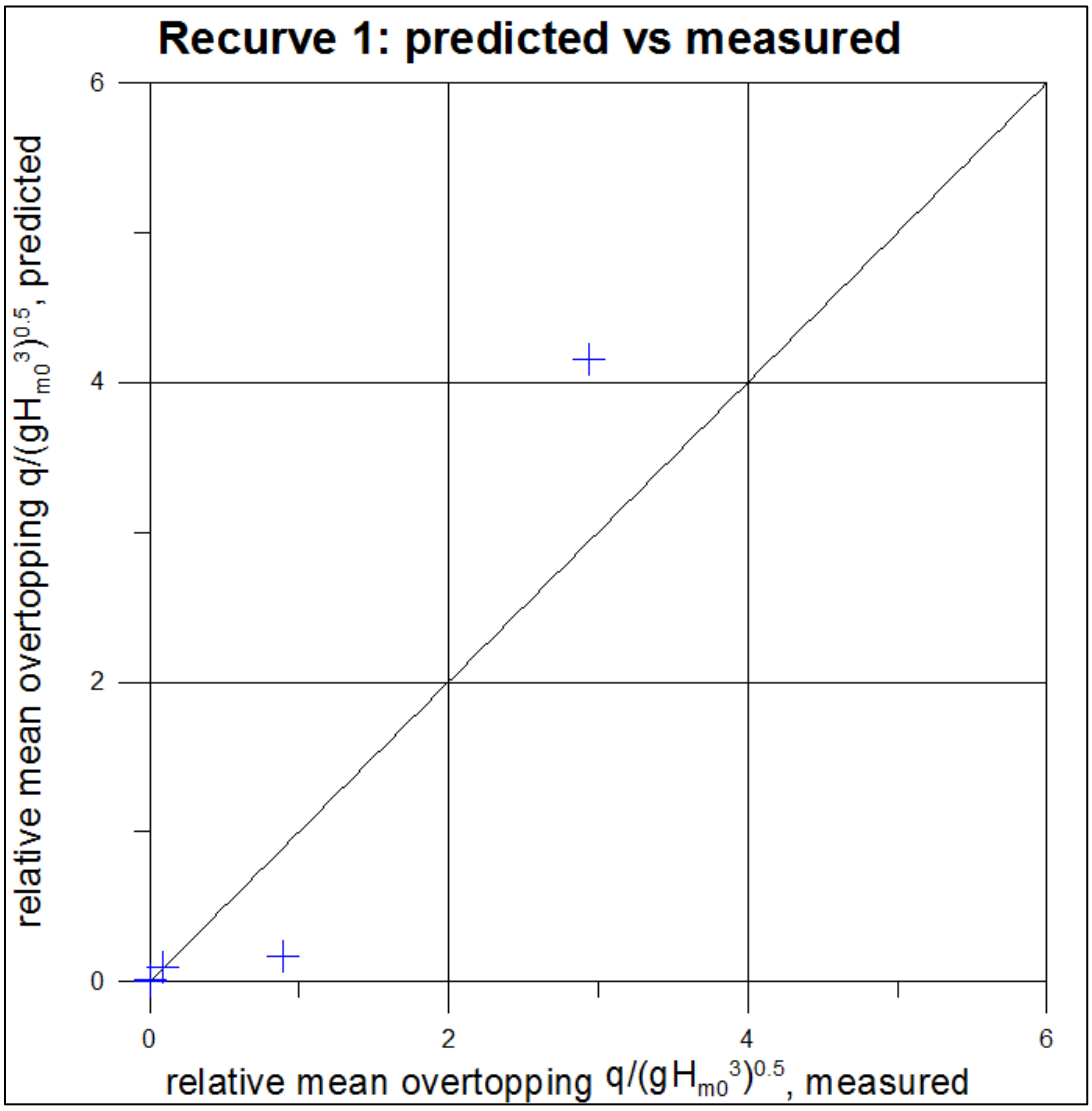

Figure 58: Recurve 1: predicted versus measured overtopping rate

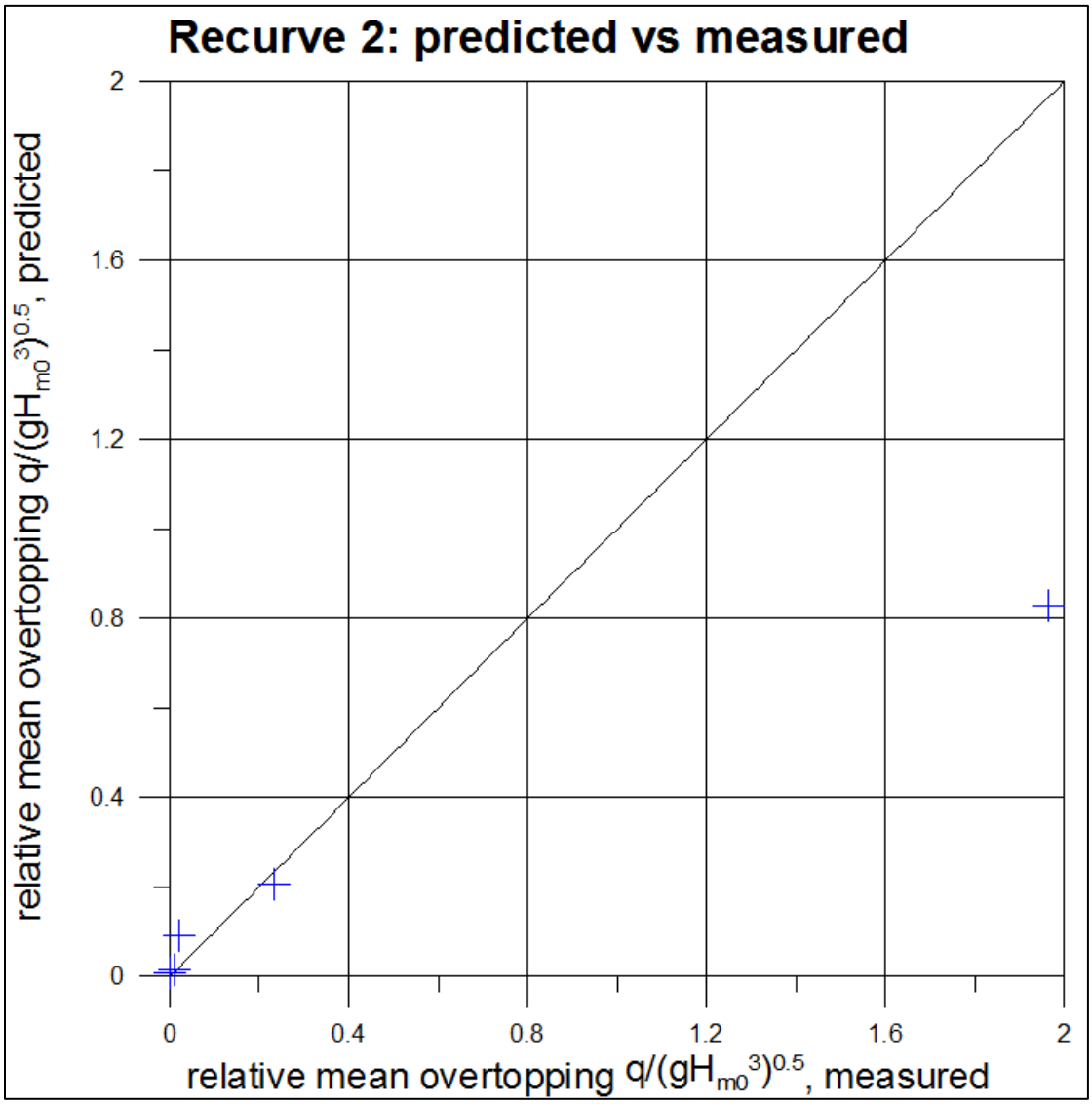

Figure 59: Recurve 2: predicted versus measured overtopping rate

5.4 Other considered factors

The reduction in overtopping is only one of many other factors such as safety, other uses (e.g. aesthetics) and cost, which are considered in the process of deciding which type of wall section will be designed and built. This section briefly discusses the other deciding factors.

5.4.1 Safety evaluation for pedestrians, vehicles and buildings

Table 18 gives a summary of the average prototype overtopping rates measured from the performed physical model tests. A case number is allocated for each condition. To assess these overtopping rates

for the tested case using prototype values, the allowable overtopping rates (as presented in Table 1) are considered.

Table 18: Summary of average prototype overtopping rates

	Vertical wall				
Case number	1	2	3	4	5
Water level (m)	10.8	10.4	10.0	9.4	9.0
Water depth at toe (m)	2.4	2.0	1.6	1.0	0.6
Freeboard Rc (m)	1.6	2.0	2.4	3.0	3.4
Overtopping (l)	454.85	454.78	312.64	127.82	29.08
Overtopping rate (l/s per m)	18.19	18.19	12.51	5.11	1.16

	Recurve 1				
Case number	6	7	8	9	10
Water level (m)	10.8	10.4	10.0	9.4	9.0
Water depth at toe (m)	2.4	2.0	1.6	1.0	0.6
Freeboard Rc (m)	1.6	2.0	2.4	3.0	3.4
Overtopping rate (l/s per m)	11.47	3.82	0.38	0.02	0.00

	Recurve 2				
Case number	11	12	13	14	15
Water level (m)	10.8	10.4	10.0	9.4	9.0
Water depth at toe (m)	2.4	2.0	1.6	1.0	0.6
Freeboard Rc (m)	1.6	2.0	2.4	3.0	3.4
Overtopping rate (l/s per m)	6.13	1.05	0.09	0.05	0.00

Vertical wall

For the vertical wall, the measured overtopping rates (Cases 1 to 5) lead to some unsafe situations for pedestrians, vehicles and buildings. It will be unsafe for both unaware and aware pedestrians behind the vertical seawall in these cases. In Cases 1 to 3, it will even be dangerous for trained staff who are well shod and protected, to walk behind the sea wall. It is possibly safe for trained staff only in Cases 4 and 5, provided that there are no falling jets and the overtopping flows are at lower levels only.

In terms of vehicles, it is unsafe to drive at a moderate or high speed during all the measured condition. However, for all cases, safe driving at slow speeds is possible, provided that there are no falling jets and the overtopping flows are at lower levels only.

For the vertical wall, all measured cases have the possibility to cause structural damage to buildings

Recurve 1

The results of the physical model tests show that the Recurve 1 profile creates safer conditions than the vertical wall. For Case 6 and possibly for Case 7, it is unsafe for trained staff, well shod and protected, to walk behind the wall. With Case 8 it is unsafe for unaware and aware pedestrians, but it will be safe for trained staff. Case 9 and 10 create safe conditions even for unaware pedestrians who have no clear view of the sea, are easily upset or frightened, and walk on a narrow walkway or close to the edge of the walkway.

It will be safe to drive at a moderate or high speed with impulsive overtopping which leads to falling or high jets in Cases 9 and 10 only. However, driving at a low speed is possible in all cases provided that overtopping by pulsating flows occur only at low levels and there are no falling jets.

No damage to buildings will occur in Case 10 only. In Case 9, minor damage to buildings may occur. Cases 6 to 8 all have the potential to cause structural damage to buildings.

Recurve 2

Recurve 2 proves to be the safest seawall profile under the measured conditions. Case 10 creates conditions that are safe for unaware pedestrians who have no clear view of the sea, are easily upset or frightened, and walk on a narrow walkway or close to the edge of the walkway. For Cases 13 and 14, it is safe for aware pedestrians who have a clear view of the sea, are not easily upset or frightened, are able to tolerate getting wet and who walk on a wider walkway. Cases 11 and 12 are still safe for trained, well protected staff.

It is safe for driving at moderate or high speed in Cases 14 and 15, provided that no impulsive overtopping giving falling or high velocity jets occur. All cases for the Recurve 2 profile provide safe conditions for driving at a low speed with overtopping by pulsating flows at low levels only and with no falling jets occuring.

In terms of the safety of buildings, only Case 15 will not cause any damage to buildings. Cases 11 to 14 are all capable of causing structural damage to buildings.

5.4.2 Additional factors to be considered

In terms of constructability, the 0.6 m overhang of Recurve 1 will be easier to build than the 1.2 m overhang of Recurve 2. The moments and forces on the larger overhang will be greater than on the smaller overhang.

A cost analysis is one of the factors to consider when deciding whether to recommend a Recurve 1 or Recurve 2 seawall. The cost analysis should include the cost of construction as well as the estimated cost of repairing damage after storms of different return periods occur.

When deciding between a Recurve 1 or Recurve 2 seawall, it should be considered how frequently the relative freeboard will be less than 2.4 meters. If it is seldom the case that the freeboard reaches a level less than 2.4 m, the difference in the performance between Recurve 1 and Recurve 2 in reducing overtopping can be negligible.

5.5 Applicability of results to a case study

The applicability of the results and findings of the physical model tests are illustrated with the aid of a case study of the wave overtopping problem at Strand. Strand is situated on the coast of False Bay, South Africa.

Strand's coastal defences consist mainly of a vertical wall, and in one location, a recurve wall. However, both the vertical and the recurve walls are damaged and have reached the end of their design life. Figure 60 shows the damaged recurve wall at Strand.

Strand has a popular recreational beach. Stakeholders will not approve a high seawall that obstructs the view of the sea from the road along the beach. By designing a recurve wall, the crest level of the structure can be lower than a vertical wall to allow for the same overtopping rate. When the allowable overtopping limit is selected, the crest level of the recurve wall can be calculated by using the graph in Figure 50.

The overtopping hazard in Strand was evaluated as part of the project “Coastal Zone Study and Protection Works between Gordon’s Bay and Zeekoevlei Canal Outlet”, conducted by PD Naidoo & Associates Consulting Engineers (PDN). For the purpose of this case study, the proposed overtopping guideline along with the wave conditions and water-levels as described in the mentioned project, will

be used in the calculations. Table 19 gives a summary of these parameters as used in the case study (Institute of Water and Environmental Engineering, 2012).

Figure 60: Current recurve wall in Strand

Table 19: Summary of used parameters

Overtopping limit (q)	1.0 l/s per m in a 1 in 20 year event
Beach level is at Land Levelling Datum (= mean sea-level)	LLD
Water-level above LLD for 1 in 20 year event	+1.6 m LLD
Significant wave height at -10 m for 1 in 20 year event (H_s)	1.7 m
Depth-limited significant wave height at seawall	1.12 m

The overtopping limit was selected in accordance with the guidelines in Table 1. This selection is somewhat subjective as these are only guidelines. A lower allowable overtopping limit will result in a higher seawall. Therefore a compromise in allowable overtopping has to be made to limit the wall height and minimise the obstruction of the line of sight to the sea horizon for pedestrians and car drivers and their passengers.

As the overtopping limit is selected and the significant wave height is known, the relative allowable mean overtopping rate is calculated as follows:

$$\frac{q}{\sqrt{gH_{m0}{}^3}} = \frac{1.0}{\sqrt{(9.81)1.12^3}} = 0.269$$

The calculated relative overtopping rate of 0.269 is plotted as a straight line on the graph as illustrated in Figure 61 indicated as "CASE STUDY" on the legend. The point of intersection between the calculated relative overtopping rate and each seawall profile type is read from the graph. Since the relative freeboard and the water-level are now known, the required crest level of each wall type can be calculated. Table 20 presents the calculated results.

For the selected allowable overtopping rate for a 1 in 20 year storm event, the required wall height for a vertical wall is more than 1 m higher than for the recurve walls. Both Recurve 1 and 2 offer a good alternative to a vertical wall to reduce overtopping. With the lower required wall height, obstruction of the sea view can possibly be avoided. When deciding between Recurve 1 and 2, other factors, as mentioned in Section 5.4.2, should be considered. However, it is clear that a recurve wall will be a better solution for coastal defence at Strand than a vertical wall.

Since the current Strand seawall heights range from +2.0 to +4.0 m LLD, a seawall height of +3.37 or +3.60 m LLD could be acceptable at the Strand. However, further studies should investigate how such a seawall will affect the line of sight to the sea for road and promenade users.

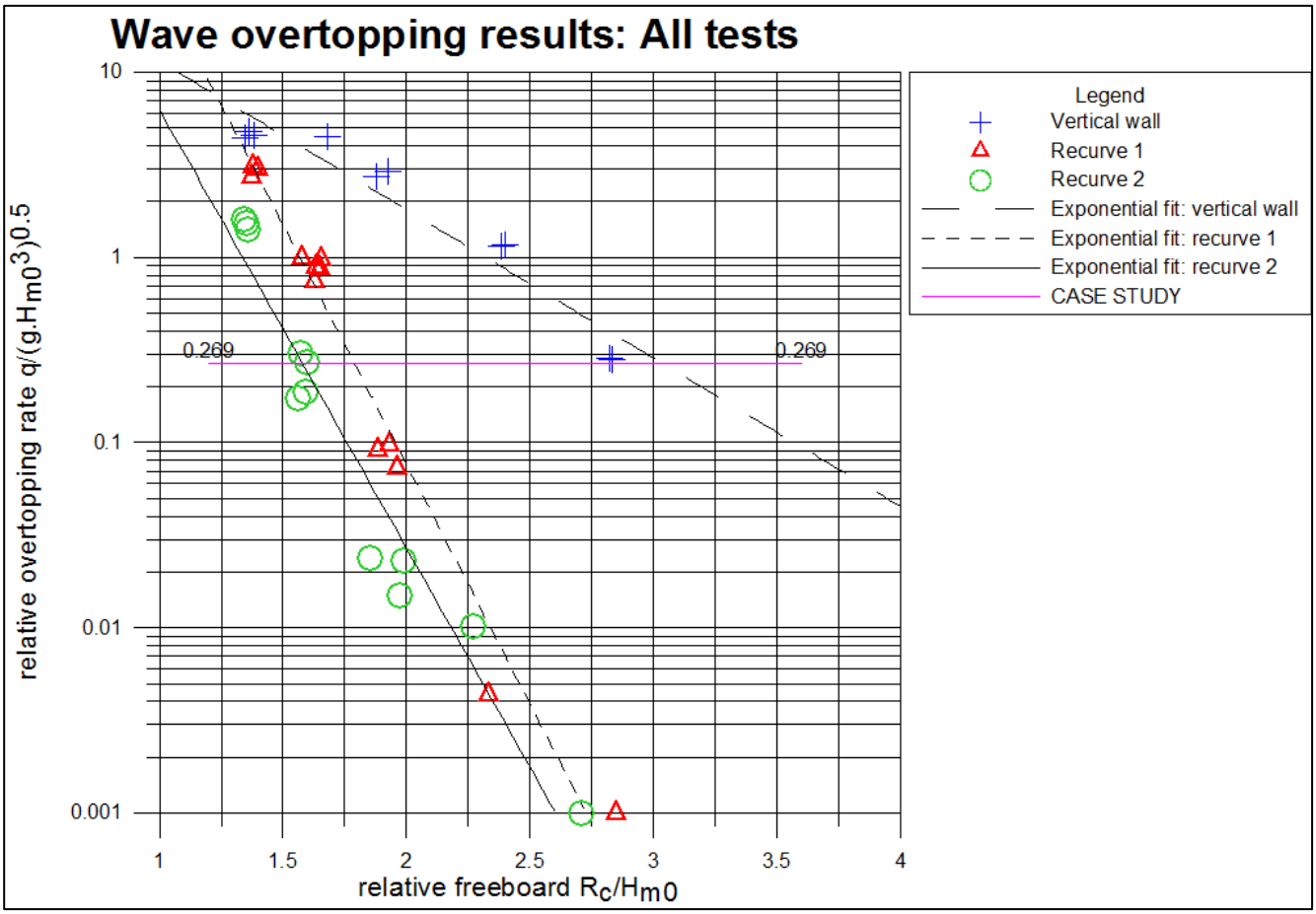

Figure 61: Example of how to apply results of this project in case study

Table 20: Results for case study calculations

Seawall profile	Relative freeboard	Freeboard (m)	Crest level (m LLD)
Recurve 2	1.578	1.77	+3.37
Recurve 1	1.789	2.00	+3.60
Vertical wall	3.032	3.40	+5.00

Chapter 6: Conclusion and recommendations

6.1 General

Higher wave heights resulting from the expected rise in sea-level will cause larger wave overtopping over seawalls at the back of beaches. To address this problem, the crest level of existing coastal structures can be raised. However, raising the crest level could obstruct the view of the sea. This project investigates the use of recurve walls as a possible solution as the crest level of recurve walls can be lower than that of vertical walls with the same overtopping rate. The use of recurve walls is not only a solution mitigating the impact of sea-level rise, but also applies to the design of new seawalls.

Using rates obtained from physical model tests, the project aims to compare overtopping rates for a vertical seawall without a recurve, with seawalls with recurves. The second objective of the study is to investigate the influence of the overhang length of the recurve wall on overtopping rates.

6.2 Findings from literature review

Two proposed recurve profile shapes are described in the literature review. The first recurve profile shape was proposed by Berkeley-Thorn and Roberts (1981) and is located at the crest of a sloping seawall. This recurve profile was used in a number of studies and Besley (1999) claims that it is very effective, while other profiles may be found to be significantly less so.

The second recurve profile, namely the Flaring Shaped Seawall (FSS), was proposed by Kamikubo (2000 & 2003). The FSS uses a deep circular cross-section. The non-overtopping FSS has a significantly lower crest height compared with a conventional wave absorbing vertical seawall. Although Kortenhaus et al. (2003) suggest that the profile of the FSS will be difficult to form with reinforced concrete, a FSS has been built in Japan.

Within the framework of the CLASH project, Pearson et al. (2004) present a decision chart as design guidance for recurve walls. This framework has been applied in the EurOtop manual.

Based on literature reviewed, it was found that scale effects have little influence on wave overtopping of vertical seawalls, provided the scale is large enough to reduce the effect of viscosity and surface tension to acceptably low levels. Laboratory effects also play a small role, provided the model tests are carefully executed. However, the failure to include wind in modelling can play a role in certain cases (especially for very low overtopping).

Reis et al. (2008) suggest that tests should be repeated, as the mean overtopping rates varies from test to test, even if performed under the same conditions. The number of waves per test and the largest wave heights in the wave train are also very important.

6.3 Findings of physical model tests

Physical model tests were performed on three different seawall profiles: a vertical wall and a recurve section with a short and a long seaward overhang, denoted Recurve 1 and Recurve 2 respectively.

The results of the model tests indicate that the use of recurve walls offers a definite reduction in wave overtopping rates compared with vertical walls. The relative freeboard of the structure influences the reduction in overtopping of recurve walls. The highest reduction in overtopping of recurve walls compared with vertical walls, occurs for the highest relative freeboard cases. As the relative freeboard decreases, the effectiveness of recurve walls to reduce overtopping also decreases. However, even for the lowest relative freeboard cases, recurve walls offer a significant reduction in overtopping compared with the vertical wall.

The results also indicate that Recurve 2, with a large seaward overhang, proves to be more effective in reducing overtopping than Recurve 1, which has a small overhang. Recurve 1 has a seaward overhang of 0.6 m, whereas Recurve 2 has a seaward overhang of 1.2 m (prototype dimensions).

For cases with high freeboard or large wave heights when R_c/H_{m0} >2.2, both recurves effectively reflects the splash from the incident breaking waves. Consequently, the length of the seaward overhang of the recurves becomes less important in reducing overtopping.

Also when $R_c/H_{m0} \leq 1.4$, the length of the seaward overhang is of lesser importance. For the lowest two freeboard cases, the reduction in overtopping for Recurve 1 is 37% and 79%, and for Recurve 2, 66% and 94% respectively.

By further investigating the influence of the overhang length on the mean overtopping rate as a function of freeboard, it was found that all freeboard cases follow the same trend, namely: as the overhang length increases, the mean overtopping rate decreases. The largest reduction in relative mean overtopping occurs between the vertical wall and Recurve 1. The reduction in overtopping rate between Recurve 1 and Recurve 2 is smaller, but still significant. However, as the freeboard increases, the reduction in overtopping between Recurve 1 and Recurve 2 becomes less significant.

The results of tests performed under the same conditions, but with varying peak wave periods of 8, 10 and 12 seconds, show that the mean overtopping rate is fairly sensitive to the peak wave period.

The results of the different seawall profiles have also been compared with the predicted overtopping rates calculated by the EurOtop calculation tool. This comparison is made to get an indication how the results of this project compare with other physical model studies. Both the probabilistic and deterministic (overtopping has been increased by one standard deviation in EurOtop) approaches are used to calculate the overtopping rate.

In general, the measured overtopping rates, follow the trend of the predicted EurOtop overtopping rates. However, in some cases the overtopping rates are underpredicted and others overpredicted. The conditions for this project's model tests do not exactly correspond to the case in the EurOtop calculation tool. This could possibly explain the deviations between the measured overtopping rates, and the predicted overtopping rates.

6.4 Conclusions

For all modelled cases a recurve seawall proves to be more effective in reducing overtopping at the back of a beach compared to a vertical seawall without a recurve. The reduction of overtopping can be as high as 100%, depending on the freeboard, wave conditions and overhang length.

The length of the seaward overhang influences the overtopping performance of the seawall. As the overhang length increases, the reduction in overtopping also increases. However, for high freeboard cases, the length of the seaward overhang becomes less important.

6.5 Recommendations for further research

This project investigated the influence of the recurve overhang on overtopping rates. However, to present comprehensive design guidelines, additional model tests are required.

Figure 52 gives an indication of the influence of the overhang length on the mean overtopping rate. The figure presents the relative mean overtopping rate versus the relative overtopping length as a function of freeboard. However, to be certain of the presented trend, it is recommended that further model tests are performed with relative overhang lengths between 0.3 and 0.7.

Figure 52 also illustrates that as the relative overhang length increases, the reduction in relative overtopping will, at a certain overhang length, remain constant. However, it is recommended that further tests are performed with relative overhang lengths from 1 to 1.2, in order to reach a more rigorous conclusion.

Physical model tests were performed for waves with a peak period of 10 seconds. To test the sensitivity of the overtopping rates to the peak period of the waves, some tests were also performed with peak periods of 8 and 12 seconds. As these results indicate that overtopping rates are fairly sensitive to the wave period, Figure 53, it is recommended that further tests are performed with a range of wave periods.

The measured overtopping rates were compared to the overtopping rates predicted by the EurOtop calculation tool. To fully evaluate the model tests by comparing them with the CLASH predictions, further comprehensive tests are required.

This project tested two different recurve angles. Tests have been done to establish the optimal geometry of a wave return wall on a smooth dike. Among other properties, the optimal angle for a recurve wall on a smooth dike was investigated (Van Doorslaer & De Rouck, 2010). Further research should be done on the optimal geometry for a recurve wall at the back of a beach.

As this project did not investigate the forces acting on the recurve wall, it is also recommended that further research investigates the forces on recurve walls with different overhang lengths.

References

Allsop, N. W. H., 2013. *E-mail correspondence,* United Kingdom: HR Wallingford.

Allsop, N. W. H., Alderson, J. & Chapman, A., 2007. *Defending buildings and people against overtopping,* Wallingford: HR Wallingford.

Bennett, A., 2009. *Picasa web albums.* [Online]
Available at: https://picasaweb.google.com/lh/photo/oB0fbmHvDp-SBb1NKavksQ
[Accessed 16 September 2013].

Berkeley-Thorn, R. & Roberts, A. G., 1981. *Sea defence and coast protection works.* London: Thomas Telford Ltd.

Besley, P., 1999. *Wave overtopping of seawalls.* UK: Environment Agency, R&D Technical Report W178.

CIRIA, CUR & CETMEF, 2007. *The Rock Manual. The use of rock in hydraulic engineering (2nd edition).* London: C683, CIRIA.

De Rouck, J., Geeraerts, J., Troch, P., Kortenhaus, A., Pullen, T. & Franco, L., 2005. *New results on scale effects for wave overtopping at coastal structures,* Ghent, CLASH D46: Final Report: Ghent University.

EurOtop, 2007. *Wave overtopping of sea defences and related structures: Assessment manual.* [Online]
Available at: www.overtopping-manual.com
[Accessed 5 October 2012].

Franco, L., de Gerloni, M. & van der Meer, J. W., 1994. *Wave overtopping on vertical and composite breakwaters.* Kobe, Proc. of 24th International Conference on Coastal Engineering (ICCE).

Grainger, K., 2009. *Geograph.* [Online]
Available at: http://www.geograph.org.uk/photo/1510021
[Accessed 16 September 2013].

Hawaii Real Estate, n.d. *Ocean Front Hawaii.* [Online]
Available at: http://www.drhank.com/kona/
[Accessed 16 September 2013].

Herbert, D. M., Allsop, N. W. H. & Owen, M., 1994. *Overtopping of sea walls under random waves,* Wallingford: HR Wallingford, Report SR 316.

HR Wallingford, n.d. *Wave overtopping.* [Online]
Available at: http://www.overtopping-manual.com/calculation_tool.html
[Accessed 9 October 2013].

Hughes, S. A., 1995. *Physical models and laboratory techniques in coastal engineering.* Vicksburg, USA: Coastal Engineering Research Center.

Institute of Water and Environmental Engineering, 2012. *Physical model tests of Strand seawall options,* Report submitted to PD Naidoo & Associates, Stellenbosch: University of Stellenbosch.

Kamikubo, Y., Murakami, K., Irie, I. & Hamasaki, Y., 2000. *Study on practical application of a non-wave overtopping type seawall.* Sydney, Proc. of 27th ICCE Volume 3, pp. 2215-2228.

Kamikubo, Y., Murakami, K., Irie, I., Kataoka, Y. & Takehana, N., 2003. *Reduction of wave overtopping and water spray with using Flaring Shaped Seawall.* Honolulu, The International Society of Offshore and Polar Engineers, pp. 671-675.

Kamikubo, Y., n.d. *Flaring Shaped Seawall (FSS).* [Online]
Available at: http://y-page.kumamoto-nct.ac.jp/u/kamikubo/fss.html
[Accessed 16 September 2013].

Kortenhaus, A., Pearson, J., Bruce, T., Allsop, N. W .H. & van der Meer, J. W., 2003. *Influence of parapets and recurves on wave overtopping and wave loading of complex vertical walls,* Netherlands: Infram publication no. 17.

Mansard, E. P. D & Funke, E. R, 1980. *The measurement of incident and reflected spectra using a least squares method,* Sydney, Proc. of 17th ICCE, pp.154-172.

Noble Consultants, Inc., 2011. *Seawalls, revetments, dikes & levees.* [Online]
Available at: http://www.nobleconsultants.com/projects/civil-structural-port-harbor-engineering/seawalls-revetments-dikes-levees/#ocean
[Accessed 16 September 2013].

Owen, M. W. & Steele, A. A. J., 1991. *Effectiveness of recurve wave return walls,* Wallingford, Report SR 261: HR Wallingford.

Pearson, J., Bruce, T., Allsop, N. W. .. & Gironella, X., 2002. *Violent Wave Overtopping-Measurements at large and small scale.* Cardiff, Proc. of 28th ICCE, pp. 2227-2238.

Pearson, J., Bruce, T., Allsop, N. W. H., Kortenhaus, A. & van der Meer, J. W., 2004. *Effectiveness of recurve walls in reducing wave overtopping on seawalls and breakwaters,* Netherlands: Infram publication no.21.

PIANC, n.d. *PIANC Open Teaching Material.* [Online]
Available at: http://www.kennisbank-waterbouw.nl/EC/CLM01060003.html
[Accessed 16 September 2013].

Pullen, T., Allsop, W., Bruce, T. & Pearson, J., 2008. *Field and laboratory measurements of mean overtopping discharges and spatial distributions at vertical seawalls,* Ref. CENG-02238: Elsevier.

Reis, M. T., Neves, M. G. & Hedges, T., 2008. Investigating the lengths of scale model tests to determine mean wave overtopping discharges. *Coastal Engineering Journal*, 50(4), pp. 441-462.

Rossouw, J., 1989. PhD Thesis: Design waves for the South African coastline, Stellenbosch: University of Stellenbosch.

Roux, G. B., 2013. *MSc Thesis: Reduction of seawall overtopping at the Strand,* Stellenbosch: University of Stellenbosch.

Schoonees, J. S., Lynn, B. C., le Roux, M. & Bouton, P., 2008. *Development set-back line for southern beaches of Richards Bay,* Stellenbosch: WSP.

Schoonees, J. S. & Theron, A. K., 2003. *Shoreline stability and sedimentation in Saldanha Bay,* Stellenbosch: CSIR.

Schüttrumpf, H. & Oumeraci, H., 2005. *Scale and model effects in crest level design.* Höfn, Iceland, Proc. of 2nd Coastal Symposium.

Soltau, C., 2009. *MSc Thesis: The cross-shore distribution of grain size in the longshore transport zone,* Stellenbosch: University of Stellenbosch.

U.S. Army Corps of Engineers, 2001. *Coastal Engineering Manual.* Engineer Manual 1110-2-1100 (in 6 volumes) ed. Washington, D.C.: U.S. Army Corps of Engineers.

US Army Corps of Engineers, 1991. *Reduction of wave overtopping by parapets,* REMR: Technical Note CO-RR-1.5.

Van Doorslaer, K. & De Rouck, J., 2010. *Reduction of wave overtopping on a smooth dike by means of a parapet.* ASCE, Proc. of 32nd ICCE.

Veale, W., Suzuki, T., Verwaest, T., Trouw, K. & Mertens, T., 2012. *Integrated design of coastal protection works for Wenduine, Belgium,* Antwerp: Flanders Hydraulics Research.

West Hawaii Today, 2013. *Fun in the Sun.* [Online]
Available at: http://westhawaiitoday.com/sections/news/local-news/fun-sun.html
[Accessed 16 September 2013].

West, I., 2013. *Sandbanks Sand Spit.* [Online]
Available at: http://www.southampton.ac.uk/~imw/Sandbanks.htm
[Accessed 16 September 2013].

Willson, A., 2008. *flickriver.* [Online]
Available at: http://www.flickriver.com/photos/angus-willson/2668996756/
[Accessed 16 September 2013].

WNNR, 1983. *Valsbaai: Velddataverslag Volume II: Figure (C/SEA 8219/2),* Stellenbosch: WNNR.

WSP Africa Coastal Engineers, 2012. *Coastal processes setback line for the Duin & See development between Great Brak Rriver and Glentana,* Stellenbosch: WSP.

Appendix A: Long section of the flume bed

Long section of flume layout